The Function of Backup Pathways of Non-Homologous End Joining in Relation to Growth State and Lesion Quality in Cells of Higher Eukaryotes

Inaugural-Dissertation

zur

Erlangung des Doktorgrades Dr. *rer. nat.* der Fakultät

Biologie und Geografie

an der Universität Duisburg-Essen

Standort Essen, Germany

vorgelegt von

Satyendra Kumar Singh

aus

Mirzapur,Uttar Predesh, Indien

Juni 2010

Die der vorliegenden Arbeit zugrunde liegenden Experimente wurden am Institut für Medizinische Strahlenbiologie an der Universität Duisburg-Essen, Standort Essen, durchgeführt.

1. Gutachter: Prof. Dr. George Iliakis

2. Gutachter: Prof. Dr. Ralf Küppers

3. Gutachter: Prof. Dr. Peter Bayer

Vorsitzender des Prüfungsausschusses: Prof. Dr. Ralf Küppers

Tag der mündlichen Prüfung: August 5th 2010

“Try not to become a man of success, but rather try to become a man of value.” *Albert Einstein*

“There are two kinds of people; those who do the work and those who take the credit. Try to be in the first group; there is less competition there.”

Indira Gandhi

Dedicated to

My dearest Brother Sumit Kumar Singh

(10 Nov 1981 – 25 July 2008)

"The saddest summary of a life contains three descriptions: could have, might have, and should have." *Louis E. Boone*

Table of content

Table of content I

Figures and Tables VI

Abbreviations IX

Abstract XII

1. Introduction *1*

1.1. Preamble **1**

1.2. Homologous Recombination Repair (HRR) **2**

1.3. Non-homologous end joining (NHEJ) **5**

1.3.1. Detection of DSBs and tethering of DNA ends 6

1.3.1.1. The Ku70/Ku80 heterodimer 6

1.3.1.2. DNA-PKcs 6

1.3.2. Processing of DNA Ends 9

1.3.2.1. Artemis 9

1.3.2.2. DNA polymerase μ and λ 9

1.3.2.3. Polynucleotide Kinase (PNK) 10

1.3.2.4. Other DNA end processing enzymes 10

1.3.3. Ligation of the DNA ends 11

1.3.3.1. The Ligase IV-XRCC 4 complex 11

1.4. Back up pathways of NHEJ (B-NHEJ) **11**

1.4.1. The Mre11-Rad50-Nbs1 (MRN) complex and CtIP 13

1.4.2. Poly (ADP-ribose) polymerase 1, Xrcc1 and DNA ligase III 14

1.4.3. Histone H1 15

1.5. Regulation of DSB repair pathway choice by DNA-PKcs **15**

1.6. Growth factor signaling and DNA double strand break repair **17**

1.7. Defining Characteristics of IR-induced DNA damage **20**

1.7.1. Linear energy transfer (LET) 20

1.7.2. Complex lesions induced by IR 22

1.7.3. Principles of measurement of clustered DNA lesions 23

1.8. IR induced heat labile sites and their contribution to DSB induction 24

1.8.1. Measurement of prompt DSBs in mammalian cells 24

1.9. Heavy ion irradiation facility at the GSI in Darmstadt 26

1.10. Aim and Scope of the work 27

1.10.1. Cell cycle dependent fluctuations of B-NHEJ activity 28

1.10.2. The Growth state dependence of B-NHEJ 28

1.10.3. Determination of B-NHEJ activity by PFGE after exclusion of HLSs 28

2. Materials and Methods 30

2.1. Material 30

2.1.1. Laboratory Apparatus 30

2.1.2. Disposable Elements 31

2.1.3. Chemical Reagents 32

2.1.4. Antibodies 34

2.1.5. Buffers and solutions 34

2.2. Methods 37

2.2.1. Cell lines and cell culture 37

2.2.2. Radiation 38

2.2.2.1. X-ray irradiation (low LET) 38

2.2.2.2. Heavy ion irradiation (high LET) 38

2.2.3. The GSI Accelerator Facilities 39

2.2.4. Cell sorting methods 40

2.2.4.1. Cell cycle analysis by flow cytometry 40

2.2.4.2. Cell freezing 41

2.2.4.3. Cell staining for sorting 41

2.2.4.4. Cell sorting 42

2.2.5. Centrifugal elutriation 42

2.2.6. Asymmetric field inversion gel electrophoresis (AFIGE) 42

2.2.7. Methods to obtain plateau phase culture 44

2.2.7.1. Normal growth into a plateau-phase 44

2.2.7.2. Artificially generated non-growing cells 44

2.2.8. Clonogenic survival assay 45

2.2.9. Methods to monitor Heat Labile Sites (HLSs) 45

2.2.9.1. Low temperature lysis 45

2.2.9.2. Measurement of induction of HLSs induction into DSBs at different temperature 46

2.2.10. Electrophoresis and Immunoblotting 46
2.2.10.1. Cell extracts preparation and electrophoresis 46
2.2.10.2. Immunoblotting 47

3. Results ***48***

3.1. Cell cycle dependent regulation of B-NHEJ **48**
3.1.1. Experimental design 48
3.1.1.1. Control experiments designed to standardize sorting conditions 48
3.1.2. Repair of DNA DSBs throughout the cell cycle in wt MEFs 49
3.1.3. Repair of DSBs throughout the cell cycle in D-NHEJ deficient MEFs 51
3.1.4. Repair of DSBs throughout the cell cycle in *Rad54*$^{-/-}$ MEFs 53
3.1.5. DSB rejoining throughout the cell cycle in HRR and D-NHEJ deficient MEFs 54

3.2. Marked dependence on growth state of the efficiency of B-NHEJ **56**
3.2.1. B-NHEJ is compromised in non-cycling D-NHEJ mutants across species 56
3.2.2. DNA-PKcs inhibitors are more efficient in plateau-phase 61
3.2.3. Kinase dead DNA-PKcs cells show dominant negative effect 62
3.2.4. Effect of DNA-PKcs autophosphorylation sites mutants on DSB repair 63
3.2.5. Effect of phosphomimicking mutants of DNA-PKcs on DSB repair 66
3.2.6. Effect of different levels of DNA-PKcs on DSB repair 66
3.2.7. Repair kinetics of double knock out of D-NHEJ proteins 66

3.3. Effect of EGFR signaling over DSB repair by B-NHEJ **67**
3.3.1. B-NHEJ inhibition in plateau phase cells generated by serum deprivation 67
3.3.2. Inhibition of B-NHEJ by serum deprivation is reversible 68
3.3.3. Reversal in B-NHEJ is not a very fast process 69
3.3.4. Relationships between time of incubation and serum concentration for B-NHEJ recovery 71
3.3.5. Repair after chemical inhibition of EGFR 72
3.3.6. Expression levels of proteins implicated in B-NHEJ 75

3.4. B-NHEJ contributes to cell survival **75**

3.5. Backup pathways of NHEJ after exclusion of heat labile site (HLSs) **79**
3.5.1. The function of B-NHEJ is demonstrated under low-temperature lysis (LTL) 80
3.5.2. Lysis at 37°C is equivalent to HTL 87
3.5.2.1. Effect of lysis on dose response and repair kinetics 88
3.5.3. Estimation of HLSs induction at 37°C in naked DNA and in intact cells during repair 90
3.5.4. Conversion of HLSs induced in intact cells into DSBs *in vitro* 90

3.5.5. Thermally unstable sugar adducts are induced after irradiation of naked DNA 91
3.5.6. Protein during incubation at elevated temperatures accelerates SA-2 conversion 93

3.6. Effect of high LET radiation on the repair of DSBs by B-NHEJ 95
3.6.1. Induction of HLSs by heavy ions 95
3.6.2. Effect of lesion complexity on B-NHEJ efficiency 97

4. Discussion 99

4.1. The function of B-NHEJ is enhanced in G2 99
4.1.1. Background 99
4.1.2. Methodology 100
4.1.3. HRR throughout the cell cycle 101
4.1.4. Enhanced function of B-NHEJ in G2 102

4.2. Marked dependence on growth state of B-NHEJ 103
4.2.1. Growth state as a determinant of B-NHEJ efficiency 103
4.2.2. Dependence of D-NHEJ on growth state 104
4.2.3. B-NHEJ is not compromised in DNA-PKcs$^{-/-}$ cells at plateau phase of growth 105
4.2.4. Effect of growth factor signaling in double knockout of DNA-PKcs and Ku80 105
4.2.5. Inhibition of D-NHEJ with inhibitor of DNA-PKcs allows the function of B-NHEJ in repair proficient cells 106
4.2.6. DNA-PKcs act as regulator of B-NHEJ in plateau phase of growth 107
4.2.7. D-NHEJ deficient cells show enhanced radiosensitivity in the plateau-phase of growth 108
4.2.8. Growth factor signaling and its effect on B-NHEJ 108

4.3. Prompt and temperature dependent DSBs 110
4.3.1. Robust B-NHEJ activity detectable after LTL 111
4.3.2. Independent lines of investigation provide strong evidence for a robust function of alternative pathways of NHEJ in D-NHEJ deficient cells 111
4.3.3. Why does DSB repair appear slow after LTL? 113
4.3.4. Induction and repair of DNA DSBs after heavy ion irradiation 114
4.3.5. Efficiency of B-NHEJ after heavy ion irradiation 115

5. Summary 116

6. Reference List 118

7. Appendix 138

8. Acknowledgement 140

9. Curriculum Vitae ***142***

10. Publications and Conferences ***144***

11. Declaration ***146***

Figures and Tables

Figure 1.1: Schematic diagram showing the main steps of HRR……..……..…**3**

Figure 1.2: Proposed model of the DNA-PK dependent pathway of non-homologous end joining……...……...…….....**7**

Figure 1.3: The major domains of DNA-PKcs. ……...…….……...……..**8**

Figure 1.4: Role of B-NHEJ revealed in cells deficient in D-NHEJ and HRR or in both pathways……...……..…….....**12**

Figure 1.5: Schematic representation of B-NHEJ pathway……...……..……..**14**

Figure 1.6: A model of EGFR-mediated radioprotection…….……**18**

Figure 1.7: Blockade of EGFR-mediated DNA repair……...……..……**19**

Figure 1.8: Difference in energy deposition pattern between high and low LET radiation……...……....**22**

Figure 1.9: Prompt and temperature sensitive delayed DSB…….……**25**

Figure 2.1: Accelerator facility at GSI, Darmstadt……..……..**39**

Figure 2.2: UNILAC facility at GSI……...…….…….....**39**

Figure 2.3: SIS facility at GSI……...…….……..**40**

Figure 3.1: Scheme of sorting experiment……...…….……**49**

Figure 3.2: Rejoining of IR-induced DSBs in wt MEFs…….……...….....**50**

Figure 3.3: Rejoining of IR-induced DSBs in *LIG4*$^{-/-}$ MEFs…….……...…**52**

Figure 3.4: Rejoining of IR-induced DSBs in *Rad54*$^{-/-}$ MEFs……...…….…..**54**

Figure 3.5: Rejoining of IR-induced DSBs in *Rad54*$^{-/-}$*/LIG4*$^{-/-}$ MEFs……...…….…..**55**

Figure 3.6: Growth curve of different mouse, human and CHO cell lines……...…….…...**57**

Figure 3.7: DSB repair capacity strongly depends on growth state in *Ku70*$^{-/-}$ and *Ku80*$^{-/-}$ MEFs…….……...…….……..**58**

Figure 3.8: DSB repair capacity strongly depends on growth state in XRCC4 deficient *xr-1* cells……..……..……...……**59**

Figure 3.9: DSB repair capacity does not change in DNA-PKcs deficient cells……..**60**

Figure 3.10: Wortmannin induced inhibition of DSB repair depends on growth state in human glioma M059K cells……..…….....…...**61**

Figure 3.11: Repair kinetics of DNA-PKcs kinase dead and autophosphorylation mutants……..……..**64**

Figure 3.12: Repair kinetics of cells expressing different level of DNA-PKcs and phosphomimicking forms of DNA-PKcs……...…….……...…**65**

Figure 3.13: Repair kinetics of double D-NHEJ mutant (*Ku80*$^{-/-}$ and *DNA-PKcs*$^{-/-}$)…….……...**67**

Figure 3.14: Repair kinetics of *Lig4*$^{-/-}$ cells after serum deprivation…...……..……..……..**69**

Figure 3.15: Recovery of repair capacity as a function of serum concentration applied immediately after the end of the serum deprivation period…….…….....……..**70**

Figure 3.16: Recovery of repair capacity as function of time of incubation in growth medium supplemented with 10% serum……..…….....**71**

Figure 3.17: Relationship between time of incubation and serum concentration in the recovery of B-NHEJ…….....……**72**

Figure 3.18: Relationships between time of incubation and serum concentration in B-NHEJ recovery……...…….……..……**73**

Figure 3.19: Relationships between time of incubation and serum concentration in the recovery of B-NHEJ……...…….....……...…..**74**

Figure 3.20: Effect of the EGFR inhibitor BIBX-1382 on repair of DSBs by B-NHEJ……...**74**

Figure 3.21: Expression levels of proteins implicated in B-NHEJ in the different stages of growth…….…….…….……..…….**75**

Figure 3.22: Survival of *LIG4*$^{-/-}$ and wt MEFs at different stages of growth and phases of the cell cycle……...……...……...**78**

Figure 3.23: Survival of wt MEFs at different stages of growth and phases of the cell cycle ……...……...……..**79**

Figure 3.24: Dose response and repair kinetics of IR induced DSBs in human DNA-PKcs proficient M059K cells following high (HTL) and low (LTL) temperature lysis...……..…..**82**

Figure 3.25: Dose response and repair kinetics of IR induced DSBs in human DNA-PKcs deficient M059J cells after HTL or LTL……...……..……...**83**

Figure 3.26: Dose response and repair kinetics of IR induced DSBs in *LIG4*$^{-/-}$ MEFs after HTL or LTL……...……...…..……**84**

Figure 3.27: Dose response and repair kinetics of IR induced DSBs in *Ku70*$^{-/-}$ fibroblasts after HTL or LTL……...…….……..…..**85**

Figure 3.28: Dose response and repair kinetics of radiation induced DSBs in DNA-PKcs deficient Chinese hamster mutant *irs20* cells after lysis at 37^{o}C…….…….....…….....**86**

Figure 3.29: Dose response and repair kinetics of IR induced DSBs in human DNA-PKcs proficient M059K after LTL of different duration……..……...**88**

Figure 3.30: Dose response and repair kinetics of IR induced DSBs in human DNA-PKcs proficient M059K after LTL for different duration…….……...**89**

Figure 3.31: Conversion of HLSs induced in irradiated cells to DSBs by incubation of lysed DNA at elevated temperatures……...…..…...**92**

Figure 3.32: Induction of HLSs in irradiated lysed DNA…….....…..…..…..**93**

Figure 3.33: Conversion of HLSs in chromatin bound DNA…….….....**94**

Figure 3.34: Dose response curve of different cell lines after to heavy ions…….....**95**

Figure 3.35: Conversion of HLSs at different temperature after heavy ion irradiation…….…...**96**

Figure 3.36: Effect of lesion complexity on B-NHEJ efficiency……. ..…..**98**

Table 1: Antibodies used in western blotting analysis……..34

Abbreviations

AFIGE	Alternating Field Inversion Electrophoresis
ATM	ataxia-telangiectasia mutated
B-NHEJ	Backup-non-homologous end joining
bp	base pairs
BSA	Bovine Serum Albumin
CHO	Chinese Hamster Ovary
DAPI	4`,6-Diamidino-2-Phenylindole
Deq	Dose equivalent
DMEM	Dulbecco's Modified Eagle Medium
DNA	Deoxyribonucleic Acid
DNA-PK	DNA dependent protein kinase
DNA-PKcs	DNA dependent protein kinase catalytic subunit
D-NHEJ	DNA-PK-dependent non-homologous end joining
DSB	Double Strand Break
DTT	Dithiothreitol
ECL	Enhanced Chemoluminescence
EDTA	Ethylene Diamine Tetraacetic Acid
EGFR	Epidermal Growth Factor Receptor
et al.	et alii (and others)
FACS	Fluorescence Activated Cell Sorter
FAR	Fraction of Activity Released
FBS	Fetal Bovine Serum
FDR	Fraction of DNA Released
gm	gram
Gev	Giga electron Volt
Gy	Gray
HEPES	4-(2-hydroxyl)-1-Piperazineethanesulfonic Acid
HI	Heavy Ions

HLS	Heat Labile Sites
HRR	Homologous Recombination Repair
HTL	High Temperature Lysis
ICLs	Interstrand Crosslinks
IR	Ionizing Radiation
kDa	Kilodalton
LET	Linear Energy Transfer
LMDS	Locally Multiply Damaged Site
LTL	Low Temperature Lysis
MEF	Mouse Embryonic Fibroblast
MEK	MAPK and ERK Kinase
MEM	Minimum Essential Medium
min	minute
MQ	Milli-Q
MRN	Mre11/Rad50/Nbs1
NHEJ	Non-homologous End Joining
PAGE	Polyacrylamide Gel Electrophoresis
PARP-1	Poly (ADP-ribose) polymerase 1
PBS	Phosphate Buffered Saline
PE	Plating Efficiency
PFGE	Pulsed Field Gel Electrophoresis
PI	Propidium Iodide
PI3K	Phosphoinositol 3-Kinase
RNase	Ribonuclease
ROS	Reactive Oxygen Species
rpm	revolution per minute
SA	Sugar Adduct
SDS	Sodium Dodecyl Sulphate
SSB	Single Strand break
TEMED	Tetramethylethylenediamine

Tris	Tris-(hydroxymetheyl)-aminomethane
V(D)J	Variable (diversity) joining
WT	Wild Type
XRCC	X-ray cross complementing

Abstract

DNA double strand breaks (DSBs) are toxic lesions generated by various endogenous processes (like free radicals, V(D)J recombination etc.) and by exogenous agents such as ionizing radiation (IR) and radiomimetic drugs. DSBs are repaired by either homologous recombination (HR) or non-homologous end joining (NHEJ). Defects in any of the pathways of DSB repair lead to an increase in cell death, as well as to genomic instability that eventually leads to cancer.

Homologous recombination occurs only during late S and G2 phase of the cell cycle when sister chromatids are available in close proximity. In contrast, NHEJ is the major pathway for DSB repair as it functions throughout the cell cycle and does not require a homologous chromosome or chromatid. NHEJ repairs broken DNA ends with no homology requirement, although it occasionally uses micro-homologies. During this process, broken DNA ends are instantly captured by the Ku heterodimer (Ku70/80) that recruits DNA-PKcs to the site of the DSB. DNA-PKcs changes its conformation at the site of the DSB and dimerises to generate a scaffold for subsequent processing of the DNA ends. At the end of this process compatible ends are ligated by the Ligase IV/XRCC4 complex. This reaction is stimulated by XLF/Cernunnos, which interacts with XRCC4. We refer to this pathway as D-NHEJ to indicate its dependence on DNA-PK. In many cases, DNA ends are not compatible and need processing before ligation. Ionizing radiation, for example, induces a large number of ends that contain damaged bases and/or DNA backbone sugars that need processing before ligation. DNA polymerases (μ, λ), polynucleotide kinase and the Artemis nuclease are responsible for this end processing and the occasionally required subsequent DNA polymerization.

Cells with mutations in components of D-NHEJ still remain capable of repairing the majority of IR induced DSBs albeit with slower kinetics and in an error prone manner. Unexpectedly, this pathway is not sensitive to mutations in genes required for homologous recombination repair (HRR). We therefore, refer to this form of DSB repair as a distinct form of end joining that is normally suppressed by D-NHEJ. However, when D-NHEJ is genetically or chemically compromised, this form of end joining acts like a backup and repairs the majority of DSBs in the genome, albeit slower and often incorrectly. We proposed the term B-NHEJ for this form of

nonhomologous end joining to differentiate it from D-NHEJ and to indicate its putative backup function.

The operation of B-NHEJ could be demonstrated at the chromosomal level using human peripheral blood lymphocytes and inhibitors of D-NHEJ. Biochemical studies implicate DNA Ligase III in B-NHEJ and suggest that the repair module PARP-1/XRCC1/DNA Ligase III, already known to be involved in single strand break (SSB) repair, also contributes to DSB repair.

I have investigated the cell cycle dependence of B-NHEJ and found that B-NHEJ is enhanced in the G2 phase of the cell cycle. Further studies that form one focus of this thesis examine the growth state dependence of B-NHEJ. I found that B-NHEJ is compromised as cells enter the plateau phase of growth. I examined the generality of this observation using diverse D-NHEJ mutants, as well as in wild type cells after chemical inhibition of D-NHEJ. Interestingly, DNA-PKcs mutant and knockout cell lines do not show this inhibition in DNA DSB repair capacity in plateau phase of growth. This result indicates towards pathways regulatory activity of DNA-PKcs. Furthermore, I examined the consequences of this growth-state-dependent B-NHEJ inhibition by investigating cell radiosensitivity to killing. Changes in chromatin structure were investigated as possible causes of the observed effect, as well as changes in growth factor signaling. Finally, the thermal stability of lesions causing DSBs and their reparability by B-NHEJ and D-NHEJ is investigated. We found that thermally sensitive lesions transformed into breaks even at 37°C inside the cells too.

The results uncover important properties of B-NHEJ that require further in depth investigation and point to characteristics of the chemical alterations in the DNA that underlie DSBs that need further characterization.

1. Introduction

1.1. Preamble

The DNA double-strand breaks (DSBs) are considered as the most lethal form of DNA damage. They can be generated by exogenous agents such as IR (ionizing radiation), topoisomerase inhibitors, radiomimetic drugs and by cellular processes such as meiosis, V(D)J recombination, class switch recombination, stalled DNA replication forks and reactions that generate ROS (reactive oxygen species) (Helleday et al., 2007). In contrast to the programmed nature of DSBs induced by cellular processes such as V(D)J recombination or class switch recombination, DSBs are randomly induced by the IR, which is problematic in efficient repair. In addition, due to the nature of energy deposition events, an irradiated cell may recognize DSB lesions far more massively than those induced by programmed cellular processes. All these characteristics generate special processing requirements that can be understood only after defining the properties of the spectrum of DSBs induced.

In addition, it is important to point out that IR induces multiple forms of DNA damage, including damages to the bases and cleavage of the DNA backbone that results into DNA SSBs (single strand breaks). These types of DNA damages are repaired by the BER (base excision repair) and the SSB repair pathways (Almeida and Sobol, 2007; Dianov and Parsons, 2007). In their simplest form, DNA DSBs are generated when two SSBs are induced on opposite strands about 10 bp apart. DNA termini (either of SSBs or DSBs) frequently contain 3`-phosphate or 3`-phosphoglycolate groups, which need to be removed before ligation. Moreover, the DNA surrounding the DSB may contain additional forms of IR induced DNA damage, thus generating a form of lesion which is collectively termed as complex or clustered lesions (Georgakilas, 2008; Sutherland et al., 2002). These lesions are thought to be difficult to repair, first because of the additional destabilization they generate in the DNA molecule, and second because of the problems caused by their simultaneous enzymatic processing. If left unrepaired these lesions may lead to cell death, and in general misrepaired DSBs have the potential of causing chromosomal translocations and genomic instability (Olive, 1998).

Higher eukaryotic cells have developed efficient mechanisms to sense and repair DNA DSBs and

thus to maintain genomic stability. These DNA damage response (DDR) pathways consist of several major steps including sensor, mediator, transducer and effector proteins. Ultimate goal of the sensing is the coordination of repair of the cell cycle and other vital cellular processes.

There are two fundamentally different ways of repairing DSBs: (1) homologous recombination (HR)-mediated repair and (2) non-homologous end joining (NHEJ). It remains unknown on what basis the cell decides which pathway to use for the repair of a particular DSB. Equally unknown is also whether the pathway selection decision fundamentals are affected by the nature of the DSB and by its association with other forms of damage to generate a complex lesion. Further issues of interest include the discovery (also from our laboratory) of additional pathways of DSB repair that increase the dimensions of the cellular repair decision space.

The present work addresses two important aspects of DSB processing. First, we examine the nature and some defining characteristics of a newly discovered alternative pathway of DSB repair. Second, we address important issues of the chemical nature of DSBs as they relate to their thermal stability. Before we provide a detailed outline of the aims of the present work, we discuss briefly DSB repair pathways and IR induced DNA damage characteristics to generate the framework of our arguments and facilitate the interpretation of the results obtained.

1.2. Homologous Recombination Repair (HRR)

HRR is a repair pathway found in all forms of life. It provides high fidelity, template-dependent repair or tolerance of complex DNA damages including DNA gaps, DNA DSBs and DNA interstrand crosslinks (ICLs). It requires a DNA sequence homologous to the one containing the DNA damage and utilizes either the sister chromatid or the homologous chromosome for error-free restoration of the DNA molecule. HRR is the primary mechanism of DSB repair in yeast and bacteria. Its contribution to DSB repair in vertebrate cells remains uncertain, but in principle it could operate in G1 phase using the homologous chromosome, and in S and G2 phase using the sister chromatid (Lee et al., 1997). In addition to the repair of DNA DSBs, HRR has also been implicated in several other biological processes. It is involved in meiotic cross over, which are responsible for the allelic rearrangement in the gametes, and is necessary for proper chromosome segregation. It is also important for mating type switching in yeast and epitope immunoglobulin

class switching in many organisms (see Figure 1.1 for an outline of HRR steps).

The initial steps of HRR consist of 5' DNA end resection and the subsequent invasion of the remaining 3`-OH end into a template duplex DNA to initiate repair synthesis. The nucleolytic resection of the DNA ends at the DSB in the 5` to 3` direction leads to a 3`single-stranded overhang at both DNA ends that initiate the process. This reaction is mediated by the Mre11/Rad50/Nbs1 (MRN) complex and CtIP (Limbo et al., 2007; Takeda et al., 2007). The generated ssDNA is initially bound by the eukaryotic ssDNA binding replication protein A (RPA), which has higher affinity for ssDNA than Rad51 (Sung and Klein, 2006; Wold, 1997). Rad51 is the eukaryotic RecA homolog that catalyzes homology search and DNA strand exchange (Sung, 1994). Similar to RecA, Rad51 binds cooperatively to ssDNA in a ternary complex with ATP at a stoichiometry of 1 protomer per 3-4 nucleotides and forms a right handed filament with a helical pitch of 130 Å (Conway et al., 2004).

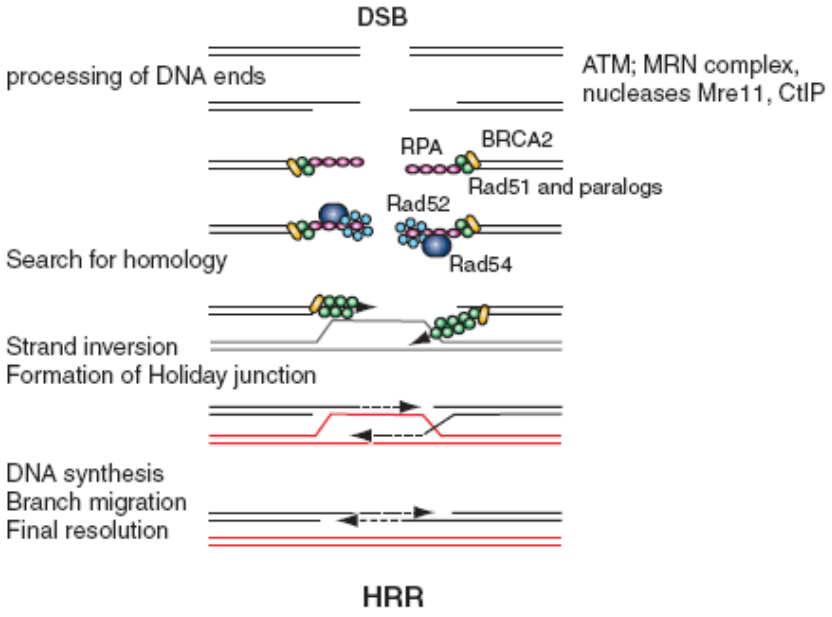

Figure 1.1: Schematic diagram showing the main steps of HRR

RPA is a heterotrimeric ssDNA-binding protein involved in all DNA metabolic processes generating ssDNA (Wold, 1997). There are five human Rad51 paralogs Rad51B, Rad51C,

Rad51D, Xrcc2 and Xrcc3. Rad51C associates with Xrcc3 and is also found in a complex with Rad51B, Rad51D and Xrcc2 (Masson et al., 2001). Genetic analysis suggests non-overlapping functions of Rad51C-Rad51D-Xrcc2 and Xrcc3-Rad51C complexes (Yonetani et al., 2005). In yeast, Rad52 accelerates displacement of RPA from ssDNA by Rad51 (Sugiyama and Kowalczykowski, 2002), and allows efficient Rad51-mediated recombination involving RPA coated ssDNA. Unlike yeast, mouse Rad52 mutants display extremely mild recombination defects and no radiosensitivity to killing (Rijkers et al., 1998). Genetic experiment in chicken DT40 cells suggests a partially overlapping function of Xrcc3 and Rad52 (Fujimori et al., 2001). It is not clear which mammalian protein has taken over the functions exerted by yeast Rad52 protein, but possible candidate is BRCA2, which is not found in budding yeast. BRCA2 is required for IR-induced Rad51 focus formation *in vivo* (Tarsounas, Davies, and West, 2003) and it is recruited to DSBs with the help of BRCA1.

Rad54 is a core factor of HRR in budding yeast and its deficiency generates DNA damage sensitivity identical to that of Rad51 mutants (Heyer et al., 2006). In mice, Rad51 is essential whereas Rad54 deficient cells or mice are viable (Sharan et al., 1997). Rad54 is a bidirectional motor protein that translocates at ~300bp/s on dsDNA powered by the hydrolysis of ATP. Rad54 associates with and stabilizes the Rad51 presynaptic filament assisting its targeting to the pairing site. Its similarity to Snf2-like chromatin remodeling factors and the ability to slide nucleosomes suggest a role in chromatin remodeling during HRR (Zhang et al., 2007).

Homology search and DNA strand invasion are collectively called synapsis and catalyzed by the core proteins discussed above. These generate the D-loop intermediate, where the 3`-end of the invading strand primes DNA synthesis of template duplex DNA leading to the generation of a Holliday junction and the association of several proteins that are involved in resolving this structure in a specific manner. The ResolvaseA activity cleaves Holliday junctions into cross over and non-cross over products. An alternative mechanism involves BLM DNA helicase with the type I topoisomerases TOPOIIIα (Plank and Hsieh, 2006; Wu et al., 2006). In a process termed dissolution, BLM migrates the two junctions towards each other and TOPOIIIα removes the hemi-catenates that topologically link two duplexes.

All proteins involved in HRR are known to be expressed in the majority of mammalian cells. It is

therefore thought that this pathway plays a significant role in the repair of DNA DSBs in higher eukaryotes. Mutant cell lines with defects in Rad51 paralogs Xrcc2 and Xrcc3 are radiosensitive to killing (Cui et al., 1999). Furthermore, the same cells, as well as cells with defects in BRCA1 and BRCA2, are defective in the repair of enzymatically induced DSBs in model system for HRR (Jasin, 2002).

Although, the above evidence clearly implicates HRR in the repair of DSBs, it is not yet known how HRR proteins are recruited to repair IR induced DSBs. This is because cells with defects in Xrcc2 and Xrcc3, and despite their increased radiosensitivity to killing, show no defects in DNA DSB repair as measured by pulsed-field gel electrophoresis (PFGE).

1.3. Non-homologous end joining (NHEJ)

In cells of higher eukaryotes, DSBs are repaired mainly by non-homologous end joining (NHEJ) (Jackson, 2002; Valerie and Povirk, 2003; van Gent, Hoeijmakers, and Kanaar, 2001a). This mode of DSB repair is homology independent and restores the integrity of the DNA molecule without necessarily preserving its sequence in the vicinity of the break (Lieber et al., 2003; Valerie and Povirk, 2003; Weterings and van Gent, 2004). It operates efficiently and removes the majority of IR induced DSBs with half times of 10-30 min. It maneuvers efficiently in all phases of cell cycle. The MRN complex may contribute to the regulation of this pathway as silencing or chemical inhibition of Mre11 reduces the efficiency of NHEJ (Dinkelmann et al., 2009; Rass et al., 2009; Xie, Kwok, and Scully, 2009).

NHEJ in higher eukaryotes requires Ku (Ku70/Ku80 heterodimer), DNA-PKcs (see Figure 1.2), XRCC4, DNA Ligase IV, Artemis and XLF (XRCC4-like factor or Cernunnos). Deletion or inactivation of any of these core NHEJ factors induces marked sensitivity to IR and to other DSB-inducing agents, and causes defects in V(D)J recombination (Bassing and Alt, 2004; Kurimasa et al., 1999; Meek et al., 2004; O'Driscoll and Jeggo, 2006). NHEJ comprises the following sequential events; (1) detection of the DSB and tethering/protection of the DNA ends; (2) DNA end processing to remove damage or nonligatable groups; and (3) DNA ligation. The different steps of NHEJ are graphically shown in Figure 1.2 and are briefly discussed next.

1.3.1. Detection of DSBs and tethering of DNA ends

1.3.1.1. The Ku70/Ku80 heterodimer

First step of NHEJ is detection of the DSB by Ku heterodimer. This is composed of two subunits Ku70 and Ku80, which are encoded by the XRCC5 and XRCC6 genes. Each comprises a central DNA binding core. The N-terminus of Ku70 contains an acidic domain that is phosphorylated *in vitro* by DNA-PKcs (Chan et al., 1999), whereas the C-terminus contains an SAP domain with putative chromatin/DNA binding activity (Lees-Miller and Meek, 2003). The C-terminal region of Ku80 forms a long flexible arm that may be involved in protein–protein interactions and in the alignment of two DNA-PKcs molecules at the site of DSB (Hammel et al., 2010; Harris et al., 2004; Zhang et al., 2004). The extreme C-terminus of Ku80, a conserved region, is required for the interaction with DNA-PKcs.

Ku binds to DNA ends with high affinity *in vitro* without sequence specificity (blunt, or with 5` or 3` overhangs). This is facilitated by the structure of the Ku70/80 DNA binding core, which adopts a pre-formed loop conformation that encircles the DNA. Once bound, Ku translocates inwards from the DNA ends making the extreme termini accessible to other proteins, such as DNA-PKcs (Yoo and Dynan, 1999). A very recent study shows that Ku also has end processing activity (Roberts et al., 2010); Ku nicks DNA 3` end of an abasic site by a mechanism involving a Schiff-base covalent intermediate with the abasic site. Ku interacts with DNA-PKcs (Lees-Miller and Meek, 2003), the XRCC4-DNA Ligase IV complex (Costantini et al., 2007), XLF (Yano et al., 2008), DNA polymerase μ (Mahajan et al., 2002) and with DNA polymerase λ in vitro (Ma et al., 2004). The interaction of DNA-PKcs, XLF, DNA polymerase μ and DNA Ligase IV with Ku are facilitated or enhanced in the presence of DNA, suggesting that binding of Ku with DNA is a prerequisite for interaction with other NHEJ proteins. A very recent study shows that Ku regulates the non-homologous end joining pathway choice of DNA DSB repair in human somatic cells (Fattah et al., 2010).

1.3.1.2. DNA-PKcs

DNA-PKcs, the product of PRKDC or XRCC7 gene, is a large polypeptide of over 4000 amino acids, and a member of the PI3KKs (phosphoinositide 3-kinase-like family of protein kinases).

The N-terminal ~250kDa of DNA-PKcs contains a putative DNA-binding domain, a leucine-rich region and a series of HEAT repeats (Gupta and Meek, 2005). The C-terminal region contains a FAT domain followed by the kinase domain and the C-terminal FATC domain. Cells that lack DNA-PKcs are highly radiosensitive and have defects in V(D)J recombination especially in the processing of coding joints. Moreover, in mice, dogs and horses DNA-PKcs deficiency is associated with a SCID phenotype (Meek et al., 2004). Ku and DNA-PKcs interact only in the presence of DNA (Suwa et al., 1994), and recruitment of DNA-PKcs at the sites of DSBs *in vivo* is Ku dependent (Uematsu et al., 2007). Inward translocation of Ku allows DNA-PKcs to interact with the extreme termini of the DNA, allowing two DNA-PKcs molecules to interact across the DSB and to form a so-called synaptic complex. This interaction stimulates the kinase activity of DNA-PKcs, promoting phosphorylation in trans across the DSB. The DNA-PKcs-Ku-DSB complex serves to tether the ends of the DSB together and is thought to protect the DNA ends from nuclease attack.

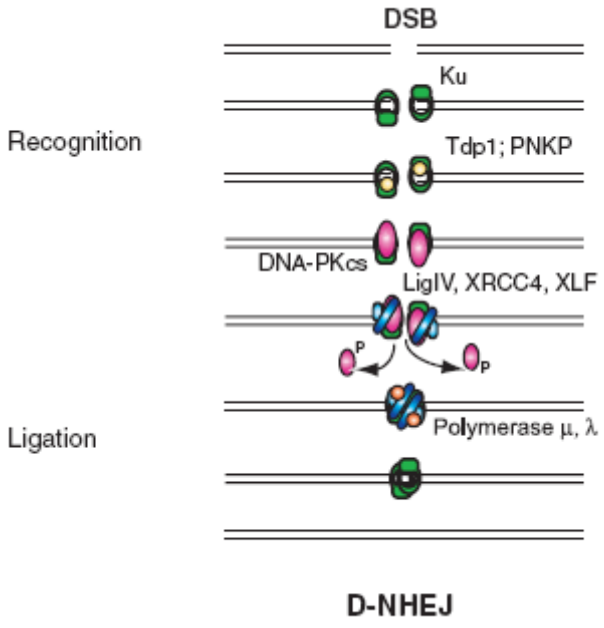

Figure 1.2: Proposed model of the DNA-PK dependent pathway of non-homologous end joining

DNA-PKcs has weak serine/threonine kinase activity that is greatly enhanced in the presence of

dsDNA ends and Ku. Like other members of the PI3KK family, DNA-PK phosphorylates many of its substrate on serine or threonine residues that are followed by glutamine residues (SQ/TQ motif) (Lees-Miller et al., 1992); however DNA-PK also phosphorylates proteins at non-SQ/TQ sites in vitro (Douglas et al., 2002). DNA-PK kinase activity is required for NHEJ (Kurimasa et al., 1999). DNA-PK phosphorylates Ku70, Ku80, XRCC4, XLF, Artemis and DNA Ligass IV *in vitro* but phosphorylation at these sites is not required for NHEJ *in vivo*. DNA-PKcs phosphorylates itself at more than 30 sites. Phosphorylation of Ser2612 and Ser2624 and Thr2609, Thr2620, Thr2638 and Thr2647 (ABCDE cluster), as well as Ser2056 and Thr3950 are all IR- inducible and DNA-PK dependent *in vivo* (Chan et al., 2002; Chen et al., 2005; Ding et al., 2003). ATM and ATR can phosphorylate Ser2612 and Thr2609, and Thr2638 and Thr2647 in response to IR or UV respectively (Chen et al., 2007; Yajima, Lee, and Chen, 2006). Figure 1.3 depicts the most important domains of DNA-PKcs.

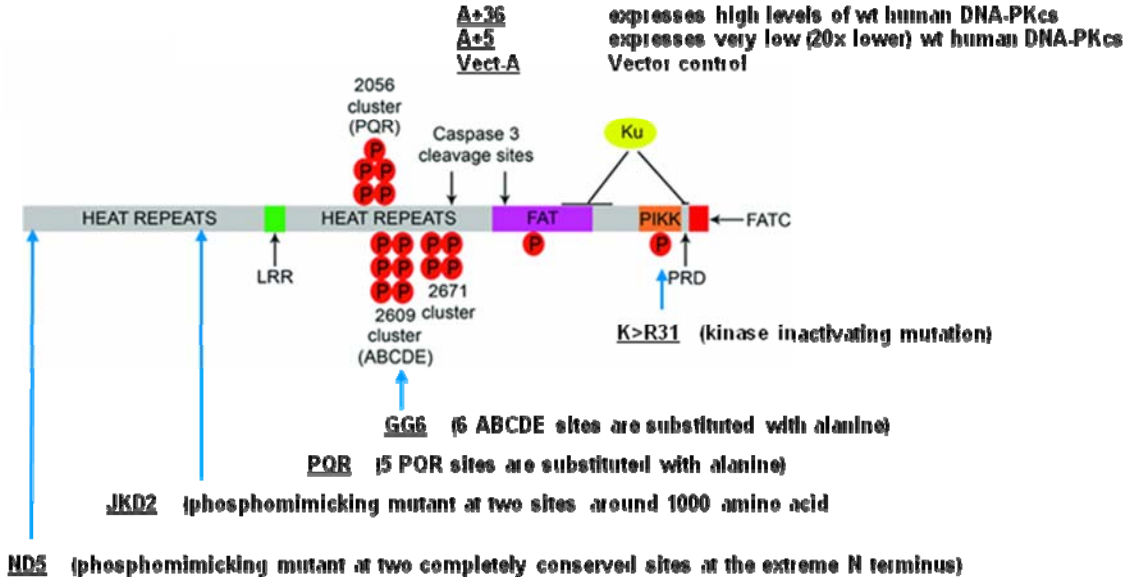

Figure 1.3: The major domains of DNA-PKcs (Brandi L. Mahaney, Biochem, J., 2009, 417; 639-50). See text for more information.

Autophosphorylation of DNA-PKcs *in vitro* results in loss of protein kinase activity and dissociation of phosphorylated DNA-PKcs from DNA bound Ku. Cells expressing DNA-PKcs mutants with serine and threonine residues in ABCDE cluster substituted with alanine, are more radiosensitive than cells expressing no DNA-PKcs at all (Convery et al., 2005). Similarly, cells in

which the protein kinase activity of DNA-PK is inhibited by a small molecule inhibitor are more radiosensitive than DNA-PK null cells and have reduced rates of HRR (Allen, Halbrook, and Nickoloff, 2003).

1.3.2. Processing of DNA Ends

Once DNA ends are detected and secured, the next step is processing of DNA termini to remove non-ligatable end groups and other lesions. Radiation generates all kind of damages to DNA that requires different combinations of processing enzymes. Candidate processing enzymes include Artemis, DNA polymerase μ and λ, PNK and possibly APLF (aprataxin and PNK-like factor) and WRN.

1.3.2.1. Artemis

Artemis possesses 5`→3` exonuclease activity and in the presence of DNA-PKcs and ATP, acquires endonuclease activity towards DNA-containing a dsDNA/ssDNA transition as well as at DNA hairpins (Ma et al., 2002). Artemis can also remove 3`-phosphoglycolate groups from DNA ends *in vitro*. Artemis defects cause RS-SCID (radiation sensitive SCID) in humans. Artemis interacts with DNA-PKcs providing a mechanism whereby it may be recruited to the DSB. Artemis deficient cells are radiosensitive, and the protein has been suggested to function in an ATM dependent pathway processing complex lesions (Jeggo and Löbrich, 2005). Artemis is also involved in NHEJ during immunoglobulin class switch recombination (Du et al., 2008).

1.3.2.2. DNA polymerase μ and λ

DNA polymerase μ and λ are recruited to DSBs via their interactions with Ku and the Ligase IV-XRCC4 complex. Recruitment of polymerase at the site of DSBs depends upon the type of damage to be repaired. Although, polymerase μ and λ carry out similar gap filling reactions, they differ in their requirements for a DNA template. Polymerase λ is largely template dependent whereas polymerase μ is less template dependent (Nick McElhinny et al., 2005). Cells lacking one or both polymerases are not hypersensitive to IR. It seems likely that polymerase μ and λ are only required for repair of a small subset of DNA breaks. DNA polymerase λ is phosphorylated in response to IR (Matsuoka et al., 2007).

1.3.2.3. Polynucleotide Kinase (PNK)

PNK has both 3`-DNA phosphatase and 5`-DNA kinase activities, suitable to remove nonligatable end groups from DNA termini. N-terminal FHA domain of PNK interacts with CK2-phosphorylated XRCC4. Knockdown of PNK in human cells renders them radiosensitive and defective in DSB repair (Rasouli-Nia, Karimi-Busheri, and Weinfeld, 2004). Radiosensitivity was attributed to a defect in NHEJ, since PNK-knockdown cells were proficient in sister chromatid exchange formation, but had an epistatic response with DNA-PKcs (Karimi-Busheri et al., 2007). PNK is also phosphorylated *in vivo* in response to IR.

1.3.2.4. Other DNA end processing enzymes

There are several additional DNA end processing enzymes involved in NHEJ. Aprataxin and PNK-like factor (APLF) has both endonuclease and exonuclease activities (Kanno et al., 2007). APLF interacts with CK2-phosphorylated XRCC4 and Ku. APLF is phosphorylated by ATM in response to DNA damage but its functional relevance is not known (Bekker-Jensen et al., 2007; Macrae et al., 2008). The Werner protein (WRN) is a member of RecQ helicase family that possesses DNA dependent ATPase, 3`-5` DNA helicase, strand annealing and 3`-5` exonuclease activities. WRN interacts with Ku, which stimulates its exonuclease activity (Cooper et al., 2000; Karmakar et al., 2002b). WRN is phosphorylated by DNA-PKcs *in vitro* and *in vivo*. Its catalytic activity is regulated by this protein (Karmakar et al., 2002a). WRN also interacts with the Ligase IV-XRCC4 complex, which stimulates its exonuclease activity *in vitro* (Kusumoto et al., 2008).

Another DNA end processing enzyme is the Mre11 nuclease. Mre11 has been implicated in the classical (D-NHEJ in our nomenclature) and backup NHEJ (see below) (Xie, Kwok, and Scully, 2009). Mre11 nuclease activity is important for DNA repair and genomic stability, and has functions distinct from those of ATM (Buis et al., 2008). Mre11 dimers may coordinate end bridging and nuclease processing in DNA DSB repair (Williams et al., 2008). DNA end processing must occur prior to ligation of the DNA ends. However, precisely when the processing enzymes are recruited to DSBs is not clear. It is possible that specific enzymes are involved in end processing and their order of recruitment is quite flexible, depending on the nature of breaks and other factors.

1.3.3. Ligation of the DNA ends

1.3.3.1. The Ligase IV-XRCC4 complex

DNA Ligase IV exists in complex with XRCC4. XRCC4 has no enzymatic activity and may act as a scaffolding protein. XRCC4 is itself a homodimer and two dimers interact to form a tetramer. XRCC4 stabilizes DNA Ligase IV and stimulates its activity (Grawunder et al., 1997). Interestingly, DNA Ligase IV has the unusual property of being able to ligate one DNA strand at a time, probably allowing processing enzymes to act simultaneously on end groups on the opposite strand (Gu et al., 2007). The Ligase IV -XRCC4 complex interacts with Ku, PNK, APLF and XLF. XRCC4 is highly phosphorylated *in vivo* (Critchlow, Bowater, and Jackson, 1997). It has been suggested that DNA-PKcs is required for DNA damage induced phosphorylation of XRCC4 (Drouet et al., 2005) and that DNA-PKcs promotes in this way DNA end ligation by DNA Ligase IV /XRCC4 complex. XRCC4 is also SUMOylated *in vivo*, and this modification is important for the nuclear localization of XRCC4 and DSB for DSB repair (Yurchenko, Xue, and Sadofsky, 2006).

1.4. Back up pathways of NHEJ (B-NHEJ)

Cells with mutations in components of D-NHEJ remain capable of repairing the majority of IR induced DSBs albeit by slower kinetics (Figure 1.4 A) (DiBiase et al., 2000). In wild type cells, DSB repair proceeds with two distinct kinetic components. A fast component repairs about 80% of DSBs within 1 h whereas a slower component repairs the remaining DSBs within a few hours. Deficiency in DNA-PK activity does not alter the half-times of either of these components of rejoining but increases from 17 to 72% the proportion of DSBs rejoining with slow kinetics. There was only a small increase in the number of unrejoined breaks in M059J as compared with M059K cells after 30 h of incubation. This observation led to the hypothesis that in cells of higher eukaryotes, an evolutionary conserved, independently active, but inherently slow NHEJ pathway is stimulated 30-fold by DNA-PKcs to rapidly remove DNA DSBs from the genome. The stimulation is expected to be local in nature and the presence of DNA-PKcs in the vicinity of the DSB is thought to determine whether rejoining will follow fast or slow kinetics.

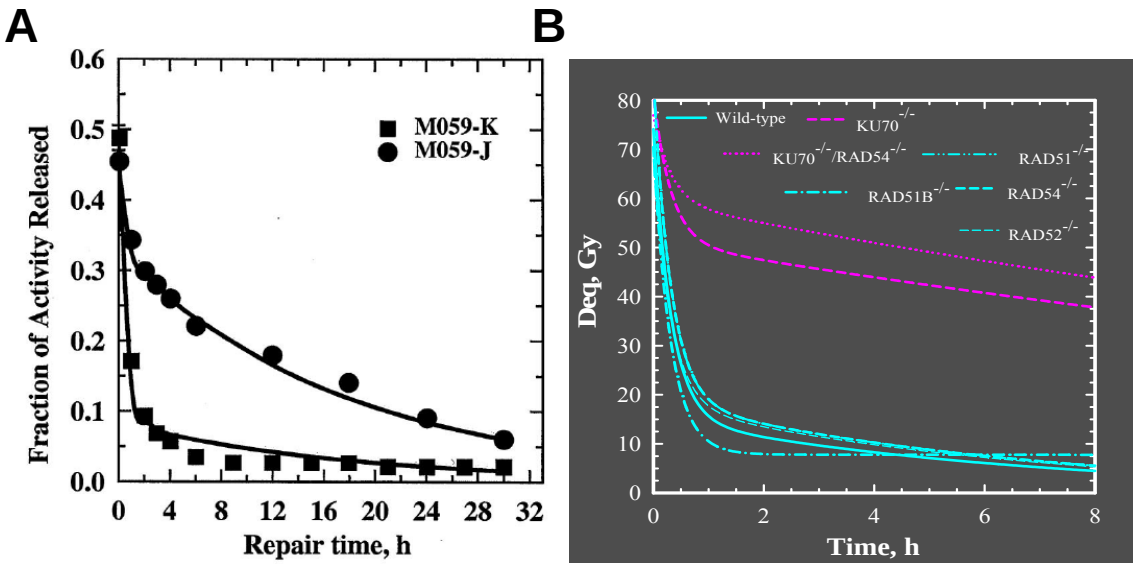

Figure 1.4: The role of B-NHEJ revealed in cells deficient in D-NHEJ and HRR, or in both pathways. Rejoining of DNA DSBs in exponentially growing wt (M059K) and D-NHEJ deficient (M059J) cells (A) (Dibiase et al. Cancer Research 60, 1245-1253, March 1, 2000) and repair after IR in wt and D-NHEJ, HRR, and D-NHEJ and HRR double mutants in DT40 cells (B) (Wang et al, Oncogene, 2001 Apr 26; 20 (18): 2212-24)

The above observations suggest a slow pathway capable of removing DSBs from the DNA when the fast DNA-PK dependent pathway is inactive and point immediately to HRR that is known to be a slow process. To address this question, a comprehensive study using the hyper recombinogenic DT40 cells and a number of mutants derived from them was carried out. These studies, which are summarized in Figure 1.4 B, showed that DT40 cells rejoin IR-induced DSBs with half times of 13 min and 4.5 h, and with contributions by the fast (78%) and slow (22%) components of rejoining similar to those of other vertebrate cells with 1000-fold lower levels of HRR. In the same set of experiments, it was further shown that deletion of Rad51B, Rad52 and Rad54 leaves the rejoining half times unchanged, as well as the contribution of the slow component. Similar conclusions were also derived using a conditional knockout mutant of Rad51. On the other hand, the expected reduction (to 37%) in the contribution of the fast component was observed in $Ku70^{-/-}$ DT40 cells, but the slow component, operating with half time of 18.4 h, was still able to rejoin the majority (63%) of DSBs. A double mutant $Ku70^{-/-}/Rad54^{-/-}$ showed half times similar to $Ku70^{-/-}$. These results indicated that defects in several genes

involved in HRR such as Rad51, Rad52, Rad54, and the paralog Rad51B had no effect on the rejoining kinetics even when D-NHEJ was compromised by Ku70 knockout.

Thus, the residual rejoining of DSBs observed in cells with defects in D-NHEJ cannot be attributed to HRR, which, under these conditions appears to be responsible for the repair of small subset of the IR induced DSBs (less than 10%). It was therefore suggested that it reflects an alternative form of end joining that operates as a backup to D-NHEJ and is therefore termed B-NHEJ (Some people also use the term alternative NHEJ). B-NHEJ activity is normally suppressed by D-NHEJ (Perrault et al., 2004). However, when D-NHEJ is genetically or chemically compromised, this form of end joining acts and restores integrity in the genome by repairing the majority of DSBs, albeit frequently with errors (Bennardo et al., 2008; Busuttil et al., 2008; Iliakis et al., 2004).

B-NHEJ has been shown to be involved in CSR, and under certain conditions in V(D)J recombination (Corneo et al., 2007). B-NHEJ also contributes to chromosomal translocations that give rise to lymphoid malignancies (Boboila et al., 2010b; Nussenzweig and Nussenzweig, 2007; Yan et al., 2007). B-NHEJ has major role in chromosomal translocation and is suppressed by D-NHEJ (Boboila et al., 2010a; Simsek and Jasin). Biochemical studies implicate DNA ligase III in B-NHEJ (Audebert, Salles, and Calsou, 2004; Wang et al., 2005) and suggest that the repair module PARP-1/Xrcc1/DNA ligase III (Audebert, Salles, and Calsou, 2004; Wang et al., 2006), that is already known to process single strand breaks (SSBs) (Caldecott, 2001), also contributes to DSB repair. A recent study has shown that 53BP1 favors long-range CSR in part by protecting DNA ends against resection, which prevents B-NHEJ dependent short-range rejoining of intra-switch region (Bothmer et al., 2010). Additional proteins, recently implicated in B-NHEJ are discussed next. A schematic diagram of B-NHEJ is shown in Figure 1.5.

1.4.1. The Mre11-Rad50-Nbs1 (MRN) complex and CtIP

The 3`-5` exonuclease activity of Mre11 has previously been suggested to be involved in microhomology-based end joining, where it degrades mismatched DNA ends until sequence identity is revealed (Paull and Gellert, 2000). During V(D)J recombination, NBS1 is required for B-NHEJ of hairpin coding ends, whereas it suppresses B-NHEJ of signal ends and promotes

proper resolution of inversional recombination intermediates (Deriano et al., 2009). A recent study has implicated Mre11 in B-NHEJ, as silencing or chemical inhibition reduces efficiency of B-NHEJ, whereas overexpression of Mre11 stimulates the resection of ssDNA and increases B-NHEJ (Dinkelmann et al., 2009; Rass et al., 2009; Xie, Kwok, and Scully, 2009). An *in vitro* study with *Xenopus laevis* egg extract showed that the MRN complex is not required in classical NHEJ but is necessary for resection-based end joining of mismatched DNA ends (Taylor et al., 2010). CtIP is a cell cycle regulated protein which has highest expression in S and G2 phase (Limbo et al. 2007). Nbs1, a subunit of MRN complex has role in tethering Ctp1 (yeast ortholog of CtIP) and Mre11-Rad50 to coordinate DNA DSB processing and repair (Willams et al. 2009).

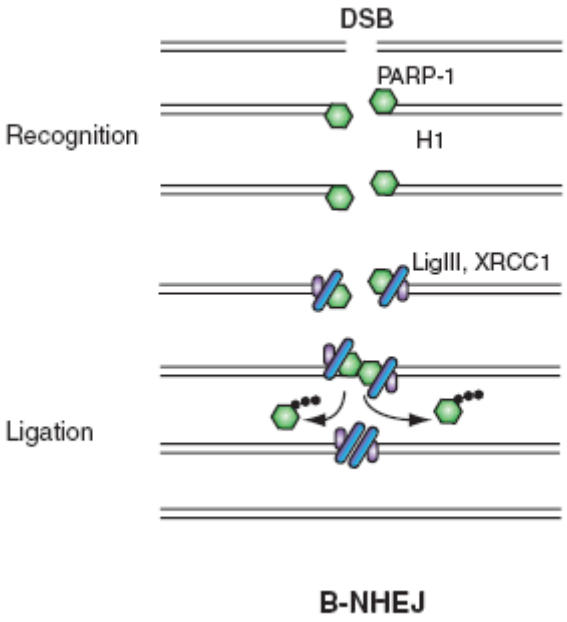

Figure 1.5: Schematic representation of B-NHEJ pathway.

1.4.2. Poly (ADP-ribose) polymerase 1, Xrcc1 and DNA ligase III

PARP-1 is an abundant nuclear protein that binds to both single strand breaks (SSBs) and DSBs. It is involved in many cellular processes including base excision repair (BER) and HRR (Helleday, Bryant, and Schultz, 2005). PARP-1 binds to DNA ends and it is in direct competition

with Ku, but Ku has higher affinity for DSBs (Wang et al., 2006). Fractionation of Xenopus extracts identified DNA ligase III in an active fraction, devoid of DNA-PK, that promote an error prone, microhomology-driven form of NHEJ (Goettlich et al., 1998). Up-regulation of WRN and DNA ligase III in chronic myeloid leukemia has implicated them in DSB repair and the resultant genomic instability that drives disease progression (Sallmyr, Tomkinson, and Rassool, 2008). There is evidence for the involvement of PARP-1 in DSB rejoining (Rudat et al., 2001; Süsse et al., 2004). Recently PARP-1 has been implicated in B-NHEJ and in immunoglobulin CSR. The authors showed that PARP-1 favors repair of switch regions through a microhomology–mediated repair pathway and that PARP-2 is a novel translocation suppressor during CSR (Robert, Dantzer, and Reina-San-Martin, 2009).

1.4.3. Histone H1

A recent study from our lab has implicated histone H1 as an accessory factor of DNA Ligase III and thus as a putative component of B-NHEJ (Rosidi et al., 2008). In this study, extract fractionation was combined with proteomic analysis to identify histone H1 as an end-joining factor. It is thought that histone H1 supports B-NHEJ by aligning the DNA ends in preparation for the DNA end-ligation step. Other studies suggest an inhibitory role for histone H1 in D-NHEJ through interference with DNA Ligase IV/XRCC4 (Kysela, Chovanec, and Jeggo, 2005). A marked inhibition of DNA end joining is observed under these conditions, which is partially rescued by histone H1 phosphorylation by DNA-PK. Since phosphorylation reduces the affinity of histone H1 for DNA binding, it could be possible that phosphorylation by DNA-PK is a mechanism for removing histone H1 from DNA (Kysela, Chovanec, and Jeggo, 2005) in preparation of Ku binding and initiation of D-NHEJ. As mentioned above, the repair module PARP-1/DNA Ligase III/XRCC1 utilizes histone H1 as an alignment factor. There is evidence that loss of histone H1 occurs during senescence (Funayama et al., 2006). This finding is unexpected as histone H1 facilitates chromatin condensation and acts mainly as transcriptional repressor (Hayes and Hansen, 2001).

1.5. Regulation of DSB repair pathway choice by DNA-PKcs

The idea that the two DSB repair pathways, D-NHEJ and HRR, compete for DSB was suggested

by early experiment showing that plasmid DNA transferred into mammalian cells could be repaired by either pathway, and by biochemical studies showing both D-NHEJ and HRR proteins bind to broken ends. MRE11 influences both pathways, raising the possibility that the competition between the two pathways might be actively controlled. Several other proteins are now implicated in both pathways, including BRCA1, histone H2AX, PARP-1, RAD18, DNA-PKcs, and ATM (Shrivastav, De Haro, and Nickoloff, 2008). Although, D-NHEJ factors are recruited to DSBs more rapidly than HRR factors, D-NHEJ and HRR factors are recruited independently. There is a significant period of time when both sets of factors are present at the damaged site (Kim et al., 2005), consistent with the notion that pathway choice may be regulated by one or more proteins that act in both pathways.

Increased HRR in cells with D-NHEJ defects can be explained by a passive competition model. However, several lines of evidence suggest that DNA-PKcs is an active regulator of DSB repair pathway choice. First evidence for this was the puzzling finding that inactivation of NHEJ by elimination of DNA-PKcs increased HRR (Allen et al., 2002), but chemical inhibition of DNA-PKcs had the opposite effect (Allen, Halbrook, and Nickoloff, 2003). Phosphorylation of DNA-PKcs is important for NHEJ, and biochemical experiments indicate that phosphorylation of the T2609 cluster causes DNA-PKcs to dissociate from broken DNA ends (Ding et al., 2003; Shrivastav, De Haro, and Nickoloff, 2008). Together, these results suggested a model in which chemically inhibited DNA-PKcs fails to dissociate from ends and thereby blocks access to other D-NHEJ repair factors, as well as to HRR repair factors. The importance of DNA-PKcs phosphorylation for HRR was underscored by a study showing that complementation of DNA-PKcs null CHO V3 cells with DNA-PKcs lacking the T2609 cluster sites gives the same phenotype as chemical inhibition of wild-type DNA-PKcs, i.e., HRR was suppressed. Thus, blocking phosphorylation of the T2609 cluster converts DNA-PKcs into a dominant-negative regulator of HRR (Cui et al., 2005).

The idea that DNA-PKcs regulate DSB repair pathway choice gained additional support when the Meek laboratory identified DNA-PKcs splice variants that lack the kinase domain. Given the importance of DNA-PKcs kinase activity for NHEJ (Convery et al., 2005), it was not surprising that these kinase-inactive variants did not complement the radiosensitivity of DNA-PKcs null

cells. However, the variants were particularly interesting because they had dominant negative effects on HRR, and therefore mimicked chemically inhibited full-length DNA-PKcs and the T2609 cluster mutant. These variants are expressed along with the full-length DNA-PKcs only in quiescent cells, but they do not have a dominant negative effect on NHEJ. These results suggest that co-expression of full-length DNA-PKcs and kinase-inactive variants limit HRR in quiescent cells, which lack the preferred sister chromatid repair template, while simultaneously maintaining a high capacity for DSB repair by NHEJ (Convery et al., 2005).

Although these results are in line with the notion that DNA-PKcs may be a regulator of DSB repair pathway choice in higher eukaryotes, it should be kept in mind that all above experiments have been carried out under the premise that no other repair pathways, such as B-NHEJ, are operational. Inclusion of additional repair pathways will add possibilities that have not been considered in the interpretation of the results obtained.

1.6. Growth factor signaling and DNA double strand break repair

Growth factor signaling has an important role in DNA damage response. Radioresistance of several solid tumors has been successfully correlated with higher levels of EGFR expression. The epidermal growth factor receptor (EGFR) is a 170-kDa cell surface receptor that plays a pivotal role in cell proliferation, cell migration, and cell survival. EGFR is frequently expressed at elevated level in multiple cancers of epithelial origin (Normanno et al., 2006). EGFR belongs to a subfamily of four closely related growth factor receptors (HER-1/ErbB1, HER-2/neu/ErbB2, HER-3/ErbB3, and HER-4/ErbB4) that bind EGFR ligands such as the epidermal growth factor (EGF) and tumor necrosis factor-α (TNF-α). Ligand binding induces receptor dimerization, which then undergo intermolecular tyrosine phosphorylation. The phosphorylated EGFR then triggers the initiation of several intracellular signaling cascades. These include the Ras/Raf/mitogen-activated protein kinase (MAPK) pathway, the phosphatidyl inositol-3-kinase (PI3K)/AKT pathway, Phospholipase Cγ-mediated generation of second messengers such as

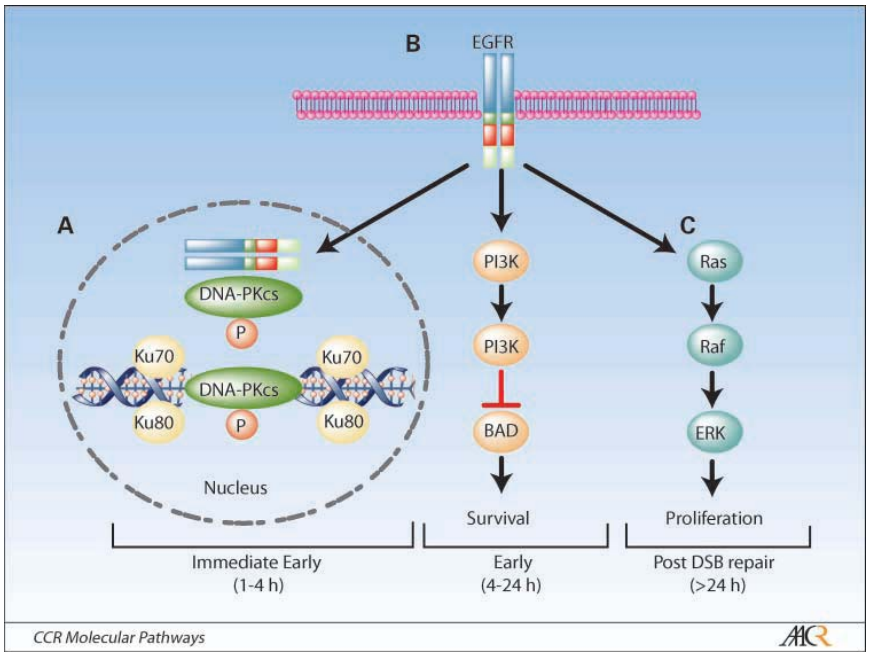

Figure 1.6: A model of EGFR-mediated radioprotection. EGFR mediated radioprotection can be temporally divided into three phases. A, an immediate early phase involves radiation-induced translocation of EGFR and interaction of DNA repair enzyme, DNA-PK. B, a second phase involves the rapid activation of EGFR-dependent PI3K and AKT, which leads to the suppression of DNA damage induced apoptosis before and after cell cycle arrest. C, a third phase involves the activation of EGFR-dependent Ras/Raf/MEK/ERK and STAT pathways that promote rapid cell proliferation. As a result tumor repopulaton occurs (Chen and Nirodi, 2007).

inositol 1,3,5-triphosphate, 1,2-diacylglycerol and calcium, which in turn activates protein kinase C, the MAP kinase, and c-jun NH2-terminal kinase pathway. EGFR mediated intracellular signaling plays a critical role in cell proliferation, cell survival, cell growth, cell migration, tumor cell invasion, and inhibition of apoptosis (Chen and Nirodi, 2007). (Figure 1.6)

Several studies have shown that EGFR is an important determinant of radiation response and that it has a radioprotective function (Akimoto et al., 1999; Bonner et al., 2006; Raben et al., 2005). Based on current evidence, EGFR mediated radioprotection can be divided into three phases: (a) an immediate early response that involves DNA repair, (b) suppression of DNA damage-induced apoptosis before and after cell cycle arrest, and (c) a tumor repopulation step that offers a proliferative advantage to tumors emerging from radiation-induced cell cycle arrest. EGFR directly interacts with DNA-PKcs. EGFR is normally present in the perinuclear space in non-irradiated cells. IR induces a ligand independent translocation of EGFR to the nucleus in a

process that involves free radicals (Bandyopadhyay et al., 1998; Dittmann et al., 2005). Nuclear EGFR binds to the catalytic subunit DNA-PKcs and the regulatory subunit Ku70 of DNA-PK. There is also evidence that radiation induces the export of DNA-PKcs from nucleus into cytoplasm (Huang and Harari, 2000). Interaction of EGFR with DNA-PKcs correlates with radiation-induced DNA-PKcs phosphorylation at Thr2609 which, in concert with six other serine and threonine amino acid residues in DNA-PKcs, controls the disassembly of DNA-PKcs and the physical rejoining of DNA DSBs (Dittmann et al., 2005) (Figure 1.7)

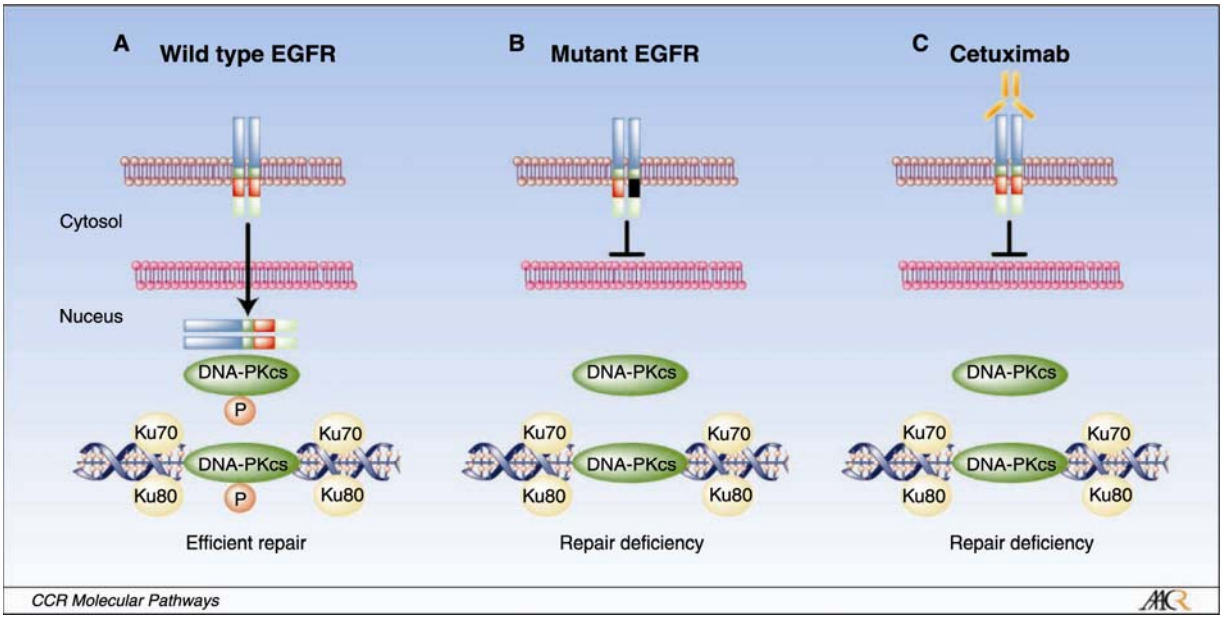

Figure 1.7: Blockade of EGFR-mediated DNA repair. A, in response to ionizing radiation, wild type EGFR translocates to the nucleus and interacts with DNA-PKcs. Radiation induced EGFR nuclear import and DNA-PKcs binding correlates with DNA-PKcs phosphorylation at Thr2609 and DNA repair. B, EGFR forms with somatic mutations in the tyrosine kinase domain are inherently defective in radiation-induced EGFR nuclear import and EGFR-DNA-PKcs interactions. Mutant EGFR abrogates radiation-induced DNA-PKcs phosphorylation at Thr2609 and compromises DNA repair and survival. C, similarly, anti-EGFR monoclonal antibodies exert a radiosensitizing effect through a blockade of EGFR nuclear import, abrogation of EGFR-DNA-PKcs binding, inhibition of DNA-PKcs phosphorylation at Thr2609, and inhibition of EGFR-dependent signaling through the Ras/raf/MEK/ERK and PI3K/AKT pathways (Chen and Nirodi, 2007).

There is evidence that IR has the ability to activate EGFR signaling, and other receptor tyrosine kinases, independently of ligand binding (Bowers et al., 2001). This activation confers a number of protective responses including increased cell proliferation and reduced apoptosis,

predominantly through the stimulation of the PI3K/Akt and Ras/MAPK pathways. Thus, activation of EGFR is believed to counteract the cytotoxic effect of radiation, and to possibly lead to the phenomenon known as "accelerated repopulation", in which the rate of tumor cell proliferation increases during the course of radiotherapy. Radiation induced activation of ATM can down regulate phosphor-ERK1/2 (part of MAPK pathway involved in EGFR signaling) and its downstream signaling via increased expression of MAP kinase phosphatase. The dephosphorylation of ERK1/2 was shown to be independent of EGFR activity and associated with radioresistance (Nyati et al., 2006). Administration of EGF prior to irradiation increases expression of the DNA repair proteins ERCC1 and Xrcc1 in DU145 and LNCaP cells. This up-regulation, which was markedly enhanced during the early response to ionizing radiation, is dependent on EGFR-ERK signaling (Yacoub et al., 2003). Upregulated XRCC1, after administration of EGF, binds the PARP auto-modification domain with high affinity (Schreiber et al., 2006).

1.7. Defining Characteristics of IR-induced DNA damage

1.7.1. Linear energy transfer (LET)

IR carries enough energy so that during the interaction with an atom, bound electrons are removed causing the atom to become ionized and thus electrically charged. Gas phase ionization potentials of molecules range between 8 and 13 eV. In solution the ionization potential can be lower by up to about 3 eV. There are several forms of electromagnetic radiation like heat waves, radio waves, infrared light, X-rays etc, but they all differ in frequency and wavelength and thus the energy of the constituting photons. Higher wavelength and lower frequency photons have lower energy compared to lower wavelength and higher frequency photons. Only the high frequency portion of electromagnetic spectrum, which includes X-rays and γ-rays is ionizing. Ionizing radiation is of two types, (1) electromagnetic wave, in which energy is carried by photons in oscillating electric and magnetic fields traveling through space at the speed of light. (2) Particulate radiation, consisting of atomic or subatomic particles (electrons, protons, etc.), which carry energy in the form of kinetic energy, or mass in motion.

LET is a measure of the energy transferred to matter as an ionizing particle travels through it.

Typically, this measure is used to quantify the effects of IR on biological specimens or electronic devices. LET is closely related to stopping power. Which is the energy loss per unit distance, dE/dx. It describes the energy loss of the particle. LET focuses upon the energy transferred to the material surrounding the particle track, by means of generation of secondary electrons. Since one is usually interested in energy transferred to the material in the vicinity of the particle track, one excludes secondary electrons with energies larger than a certain value. Since electrons of high energy have a large range, this energy limit effectively excludes electrons that travel far from the primary particle track. Hence, LET (also called "restricted linear electronic stopping power") is defined by

$$L_\Delta = \frac{dE_\Delta}{dx}$$

Where dE_Δ refers to the energy loss due to electronic collisions minus the kinetic energies of all secondary electrons with energy larger than Δ. When Δ approaches infinity, there can be no electrons with higher energy and LET becomes identical to the linear electronic stopping power.

When many ionizations occur in a relatively small volume, as when cells are exposed to high LET radiation, a multitude of damages can occur in a small region of the DNA molecule generating highly complex lesions. Such lesions may contain a multitude of DSBs and many other forms of DNA damage, which are discussed next. The ability of IR to induce this form of lesions, i.e. the DSB, is the cause of its unique effects at the cellular level. (Figure 1.8)

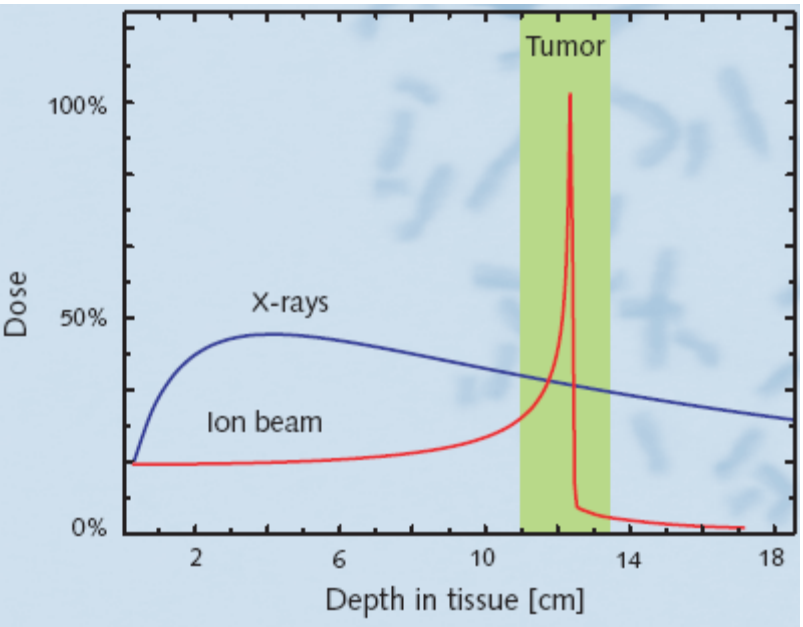

Figure 1.8: Difference in energy deposition pattern between high and low LET radiation. At cellular level, the goal of radiotherapy is to cause irreparable damage to the genetic material of the cancer cells, ultimately causing their destruction. The biological effectiveness of ion radiation in introducing genetic damage into the cancer cells is significantly greater than that of X-rays because it deposits more energy at a certain depth in the tissue making the specific targeting of the tumor possible. (GSI Darmstadt information brochure)

1.7.2. Complex lesions induced by IR

IR actually causes a range of different DNA lesions in cells. Base lesions, AP sites (apurinic or apyrimidinic), modification of sugars, single-strand breaks (SSBs) or double strand breaks (DSBs) are formed in the DNA by either direct, or by indirect effects mediated by the production of water radicals. In addition to base damage IR induces an oxidized sugar moiety in the DNA, which is either immediately modified to generate SSBs, or it is oxidized later and converted to delayed SSBs. In addition to the prompt and delayed breaks induced by radiation, additional SSBs are formed during the repair of base damage. These enzymatically induced SSBs can combine with other SSBs to generate DSBs (Wallace, 1998).

Two or more DNA lesions of the same or different nature produced in close proximity to each other on opposite DNA strands (bistranded lesion), generally within one or two helical turns of the DNA molecule, are considered complex or clustered lesions. The repair of such complex lesions is thought to be more difficult than that of simple lesions. It is therefore commonly

believed that such complex lesions contribute to the adverse effects of radiation disproportionally to their yields.

Theoretical and experimental studies suggest that the induction of clustered DNA lesions is the result of single tracks depositing energy at high LET and therefore generating many ionization events in a small volume. Clustered lesions can contain in addition to SSBs, oxidized base lesions (oxopurines and oxopyrimidines: oxobases) and AP sites (Hada and Georgakilas, 2008). The frequency of these clustered damage classes is comparable to that of frank DSBs; among all complex DNA lesions induced by IR, DSBs make up only 20% with other forms of clustered damage constituting the remaining 80% (Sutherland et al., 2000).

Additional levels of damage complexity are conceivable and may contribute to the generation of DSBs that are particularly difficult to repair. These include, in addition to base damage in the proximity of a prompt DSB also multiple DSBs induced only few (10-1000) bp apart. Finally, we will see below that chemically unstable sugar damage induces delayed DSBs through the chemical conversion of these lesions to SSBs.

1.7.3. Principles of measurement of clustered DNA lesions

There are several approaches for the detection of closely opposed oxidative DNA lesions in DNA isolated from mammalian cells, and DNA like that of T7, λ-DNA or supercoiled plasmid DNA. A unique approach for quantifying these types of bistranded damage in human cells is by using DNA repair enzymes isolated from E.coli and initially characterized by Wallace (Sutherland et al., 2000). Repair enzymes like DNA glycosylases and AP endonucleases participate in base excision repair (BER) and will also function *in vitro* on isolated DNA carrying a clustered lesion. Processing of the lesion will cleave the DNA strand and will generate a SSB in each strand. In this way a DSB will be generated from a processed cluster. Nfo or hAPE1 (Endonuclease IV) recognize mainly AP sites (abasic sites), Fpg or hOGG1 recognize oxopurines and hNth or endonuclease III recognizes mainly oxopyrimidines.

In addition to the use of above repair enzymes as damage probes, polyamines (putrescine, spermine, and spermidine) are useful for the detection of very closely spaced AP sites (1-5 bp apart), which are poorly detected by Nfo AP endonucleases (Georgakilas, Bennett, and

Sutherland, 2002). In contrast to AP endonucleases, polyamines cleave at the 3` side of the AP side. They also cleave AP sites opposite a SSB, which are resistant to cleavage by some AP endonucleases. The latter process will again result in a DSB.

1.8. IR induced heat labile sites and their contribution to DSB induction

IR induces damage to all components of the DNA molecule and much attention has been given to base damage. However, recent observations point out the importance of a sugar oxidative degradation pathway, which in most cases lead to strand break formation after exposure to IR or to radiomimetic drugs. It is well documented that some radiomimetic compounds oxidize rather specifically different positions of the 2-deoxyribose. Compounds with these properties include the antitumoral drugs bleomycin, chalicheamicin and neocarzinostatin. Bleomycin specifically oxidizes the 4-position of 2-deoxyribose, whereas chalicheamicin attacks preferentially the 4`- and 5`-positions, and neocarzinostatin is implicated in 1`-.4`- and 5`-oxidation reaction (Regulus et al., 2007). Abstraction of hydrogen at 4'-position of the deoxyribose moiety of double stranded DNA leads to concomitant formation of a strand break and a reactive aldehyde. This aldehyde is able to react with the vicinal cytosine bases and to generate an interstrand cross link. Some of these sugar modifications, however, do not cause SSBs immediately. Rather they generate an interruption of the phosphodiester bond after additional chemical processing that is influenced by the temperature at which the DNA is maintained. These sites are known as heat labile sites (HLSs) and have been extensively investigated here as they are a relevant source of DSBs.

1.8.1. Measurement of prompt DSBs in mammalian cells

In higher eukaryotes, measurement of DSBs is confounded by the large size of the DNA molecules comprising their genome. Commonly used physical methods of DSB detection relying on direct sizing of DNA molecule, such as neutral sucrose gradient centrifugation, neutral filter elution, the comet assays and pulsed-field gel electrophoresis (PFGE), require protein free DNA. Therefore, a lysis step that can be performed at different temperatures and that for PFGE has been standardized to 50°C (Blöcher and Kunhi, 1990; Schwartz and Cantor, 1984) is included in the majority of protocols.

The quality of lysis generally improves with increasing temperature between 20-50°C and is

critical not only to the magnitude of the signal measured but also to the functional dependence of this signal on radiation dose. Thus, in neutral filter elution, the shape of the dose-effect curves obtained using incomplete lysis protocols (Okayasu and Iliakis, 1989; Okayasu and Iliakis, 1991) suggest nonlinear induction of DSBs. On other hand curves obtained after lysis at elevated temperatures are compatible with the independently documented linear induction of DSBs with dose (Okayasu and Iliakis, 1989; Okayasu and Iliakis, 1991).

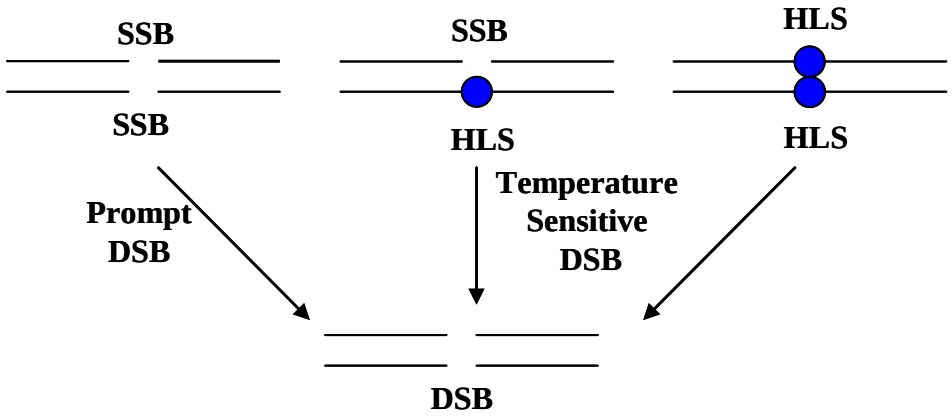

Figure 1.9: Prompt and temperature sensitive delayed DSB.

Although, incubation at high temperatures clearly improves lysis, it can also contribute indirectly to the generation of DSBs in irradiated DNA. Indeed, the γ-ray yield of DSBs in a dilute SV40 DNA solution irradiated at 2°C increased twofold when the gel electrophoresis assay was run at room temperature and quadruples after overnight incubation at 37°C (Jones, Bowell, and Ward, 1994). Similar increase in the yields of DSBs is seen after incubation of low LET-irradiated DNA at 50°C (Stenerlöw et al., 2003) but, interestingly not after exposure to high LET radiation (Yokoya et al., 2003). This increase in the yield of DSBs is thought to derive from the hydrolysis at elevated temperature of radiation induced oxidative lesions in the sugar moiety. As discussed above, these lesions initially do not disrupt the DNA sugar-phosphate backbone, but do so and cause SSBs after hydrolysis. Because hydrolysis is accelerated with increasing temperature, these lesions are therefore termed as heat-labile sites. A subset of these lesions are pH sensitive and are detected as alkali-labile sites (Jones, Bowell, and Ward, 1994).

The temperature mediated transformation of heat-labile sites to SSBs can cause DSBs if

additional heat-labile sites or SSBs are present in the opposite DNA strand, a likely event after exposure to IR that has the potential of generate clustered lesions (Georgakilas, 2008; Sutherland et al., 2000). Thus, lysis at elevated temperatures will transform certain lesions into DSBs, which were not present in the cell immediately after IR. Moreover, heat-labile sites and SSBs causing these indirect DSBs may be processed by the cells using repair pathways distinct from those employed for DSBs repair. However, this removal of heat labile sites or SSBs will also eliminate the DSBs they indirectly generate, which the assay erroneously will detect as DSB repair.

Such concerns and the conviction that heat-labile site transformation to DSBs occurs only during high-temperature (50^{o}C) prompted the development of low-temperature lysis protocols for PFGE (Karlsson et al., 2008; Rydberg, 2000; Stenerlöw et al., 2003). The reduced signal measured under low-temperature lysis conditions reduces the yield of DSBs through exclusion of those generated indirectly from HLSs. Repair kinetics measured under low-temperature lysis also showed reduced repair half-times, but the difference was really small in repair proficient cells (Karlsson et al., 2008; Rydberg, 2000; Stenerlöw et al., 2003). However similar experiments were carried out with mutants defective in D-NHEJ, where the same author reported no significant rejoining during the first hours after irradiation (Karlsson et al., 2008; Stenerlöw et al., 2003). This interpretation suggests that there is no DSB repair immediately after IR when D-NHEJ is compromised. Since several laboratories including our own have reported active processing of DSBs in D-NHEJ-deficient cells, (Iliakis et al., 2004; Perrault et al., 2004) it was important to identify the source of the discrepant interpretations. Here, we will show that they derive from the intracellular transformation of HLSs during the repair incubation period to SSBs.

1.9. Heavy ion irradiation facility at the GSI in Darmstadt

The goal of the scientific research conducted at the GSI Helmholtz Centre for Heavy Ion Research is to understand the structure and behavior of matter. The facility was established in 1969. It operates a large, in many aspects worldwide unique, accelerator of heavy-ion beams. Researchers from around the world use the facility for experiments that help point the way to new and fascinating discoveries in basic research. The research program at the GSI covers a broad range of activities extending from nuclear and atomic physics to plasma and materials research to biophysics and cancer therapy. Probably the best-known results are the discovery of six new

chemical elements and the development of a new type of tumor therapy using ion beams. Most relevant for the work described here is the medical radiation beam of heavy ions (^{14}C) that helped to establish the heavy ion therapy of human cancer in Germany. Users of the GSI facility are predominantly non-resident scientists from German Universities.

Ions are charged atoms; they are formed from neutral atoms by adding electrons to or by stripping electrons from their electron shells. Due to their charge, ions can be accelerated and steered by means of electric and magnetic fields. Ion beams have a special physical and biological effect on tissue. Certain forms of cancer can be effectively damaged with these entities while preserving the surrounding healthy tissue (see Figure 8). This is the basis of the new type of ion beam cancer therapy recently developed at the GSI. In addition to covering this very important aspect of research, the facility is also involved in research required for the radiation safety of human space exploration. ^{58}Fe ions dominate the space radiation field and the GSI can provide beams with these ions at comparable energies that can be used to study their biological effects. This research aspect was one focus of the present thesis.

1.10. Aim and Scope of the work

The debate about backup pathways of NHEJ, which our laboratory started over ten years ago, is now a hot topic of DDR (DNA damage response). Numerous studies suggest the alternative use of B-NHEJ whenever D-NHEJ is compromised. This repair pathway is certainly helpful in maintaining gross genomic stability, although it does this with a much higher error rate than D-NHEJ or HRR.

The transition of this repair pathway into the mainstream of genomic stability makes necessary to investigate all essential aspects of its organization and regulation. One aim of the present study was therefore to characterize the cell cycle, as well as the growth state dependence of B-NHEJ. We have used for this purpose pulsed-field gel electrophoresis (PFGE) as a tool to monitor induction and repair of DSBs. Since the function of B-NHEJ was challenged by the idea that it may just be an artifact of the PFGE requirement to carry out lysis at high temperatures which convert HLSs to DSBs, we invested a considerable amount of effort in clarifying this question. The results of these studies advance our understanding of DSB induction in a decisive way. In the

following paragraphs I will briefly present the framework of each aspect of these studies.

1.10.1. Cell cycle dependent fluctuations of B-NHEJ activity

HRR, due to its requirement for template, is restricted to the late S- and G2-phase. NHEJ, due to its template independence, is active throughout cell cycle. It was important to evaluate fluctuations of B-NHEJ throughout the cell cycle. The backup nature of B-NHEJ required that these studies be carried out in D-NHEJ deficient cells. When possible, HRR deficient cells had to be used as well and the results needed to be confirmed in a range of doses up to the lower limit of PFGE, 10Gy.

We used cell sorting methods to generate populations highly enriched in G1 and G2 cells. The results obtained indicate an important contribution of B-NHEJ in the repair of DNA DSBs throughout the cell cycle and showed that it is particularly active during the G2 phase of the cell cycle.

1.10.2. The Growth state dependence of B-NHEJ

We discussed above that EGFR expression correlates with radioresistance to killing and that EGFR directly interacts with DNA-PKcs. These results link growth activity to D-NHEJ. Since HRR is also dependent on growth activity by virtue of its dependence on the sister chromatid that is only present during S (partly) or G2. We inquired therefore whether B-NHEJ is also dependent on growth signaling and growth state. At first we used plateau-phase cells as a model system. We have shown earlier that at this stage of growth, B-NHEJ is compromised. Here, we confirm that the phenotype is general and discuss its possible ramifications for the use of D-NHEJ inhibitors in the treatment of human cancer.

In order to generate a better defined system to study the role of growth factor signaling in B-NHEJ, we standardized a method of serum deprivation using defined media. This system has been used to study the effect of different serum concentrations, as well as individual growth factors and growth factor inhibitors on B-NHEJ.

1.10.3. Determination of B-NHEJ activity by PFGE after exclusion of HLSs

As discussed above, the generation of HLSs by IR and their thermal transformation to DSBs may

confound the interpretation of our results. We have therefore, evaluated the contribution of HLSs in B-NHEJ by adopting a low temperature lysis protocol. In the course of these studies we discovered HLS lability at 37^{o}C, which suggested that the transformation will take place under normal conditions of growth.

2. Materials and Methods

2.1. Material

2.1.1. Laboratory Apparatus

Cell counter	Multisizer™ 3 coulter counter,Krefeld, Germany
Cell Sorter	Epics Altra Beckman Coulter, Krefeld, Germany
Centrifuge	Multifuge 3 S-R , Heraeus, Magdeburg, Germany
Centrifugal Elutriator Centrifuge	Beckman J2-21M centrifuge Beckman Coulter, Krefeld,Germany
Centrifugal Elutriator Rotor	Beckman JE-6 Elutriation Rotor, Beckman Coulter, Krefeld, Germany
CO_2- incubator	Hera Cell 240, Heraeus, Magdeburg, Germany
Flow Cytometer	Coulter Epics XL, Beckman Coulter, Krefeld, Germany
FluorImager	Typhoon 9400, Molecular Dynamics, Germany
Haemocytometer	Thoma, Superior, Germany
Inverted phase contrast microscope	Olympus, JAPAN
Laminar Flow Hood	Hera safe, Heraeus,Magdeburg, Germany
Magnetic striere	MR Hei-Mix L, Heidolph, Schwaback, Germany
Mini centrifuge	Biofuge fresco Heraeus, Magdeburg, Germany
pH-Meter	WTW, InoLab, Weiheim, Germany
SDS PAGE and blotting apperatus	Bio-Rad, Munich, Germany

Sonicator	Sonorex, RK225H, Bandelin, Germany
Water bath	GFL, Germany
weighing Machiens	BP 110 S, Sortorius, Gottingen,Germany
Western Blot imaging system	Versa Doc, Imaging System, Bio-Rad, Munich, Germany
X-Ray machine	GE-Pantak 320KeV, USA

2.1.2. Disposable Elements

0.5 and 1.5ml tubes	Greiner, Frickenhausen, Germany
12ml non-cap tubes	Greiner, Frickenhausen, Germany
15 & 50ml Centrifuge tubes	Greiner, Frickenhausen, Germany
Cell Culture Dishes, Pipettes & Flasks	Greiner, Frickenhausen, Germany
ECL developing kit	GE health care
Gel Blotting Paper	Bio-Rad, Munich, Germany
Gloves	Peha-soft® Satine, Hartmann, Heidenheim, Germany
PVDF menbrane	Amersham Hybond-P PVDF membrane, GE Healthcare

2.1.3. Chemical Reagents

Agarose	Bio-Rad, Munich, Germany
Agarose, Molecular Biology grade	Bio-Rad, Munich, Germany
Albumin, Bovine (BSA)	Roth, Karlsruhe, Germany
Bromophenol Blue	Sigma-Aldrich, Steinheim, Germany
DAPI	Sigma-Aldrich, Steinheim, Germany
DMEM	Gibco™ , Invitrogen, Karlsruhe, Germany
DMSO	Sigma-Aldrich, Steinheim, Germany
DTT	Roth, Karlsruhe, Germany
EDTA	Roth, Karlsruhe, Germany
Ethanol	Sigma-Aldrich, Steinheim, Germany
Ethidium Bromide	Roth, Karlsruhe, Germany
FBS	PAA, Cölbe, Germany
FBS	Biochrom, Berlin, Germany
FBS	Gibco™ , Invitrogen, Karlsruhe, Germany
Glycerol	Roth, Karlsruhe, Germany
Glycine	Roth, Karlsruhe, Germany
Isopropenol	Sigma-Aldrich, Steinheim, Germany
KH_2PO_4	Roth, Karlsruhe, Germany
KOH	Roth, Karlsruhe, Germany

lactic Acid	Sigma-Aldrich, Steinheim, Germany
Low Melting Agarose	Roth, Karlsruhe, Germany
Mc Coys`s	Sigma-Aldrich, Steinheim, Germany
MEM	Gibco™ , Invitrogen, Karlsruhe, Germany
NaCl	Roth, Karlsruhe, Germany
NaHCO3	Roth, Karlsruhe, Germany
Penicillin	Sigma-Aldrich, Steinheim, Germany
Propidium Iodide	Sigma-Aldrich, Steinheim, Germany
Protease	Sigma-Aldrich, Steinheim, Germany
RNase	Sigma-Aldrich, Steinheim, Germany
Rotiphorese Gel 30	Roth, Karlsruhe, Germany
See Blue Plus2 Prestained protein ladder	Invitrogen, Karlsruhe, Germany
Streptomycin	Calbiochem, Invitrogen, Karlsruhe, Germany
TEMED	Sigma-Aldrich, Steinheim, Germany
Tris	Roth, Karlsruhe, Germany
TritonX-100	Sigma-Aldrich, Steinheim, Germany
Trypsin	Biochrom , Berlin, Germany

2.1.4. Antibodies

Table 1: Antibodies used in western blotting analysis

Antibody	MW (kDa)	Type	Manufacturer	Dilution
Primary Antibodies				
DNA Ligase III	100 kDa	Monoclonal	IF3, GeneTex	1:1000
Histone H1	27/29 kDa	Monoclonal	AE-4, Acris	1:2000
PARP-1	116 kDa	Monoclonal	C-2-10, Sigma	1:2000
53BP1	220 kDa	Monoclonal, Hybridoma supernatant	Dr.Thanos Halozonetis	1:20
GAPDH	38 kDa	Monoclonal	Chemion	1:10000
Secondary Antibodies				
Anti-Mouse HRP-linked (from Horse)			Cell Signaling	1:2000
Anti-Rabbit HRP-linked (from Goat)			Cell Signaling	1:2000

2.1.5. Buffers and solutions

Coomassie Brillient Blue R 250

(0.02% Coomassie Brillient Blue R 250, 2% (w/v) Phosphoric acids, 5% Aluminium sulphate , 10% Ethanol)

DAPI solution

(2µg/ml DAPI, 0.1M Tris, 0.1M NaCl, 5mM $MgCl_2$, 0.05% TritonX-100)

Electrode buffer (4X)

(0.1M Tris, 0.768M Glycine ,pH 8.3)

Freezing Solution A

(5mM KH_2PO_4, 25mM KOH, 30mM NaCl, 20mM L (+) lactic acid, 5mM Dextrose, 0.5mM MgCl2, 200mM Sorbitol in Milli-Q H2O)

Freezing Solution B

(5mM KH_2PO_4, 25mM KOH, 30mM NaCl, 20mM L (+) lactic acid, 5mM Dextrose, 0.5mM MgCl2, 200mM Sorbitol in 80% Milli-Q H2O and 20% DMSO)

HEPES buffer

(20mM HEPES, 5mM $NaHCO_3$ resuspended in serum free media)

High Salt Buffer

(1.85M NaCl, 0.15M KCl, 5mM $MgCl_2$, 2mM EDTA, 4mM Tris-HCl, pH 7.5 and 0.5% TritonX-100 just before use)

High Temperature Lysis Buffer

(10mM Tris-HCl, 50mM NaCl, 100mM EDTA, 2% N-lauryl sarcosine (NLS), pH 7.6, and 0.2mg/ml Protease just before use)

Low Temperature Lysis Buffer (ESP buffer)

(2% N-laurylsarcosine, 1mg/ml Protease, 0.5M EDTA at pH 8.0)

PBS

(137mM NaCl, 2.7mM KCl, 10mM Na_2HPO_4, 1.76mM KH_2PO_4, pH 7.4)

PBS-T

(PBS + 0.05% Tween-20)

Resolving Buffer (4X)

(1.5 M Tris-HCl (pH 8.8), 0.4% (w/v) SDS)

RNase Buffer

(10mM Tris-HCl, 50mM NaCl, 100mM EDTA, pH 7.6, and 0.1mg/ml RNase A just before use)

SDS PAGE loading Buffer (1X)

0.125M Tris-HCl (pH 6.8), 2% (w/v) SDS, 10% Glycerol, 100mM DTT, and 0.025% Bromophenol blue)

SDS running Buffer

(1X electrode Buffer + 0.1% (w/v) SDS)

Stacking Gel Buffer (4X)

(0.5 M Tris-HCl (pH 6.8), 0.4% (w/v) SDS)

TBE (0.5X)

(45mM Tris, 45mM Boric Acid, and 1mM EDTA)

TEN Buffer

(10mM Tris-HCl, 2mM EDTA, 50mM NaCl, pH 7.5)

Transfer buffer (1X)

(200mM Glysine, 25mM Tris, 10% Methanol)

Washing Buffer

(10mM Tris-HCl, 50mM NaCl, 100mM EDTA, pH 7.6)

2.2. Methods

2.2.1. Cell lines and cell culture

The following mouse embryonic fibroblast (MEF) cell lines were used for experiments: *p53*$^{-/-}$*/LIG4*$^{+/+}$ (WT), *p53*$^{-/-}$*/LIG4*$^{-/-}$ (kind gift from Dr. F. Alt; (Frank et al., 2000), *p53*$^{-/-}$*/Rad54*$^{-/-}$*/LIG4*$^{-/-}$ (346B), *p53*$^{-/-}$*/Rad54*$^{-/-}$*/LIG4*$^{+/+}$ (347E), *Ku70*$^{-/-}$ (Ouyang et al., 1997), *Ku80*$^{-/-}$, *DNA-PKcs*$^{-/-}$ (PK33N), *Ku80*$^{-/-}$*/DNA-PKcs*$^{-/-}$ (PK80-193A) (kind gift from Dr. David J. Chen). Cells were derived from animals with the corresponding genotype and were employed in our experiments to evaluate the relative contribution of HRR, D-NHEJ and B-NHEJ in different phases of cell cycle and growth state effect experiments. *p53*$^{-/-}$*/LIG4*$^{+/+}$, *p53*$^{-/-}$*/LIG4*$^{-/-}$, 346B, 347E, *Ku80*$^{-/-}$, PK80-193A MEFs were grown in Dulbecco`s Modified Eagle`s Medium (DMEM, Sigma-Aldrich); *Ku70*$^{-/-}$, PK33N cells were maintained in Minimal Essential Medium (MEM, GIBCO) with 10% fetal bovine serum (FBS, BIOCHROM). All the cells were grown as monolayer cultures in growth medium supplemented with penicillin (100 μg/ml) and streptomycin (100 μg/ml), and were incubated at 37°C in a humidified atmosphere containing 5% CO2 and 95% air.

Chinese hamster ovary (CHO) cell lines were cultured in McCoy`s 5A used are, CHO10B4 (WT), *XRCC4* mutant (*xr1*), DNA-PKcs mutant (*irs-20*) (Stackhouse and Bedford, 1993a; Stackhouse and Bedford, 1993b; Stackhouse and Bedford, 1994), DNA-PKcs mutant (*XR-C1-3*) cells. Other culture conditions were as mentioned above. V3 cells are having a mutant and nonfunctional DNA-PKcs. These cells were transfected with several human cDNA of DNA-PKcs bearing different mutations (provided by Dr. Kathryn Meek; (Block et al., 2004)). V3 A5 and V3 A36 cells are corrected by transfection with wt gene but show low and high levels of expression, respectively. V3 GG6 and V3 PQR cells contain a mutation in ABCDE and PQR cluster respectively. V3 ND5 and V3 JKD2 cells are expressing forms of DNA-PKcs mimicking phosphorylated states; V3 ND5 cells have two substitutions with aspartic acid at the extreme N-terminal region, and V3 JKD2 cells have aspartic acid substitutions approximately 1000 amino acid from N-terminus. These cells were also grown in McCoy's 5A with 10% FBS.

M059J cells (kindly provided by Dr. J. Allalunis-Turner) are derived from a human glioma and are DSB-repair deficient due to a frameshift mutation in DNA-PKcs (Allalunis-Turner et al.,

1995). M059K cells are derived from the same tumor but have wild type DNA-PKcs and serve as repair-proficient control.

A DNA-PKcs knockout human colon cancer cell line HCT116 *DNA-PK*$^{-/-}$ was also used. These cells were grown in DMEM with 10% FBS and other growth conditions were as mentioned above.

For experiments, all the human cell lines were passaged every 3 days at 0.8 – 1 million cells in 100 mm culture dishes, and 0.3-0.35 million cells in 60 mm culture dishes. MEFs and CHO cell lines were passaged at 0.4 million cells in 100 mm culture dishes and 0.18 million in 60 mm dishes every 2 days.

2.2.2. Radiation

2.2.2.1. X-ray irradiation (low LET)

Cells were exposed to different doses of X-rays as required by the experimental protocol using a Seifert/Pantak X-ray machine operated at 320 keV, 10 mA with a 1.65 mm Al filter (effective photon energy approximately 90 keV), at a distance of 750 mm for 100 mm dishes and 500 mm for 60 mm dishes, and a dose rate of 1.3 – 3 Gy/min. Dosimetry was performed with a PTB dosimeter and Frick`s chemical dosimetry, which was used to calibrate an in-field ionization monitor. Exponentially growing cells were pre-cooled on ice for 15 min before irradiation, and the temperature of the medium was kept under 4^{o}C. During irradiation, all the dishes were kept on ice to minimize DSB repair.

2.2.2.2. Heavy ion irradiation (high LET)

In order to study the response of complex lesions and their need for B-NHEJ, as well as the induction of HLSs, we used the heavy ion radiation facility at GSI Darmstadt. Here in the heavy-ion synchrotron SIS, ion beams are accelerated up to 90 percent of the speed of light in the course of several hundred thousand revolutions. In two different experiments we used Fe and Ni ions of 1 GeV energy with corresponding LET of 150 keV/μm.

2.2.3. The GSI Accelerator Facilities

The GSI operates as a unique heavy-ion accelerator system. At this accelerator, it is possible to generate ion beams of all the elements up to the heaviest, uranium, in any state of electric charge, and to accelerate these beams to nearly the speed of light. The facility can also be used to create and accelerate beams of radioactive nuclei (see Figure 2.1). It consists of the linear accelerator UNILAC, which is a 120-meter long linear accelerator that accelerates ions up to 20 percent of the speed of light (Figure 2.2). In the heavy-ion synchrotron, SIS, the ion beam is further accelerated up to 90 percent of the speed of light in the course of several hundred thousand revolutions. SIS is the facility we used at the GSI, where we irradiated our samples with accelerated Fe and Ni ions at 1 GeV energy (Figure 2.3).

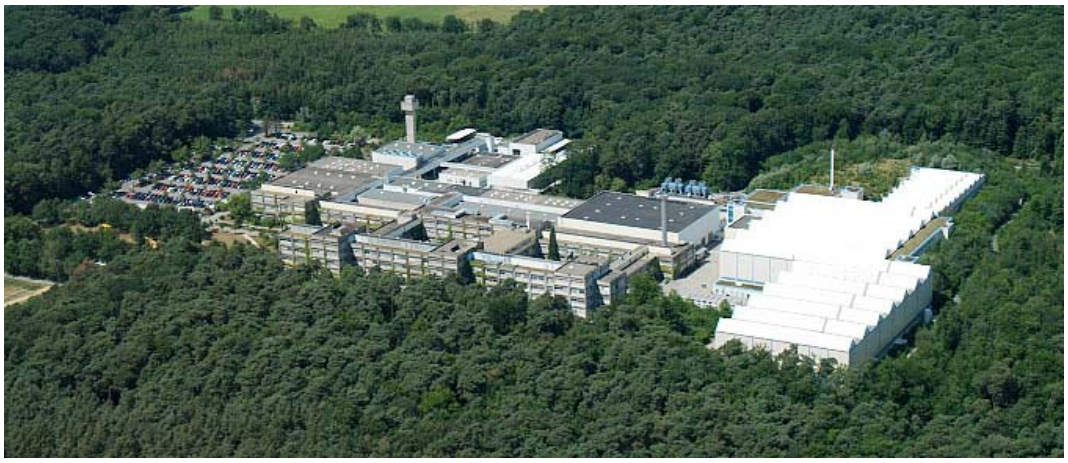

Figure 2.1: Accelerator facility at GSI, Darmstadt

Figure 2.2: UNILAC facility at GSI, Darmstadt

Figure 2.3: SIS facility at GSI

2.2.4. Cell sorting methods

2.2.4.1. Cell cycle analysis by flow cytometry

Propidium iodide binds to DNA proportional to its mass. Cell cycle distribution was assessed by measuring propidium iodide (PI) fluorescence on a flow cytometer. Cells were washed with cold PBS and trypsinized at 37°C for 5 min. Single cell suspensions were prepared in 5ml cold fresh media. About 1 million cells were collected and centrifuged at 1500 RPM, 4°C for 5 min. The cell pellets were washed with cold PBS and fixed in 70% ethanol at -20°C overnight. Supernatant was removed by centrifugation at 1500 RPM for 5 min. Pellets were washed with cold PBS and incubated in PBS containing PI (40 µg/ml) (Sigma-Aldrich) and RNase (62 µg/ml) (Sigma-Aldrich) at 37°C for 30 min in dark. Samples were measured on a flow cytometer (COULTER EPICS XL, BECKMAN COULTER) according to established protocols. Typically, 15,000 cells per sample were counted and the single cell population was gated to obtain standard histograms. Histogram files (*.HST) were generated by counting the frequency of the cell with same PI signal intensity.

The fractions of cells in the different phases of the cell cycle were calculated using the Wincycle® software. HST files were loaded into the Wincycle®. The parameter "S-phase growing order" was carefully chosen between 0, 1 or 2, until the prediction model fitted the histogram shape. Cell cycle distributions were automatically calculated.

2.2.4.2. Cell freezing

For repair experiments, after irradiation on ice, growth medium was replaced with fresh pre-warmed growth medium (42^{o}C), in order to quickly restore the temperature of the cells to 37^{o}C, and dishes were returned to 37^{o}C. Cells were processed for DNA DSBs repair analysis at various times thereafter. At 5 min before completion of the preassigned repair time interval, dishes were washed with ice cold PBS and trypsinized at 37°C for 5 min (thus, completing the pre-assigned repair time interval). After trypsinization, cells were collected in ice-cold medium. All harvesting steps were performed on ice to minimize repair.

At this stage cells are normally processed for pulse field gel electrophoresis. Since in the experiments described here cells were sorted before analysis, and because sorting is a time consuming process and only few samples can be sorted per day, cells were frozen using a special protocol that optimally preserves viability. For this purpose, cells were centrifuged at 1500 rpm for 5 min at 4^{o}C, and resuspended in ice-cold PBS. After a second centrifugation step the cell pellet was resuspended in ice cold freezing solution A (KH_2PO_4 5 mM, KOH 25 mM, NaCl 30 mM, L (+) lactic acid 20mM, Dextrose 5 mM, $MgCl_2$ 0.5mM, sorbitol 200mM) at a concentration of $2X10^7$ cells/ml and kept on ice for 3 min. Then an equal amount of the same solution but prepared with 20% DMSO was added and the suspension was gently mixed. Samples were then aliquot and snap frozen at -80^{o}C. Irradiated and non-irradiated cells were prepared in an identical manner. Before sorting, frozen cells were thawed and prepared as described below.

2.2.4.3. Cell staining for sorting

Cells were quickly thawed, resuspended in ice cold growth medium and centrifuged at 1500 rpm for 5 min at 4^{o}C. At this point, when appropriate, an aliquot was kept for measuring DSBs without further manipulations. Remaining cells were resuspended in DAPI solution (DAPI; 4, 6-diamidino-2-phenylindole 2 μg/ml, Tris 0.1M, NaCl 0.1M, MgCl2 5mM, TritonX-100 0.05%) for 30 min in ice, at a concentration of $2X10^6$ cells/ml. Before sorting the cells were gently mixed and passed through a filter to retain cell clumps. Cells prepared from irradiated samples were typically used to evaluate repair kinetics in sorted and non-sorted cell populations, whereas cells from non-irradiated samples were used to determine the background and the dose response curve

for the induction of DSBs.

2.2.4.4. Cell sorting

To obtain cells in the different phases of the cell cycle, cells were sorted using a Beckman Coulter Epics Altra Flow Cytometer equipped with a UV Laser emitting at 388 nm. Sheath fluid and sample were chilled (10^{o}C) during sorting to optimize cell recovery and reduce cell clumping. The temperature of collection chamber was 15^{o}C. Cells were collected into pre-cooled 15 ml polypropylene tubes coated with Dichlorodimethylsilane (MERCK, solution 2% in 1, 1, 1, -trichloroethane) into 0.5 ml fetal bovine serum to facilitate subsequent pelleting. Cell sorting was carried out according to DNA content and cells were obtained in G1 and G2 phases of the cell cycle. In some experiments, we also sorted cells in the S-phase. Sorted populations were reanalyzed to estimate the actual proportion of cells in the desired phase of the cell cycle. Sorted cells were collected by centrifugation at 2500 rpm, 10 min, and counted under the microscope using hemocytometer and processed for asymmetric field inversion gel electrophoresis (AFIGE).

2.2.5. Centrifugal elutriation

1.4 - 2x10^{8} cells were collected and elutriated at 4ºC using a Beckman JE-6 elutriation rotor and a Beckman J2-21M high speed centrifuge at 25 ml/min (Beckman, Krefeld, Germany). Cells were loaded at 3,000 rpm, and 250 ml fractions were collected between 2,500 and 1,500 rpm at 100 rpm steps. In this centrifugal elutriation process cells of smallest size come first and followed by bigger ones, due to this fact G1 cells come out first and then S and at last G2. During elutriation culture media with 1% serum was used. Fractions of highly enriched cells in G1 and G2 were used for experiments. Cell cycle analysis was carried out by flow cytometry as described above.

2.2.6. Asymmetric field inversion gel electrophoresis (AFIGE)

To evaluate induction of DSBs at different radiation doses, i.e. dose response experiment, non-irradiated asynchronous and sorted G1 and G2 phase cells were used. Cells were resuspended in serum-free medium (prepared with HEPES 20mM, NaHCO3 5mM to maintain pH outside the incubator) at a concentration of 6X10^{6} cells/ml and 3X10^{6} cells/ml for G1 and G2 cells respectively. Cells were then mixed with an equal volume of pre-warmed 1% agarose (50^{o}C) (BIORAD. Low Melting Preparative Grade Agarose) to reach a final concentration of 3X10^{6}

cells/ml. This cell suspension was pipette into 3 mm diameter cylindrical glass tubes and allowed to solidify in ice for several minutes. The solidified agarose-embedded cell suspension was extruded from glass tube and cut into 5 mm long blocks (for each time point at least 3 plugs were prepared). Each agarose block contains 0.2 million cells. The blocks were placed in a 60 mm Petri dish with 5 ml cold serum-free medium, and placed on ice. Irradiation was carried out on ice as described above. To evaluate the dose response, cells were exposed to 0, 10, 20, 30 and 40 Gy. Due to technical difficulties in determining the 0 h repair time point, the initial value of the repair kinetics was obtained from the dose response curve. Agarose blocks were placed in lysis buffer (10 mM Tris-HCl , 50 mM NaCl, 100 mM EDTA, 2% N-lauryl sarcosyl (NLS), pH 7.6, and 0.2 mg/ml protease just before use) immediately after irradiation. Blocks in lysis buffer were kept at 4°C for 1 h before incubation at 50°C for 16–18 h. After lysis, blocks were washed with washing buffer (10mM Tris-HCl, 50 mM NaCl, 100 mM EDTA, pH 7.6) while shaking at 37°C for 1 h. Then blocks were treated with RNase A at 37°C for 1 h in a buffer containing 10mM Tris-HCl, 50 mM NaCl, 100 mM EDTA, pH 7.6, and 0.1 mg/ml freshly added RNase A. Because this protocol includes a lysis step at 50^{o}C, we named this protocol as High Temperature Lysis (HTL). A similar protocol was also employed to prepare blocks from the repair kinetics points after sorting.

Asymmetric field inversion gel electrophoresis (AFIGE) was used for the quantification of DNA DSBs, which was carried out in a 0.5% agarose (BIORAD, Certified Molecular Biology Agarose) gel prepared with 0.5 μg/ml ethidium bromide (stock solution 10 mg/ml in water) in 0.5X TBE buffer (45 mM Tris, 45 mM boric acid, and 1mM EDTA). Agarose blocks were loaded into the wells which were sealed with 1% agarose. 1-2 h before starting electrophoresis, the buffer (0.5X TBE) was pre-cooled to 8^{o}C. AFIGE was carried out for 40 h at 8°C using alternating cycles of 50 V (1.25 V/cm) for 900s in the (forward) direction of DNA migration and 200 V (5 V/cm) for 75s in the reverse direction. During this time the temperature of TBE buffer was maintained at 8°C by circulation through an external cooling unit. After completion of electrophoresis, the gel was scanned in a FluorImager (Typhoon 9400; Molecular Dynamics).

Under the electrophoresis conditions employed here, smaller DNA fragment migrate out of the well into lane, while intact chromosomal DNA remains in the gel. To estimate remaining DSBs,

the fraction of DNA released into the lane (FDR) was measured from the EB stained gels in irradiated and non-irradiated samples using the ImageQuant 5.2 software (GE Healthcare). This parameter is defined as the fraction of DNA found in the lane and is calculated by dividing the signal in the lane with the total signal of the sample. It is equivalent to the fraction of unrepaired DNA DSBs in the sample. The FDR measured in non-irradiated cells is termed background and was subtracted from the values of FAR measured in irradiated samples to estimate the net effect of radiation.

When induction of DNA DSBs was measured at different dose of radiation in asynchronous, G1 and G2 phase cells, FDR was plotted against dose to obtain the dose response curve. For all graphs and curve fitting we used the SigmaPlot software.

To account for differences in the dose response curves in the different phases of the cell cycle and between different cell lines and experiments, and in order to facilitate the inter comparison of the results obtained, the repair kinetics are not shown as FDR versus time, but instead as Deq versus time. We used the dose response curves to estimate a Deq from each FDR value. This way of analysis has the additional advantage that it applies well to non-linear dose response curves. The repair kinetics curves were fitted by non-linear regression to calculate the repair half times. In general two components were assumed to exist in the repair curves and the fitting algorithms were selected accordingly

2.2.7. Methods to obtain plateau phase culture

2.2.7.1. Normal growth into a plateau-phase

In order to obtain plateau-phase cultures, MEFs and CHO cells were seeded at 0.18 million/60 mm tissue culture dish, 48 h later exponentially growing cells were harvested and 96 h later cells had reached the plateau-phase of growth. Human cells like M059K were grown for different periods of time to obtain cells in the different stages of growth. Distribution of cells through out the cell cycle was determined by flow cytometry as described above.

2.2.7.2. Artificially generated non-growing cells

To obtain non-growing cells in well defined conditions, MEFs were seeded at 0.4 million in 60

mm dishes. After 24 h growth medium was removed and cultures were washed with pre-warmed PBS at 37°C and replenished with pre-warmed medium without serum for 24 h. Subsequently, cells were irradiated and repair kinetics measured. In certain experiments the duration of serum deprivation varied between 4, 8, 16, and 24 h.

In some experiments serum deprived cells were treated again with different concentrations of serum 1 h before IR. Media containing different amounts of serum were added and repair kinetics obtained.

2.2.8. Clonogenic survival assay

Cell radiosensitivity to killing was determined by the clonogenic survival assay. Exponential and plateau-phase cells were irradiated at room temperature and trypsinized immediately at 37ºC. Cells were seeded into 60 mm dishes in duplicate, at various densities aiming approximately 100 colonies /dish. After an incubation period of up to 1 week, cells were stained with crystal violet and colonies of >50 cells were counted.

2.2.9. Methods to monitor Heat Labile Sites (HLSs)

2.2.9.1. Low temperature lysis

Cells were cultured, irradiated and agarose blocks with cells prepared as mentioned above in the sorting protocol. After preparation of blocks, lysis was carried out by a special two step protocol at low temperature to prepare naked chromosomal DNA without transformation of HLSs into SSBs (Karlsson et al., 2008; Stenerlöw et al., 2003). The plugs with cells were then transferred to 10 block volume of ESP lysis buffer at 4°C (2% N-laurylsarcosine (MERK), 1 mg/ml protease (Sigmal-Aldrich, all diluted in 0.5 M EDTA at pH 8.0) and incubated at 4°C for 24 h. After completion of the first step, ESP buffer was replaced with 20 block volumes of high-salt buffer (1.85 M NaCl, 0.15 m KCl, 5 mM $MgCl_2$, 2 mM EDTA, 4 mM Tris, 0.5% Triton X-100, pH 7.5; Triton X-100 was added just before use) and incubated overnight at 4^oC. Agarose blocks were washed 2X 1 h in 0.1 M EDTA and 1X 1 h in 0.5X TBE at 4°C prior to electrophoresis. The blocks were then loaded into wells in a chilled (4°C) agarose gel (BIORAD, Certified Molecular Biology Agarose) and placed in a PFGE unit. Other steps like scanning and analysis were same

as described above.

2.2.9.2. Measurement of induction of HLSs induction into DSBs at different temperature

In this experiment, 100 - 150 million cells were collect after trypsinization and prepared in agarose block as described above. Agarose blocks with cells were placed in HEPES media and were irradiated. Blocks were irradiated on ice to prevent repair. After irradiation blocks were lysed using LTL and washed 2X 1 h with TEN buffer (10mM Tris-HCl, 2mM EDTA, 50mM NaCl, pH 7.5). Blocks were distributed in individual tubes with TEN buffer (4 blocks for each tubes) and then individual tubes were placed at different temperatures in the range between 4^{o}C, 10^{o}C, 20^{o}C, 37^{o}C, or 50°C for 1, 2, 4, 8, 12, 24, or 48 h. After completion of this incubation blocks were washed 1x 1 h with 0.5X TBE, and loaded on pre-cooled agarose gel for PFGE.

In other experiments, agarose blocks were prepared, lysed using LTL and washed 2X 1 h with TEN buffer. Just before irradiation all blocks were transferred in 60 mm culture dishes filled with ice cold TEN buffer and irradiated on ice. After lysis, blocks were aliquoted in different tubes filled with TEN buffer and treated at different temperatures, as required by the experimental protocol. Then, blocks were washed 1X 1 h with 0.5X TBE and placed into the wells of a pre-cooled agarose gel.

2.2.10. Electrophoresis and Immunoblotting

2.2.10.1. Cell extracts preparation and electrophoresis

Cells were collected and were washed twice with cold PBS. Cells were mixed with 1X SDS-PAGE loading buffer (0.125M Tris-HCl (pH 6.8), 2% (w/v) SDS, 10% Glycerol, 100mM DTT, and 0.025% Bromophenol blue). Samples were denatured at 95°C for 5 min and cooled down on ice for 5 min, and sonicated for 2-3 pulses. Samples were centrifuged at 3000 RPM for 15 sec before loading. SDS-PAGE mini gels were cast (Mini-PROTEAN Tetra Cell, BIO-RAD) by following the instructions of the manufacturer. Proteins were resolved in gels with different concentrations according to their sizes; for example 15% gel for proteins smaller 50 kDa, 12% for proteins between 50-100 kDa, 10% for proteins between 100-200 kDa, and 8% for proteins larger than 200 kDa. Samples were loaded and run at constant voltage (150 V) for 1 to1.5 h

(depends upon size of protein) at RT.

2.2.10.2. Immunoblotting

After electrophoresis, gels were removed from the cassette and briefly rinsed with MQ water. PVDF membranes (GE Healthcare) and the blotting paper (BIO-RAD) were cut to the desired size. PVDF membranes were pre-soaked in 100% methanol for 1 min and rinsed in MQ water for 15 min. PVDF membranes, blotting paper and the transfer unit sponge were equilibrated in 1x transfer buffer (Glysine 200 mM (ROTH), Tris 25 mM (ROTH), 10% Methanol (Sigmal-Aldrich) at 4°C for at least 30 min. The gel, blotting papers, sponge and PVDF membrane were assembled and loaded into an electro-transfer unit (Mini Trans-Blot Electrophoretic Transfer Cell, BIO-RAD) according to the instructions of the manufacturer. Wet electro-transfers were run at 100 V, 4°C for 1 h.

After completion of transfer, the unit was disassembled and the side of the membrane on which proteins were transferred was marked. PVDF membranes were briefly rinsed with PBST (PBS + 0.05% Tween-20) and blocked in blocking buffer (PBS + 0.05% Tween-20 + 5% milk (ROTH) at RT for 1 h with gentle agitation. Primary antibodies, for DNA-Ligase III (1F3, GTX70143 GeneTex), PARP-1 (C-2-10, P-248, Sigma), Histon H1 (AE-4, Bm465, Acris), and 53BP1 antibody kindly provided by Dr. Thanos Halozonetis. Antibodies were diluted in blocking buffer 1:1000, GAPDH (Mab374, CHEMION), 1:20,000. Membranes were incubated with primaries antibodies at 4°C overnight with gentle agitation. The secondary antibodies, such as mouse IgG-HRP (Cell Signaling), rabbit IgG-HRP (Cell Signaling) were diluted 1:2000 in blocking buffer. After removing primary antibodies and washing with PBST (3x 10 min), membranes were incubated with secondary antibodies at RT for 1 h. After washing with PBST (3x 10 min), the membranes were ready for development. The ECL developing solution (GE Healthcare) was prepared according to the instructions from the manufacturer and evenly distributed on the side of the membrane on which the proteins were transferred. After 1 min incubation at RT in the dark, images were obtained using the molecular imager VersaDoc MP 4000 System (BIO-RAD).

3. Results

3.1. Cell cycle dependent regulation of B-NHEJ

3.1.1. Experimental design

Flow chart of experiment is outlined in Figure 3.1A. Cells were exposed to radiation and returned to pre-irradiation condition for repair without any manipulation. After completion of repair time interval, cells were collected and prepared for sorting. For this purpose cells were suspended in DAPI, a DNA stain. This allows the differentiation of cells on the basis of their DNA content into different phases of the cell cycle. Exponentially growing cells were gated for selection of G1 and G2 cells during sorting. All steps were carried out on ice to prevent further repair.

After staining, cells were sorted and populations enriched in specific phases of the cell cycle collected. After collection, cells were reanalyzed to quantify the degree of selection, centrifuged and prepared for pulsed-field gel electrophoresis. The charging of the cells during sorting increased their tendency to adhere to the collection vessel. Siliconization of the collection tubes before use, as well as their preconditioning with complete growth media and collection in 0.5 ml serum improved cell recovery.

3.1.1.1. Control experiments designed to standardize sorting conditions

Because cell sorting is typically carried out at 5-15^{o}C, it was important to established that cells could not repair while suspended in DAPI solution. Earlier experiments showed that after DAPI treatment repair was completely inhibited at 37^{o}C, as well as 4^{o}C. Thus, suspension of cells in DAPI solution stopped the enzymatic processes involved in DSB rejoining. This was very important because it allowed sorting without concern of the repair, as it requires the long period of time that would have complicated the interpretation of the results obtained.

On the basis of the above control experiments, experiments were carried out in the following manner. Cells were exposed to 10Gy IR, a relatively low dose for PFGE, and collected at 0.5, 1, 2, 4, and 8 h thereafter. At this point cells were stained and sorted. Residual DNA damage was measured in the initial population, as well as in sorted G1 and G2 populations. Non-irradiated

controls were also sorted and used to determine the background (FDR at 0 Gy), as well dose response of asynchronous cells and of sorted cell populations. The combined data obtained allowed the analysis of DSB repair as a function of cell cycle phases. (Figure 3.1B)

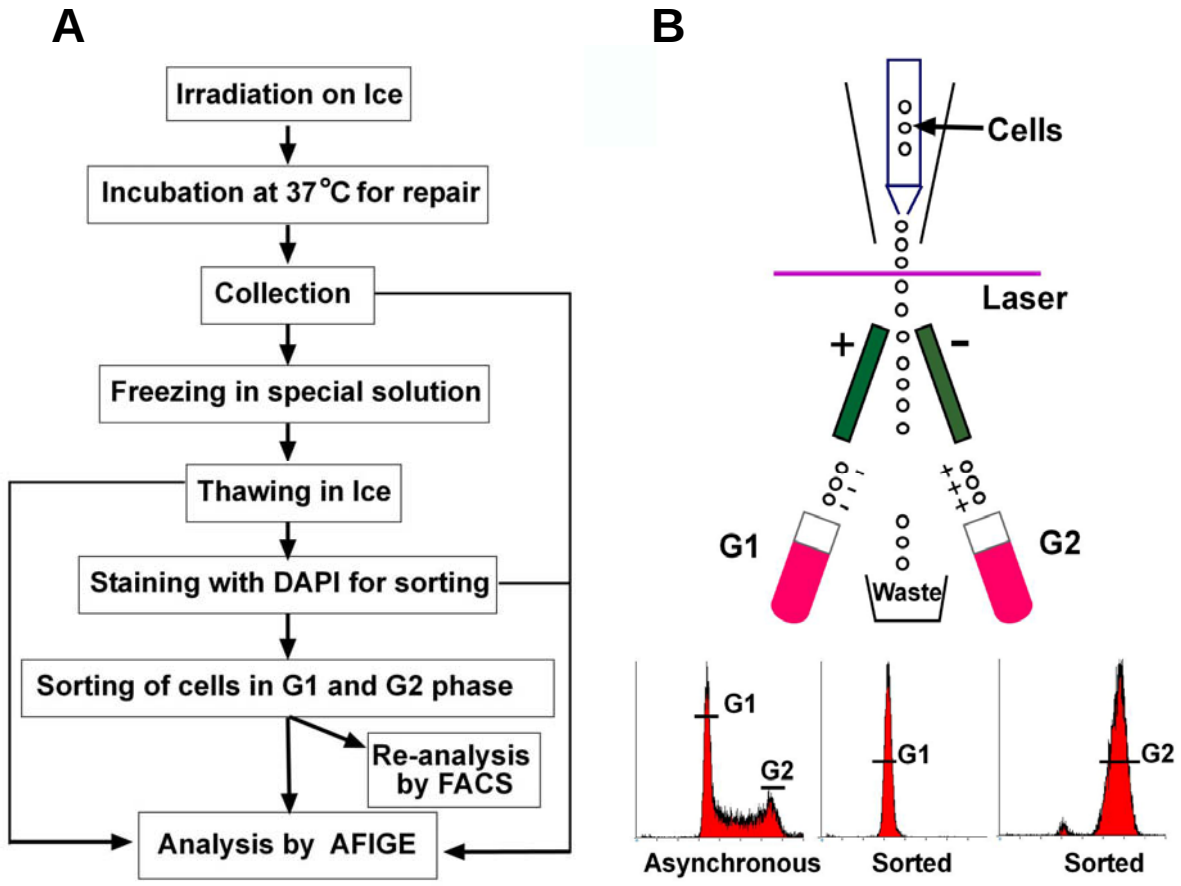

Figure 3.1: Scheme of sorting experiment. Outline of the experimental strategy (A) and schematic diagram illustrating the principle of cell sorting and typical histograms of unsorted as well as G1 and G2 populations (B).

3.1.2. Repair of DNA DSBs throughout the cell cycle in wt MEFs

Repair capacity of mouse embryonic fibroblast (MEFs) was measured in G1 and G2 phase of cell cycle and the results obtained compared to those of asynchronous cells. The results obtained with these cells are described in Figure 3.2. Top left panel shows typical gels obtained with

asynchronous cells exposed to different doses of IR in order to measure the dose response curve, as well as repair kinetics of the same cells after exposure to 10 Gy. The lower gels show repair kinetics of G1 and G2 cells, sorted from irradiated asynchronous populations at the indicated time. While release of DNA from the well into the lane as a function of dose demonstrates increase in the induction of DSBs, the gradual reduction in the amount of DNA released into the lane as a function of time after exposure is a measure of the ability of cells to repair DSBs.

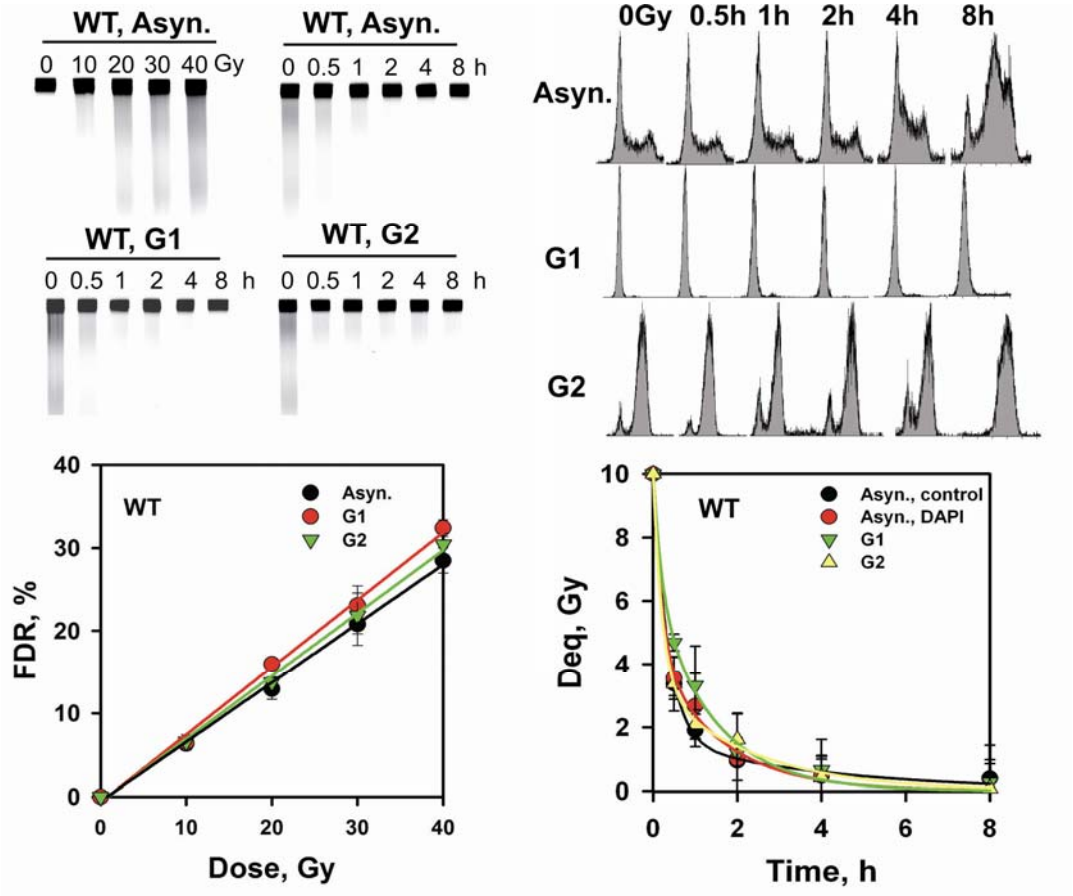

Figure 3.2: Rejoining of IR-induced DSBs in wt MEFs. Repair of asynchronously growing and sorted G1 and G2 MEFs. The left panel shows typical gels evaluating dose response and repair kinetics in different cell populations, as well as the dose response curve used for the analysis of the repair kinetics. Panels on the right show the cell cycle distributions at the time of irradiation or at different times thereafter, as well as quantification of repair kinetics. Plotted are the mean and standard deviation calculated from six determinations in two experiments.

The top right part of the figure shows the flow cytometry distribution of the initial asynchronous

population at various times after exposure to 10Gy, as well as the distribution of the sorted G1 and G2 populations. In asynchronous cells, there is an accumulation of cells in S and possibly in G2-phase at later time points, reflecting the initiation of DNA damage induced blocks in the progression through the cell cycle. Sorted G1 populations typically showed over 95% G1 cells, while sorted G2 phase populations had more than 85% G2 cells, with the remaining cells being mainly in G1 phase.

The lower left panel shows the analysis of dose response curves measured either with asynchronous cells, or with cells sorted in G1 and G2 phase of the cell cycle and plotted as FDR against radiation dose. There is only a relatively small difference in FDR as a function of dose between the different populations tested. This was expected as only S-phase cells are known to show abnormal migration patterns due to the presence of replication forks and bubbles (Iliakis et al., 1991; Metzger and Iliakis, 1991). This is also a reason for asynchronously growing cells to have lower FDR than sorted G1 and G2 cells.

This dose response curve is very important as it allowed the recalculation of the DNA repair experiments from the initially measured FDR versus time plots to dose equivalent (Deq) versus time plots. Plotting of Deq instead of FDR as a function of time has the advantage that it eliminates differences deriving from fluctuations in the migrating characteristics of the DNA. An additional advantage is that it corrects for non-linear dose response curves (not evident in this set of experiment but more obvious with other cell lines and at higher doses of radiation), which can significantly skew the repair kinetics data.

The lower panel of Figure 3.2 shows the analysis of the repair kinetics plotted as Deq versus time for asynchronous cells and sorted G1 and G2 phase cells. The initial values for Deq at t=0 h were derived from the dose response curves, as these measurement were carried out under conditions that ensure nearly complete absence of DSB repair. There is no significant difference in repair kinetics of asynchronous as compared to sorted G1 and G2 cells.

3.1.3. Repair of DSBs throughout the cell cycle in D-NHEJ deficient MEFs

It is well established that cells with mutations in KU70, DNA-PKcs or LIG4 show increased radiosensitivity to killing that is particularly pronounced during the G1 phase of the cell cycle.

These mutations are also associated with defects in the repair of DSBs (Lieber et al., 1997; Takata et al., 1998). Previous studies have implicated DNA Ligase IV and its stabilizing co-factor XRCC4, in D-NHEJ (Grawunder et al., 1998; Lee et al., 2000). However, the role of DNA Ligase IV in DSB rejoining throughout the cell cycle has not been studied. Therefore, we extended our investigations to include MEFs obtained from *LIG4*$^{-/-}$ mice.

Because *LIG4* knockout is lethal, double knockout animals with p53 were generated, *p53*$^{-/-}$/ *LIG4*$^{-/-}$. Here again G1 and G2 populations with a good degree of homogeneity could be sorted. Repair kinetics data shown in the lower left of Figure 3.3 indicate the defect in DSB rejoining in the asynchronous cells and confirm the increased DSB rejoining potential of sorted G2 cells. Perhaps the most important observation made here is that cells in all phases of the cell cycle are

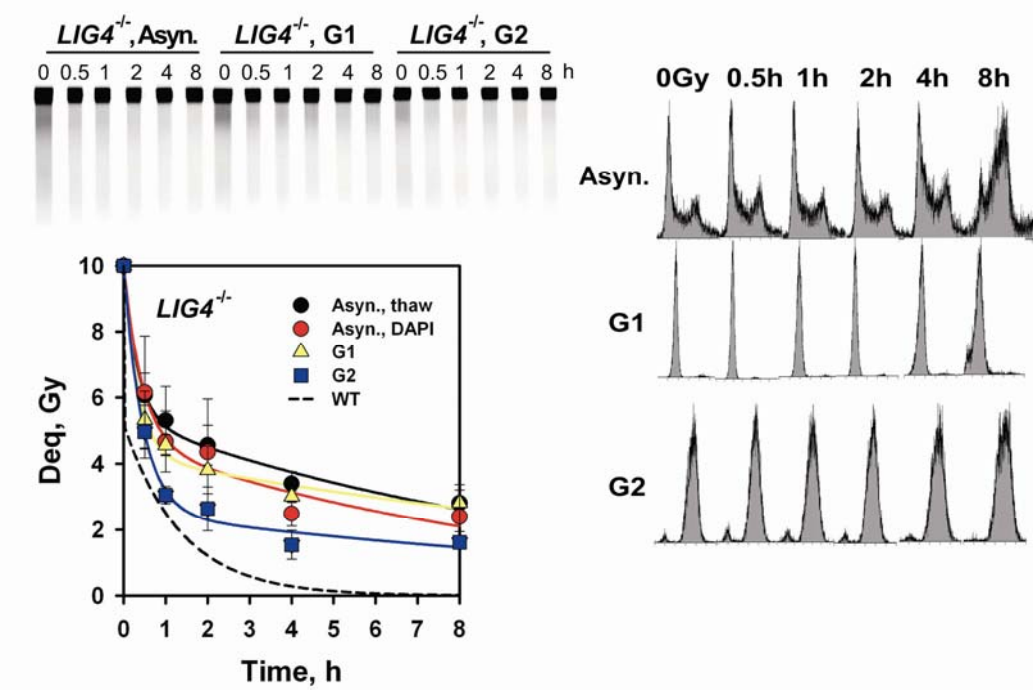

Figure 3.3: Rejoining of IR-induced DSBs in *LIG4*$^{-/-}$ MEFs. Results are obtained from two experiments and six determinations. Other details are as in Figure 3.2.

able to rejoin a large fraction of DSB despite impaired D-NHEJ. This repair of DSBs must be carried out by alternative pathways of repair. Because the most prominent of these candidate pathways is HRR, we next examined DSBs repair throughout the cell cycle in cells with defects in this repair pathway

3.1.4. Repair of DSBs throughout the cell cycle in *Rad54*$^{-/-}$ MEFs

As indicated in Figure 1.1 and as outlined in the Introduction, Rad54 is a key component of the Rad52 epistasis group of genes and is expected to play an important role in HRR. In vertebrates *Rad54* knockout causes radiosensitivity to killing (Bezzubova et al., 1997; Essers et al., 1997) and compromises genomic stability (Mills et al., 2004; Takata et al., 1998). The availability of cells with defective *Rad54* and the anticipated contribution of HRR in DSB repair during S and G2 phases (Essers et al., 1997) together with the results presented in the previous section, prompted us study the repair DSB across the cell cycle.

Figure 3.4 summarizes the results obtained. AFIGE indicated normal ability to repair DSBs and the cell sorting provided G1 and G2 populations with similar purity as for other mutants. The quantitative analysis of the results depicted in the lower left panel of Figure 3.4, shows efficient repair of DSBs in the asynchronous population. In fact no difference can be seen between this mutant and wild type MEFs suggesting that the repair defect is subtle at best. To investigate whether this effect is more pronounced in a specific phase of the cell cycle, we sorted cells in G1 and G2 phase and measured DSB repair. The results included in Figure 3.4 indicate efficient repair of DSBs in both phases of cell cycle, without any indication that cells in G2 phase have reduced repair ability. In fact, here again, G2 phase cells appeared slightly more proficient in repairing DSBs but the difference to asynchronous cells did not reach statistical significance.

These results are surprising as they indicate that *Rad54* deficiency is not accompanied by a measurable defect in DSBs rejoining in asynchronous cells, as well as in cells tested during the G1 and G2 phase of the cell cycle. But *Rad54* mutants show other homologous recombination defects, such as an order of magnitude reduction in gene targeting efficiency. These observations suggest that HRR plays an undetectable role in DSB rejoining even during G2 where it was anticipated to play a significant role. However one could also argue that defects in DSB repair are masked by the NHEJ pathway, especially by the fast D-NHEJ pathway that may be capable of efficiently removing DSBs from the genome whenever HRR is compromised. To examine this possibility we examined a double mutant with defects both in genes implicated in D-NHEJ as well as in HRR.

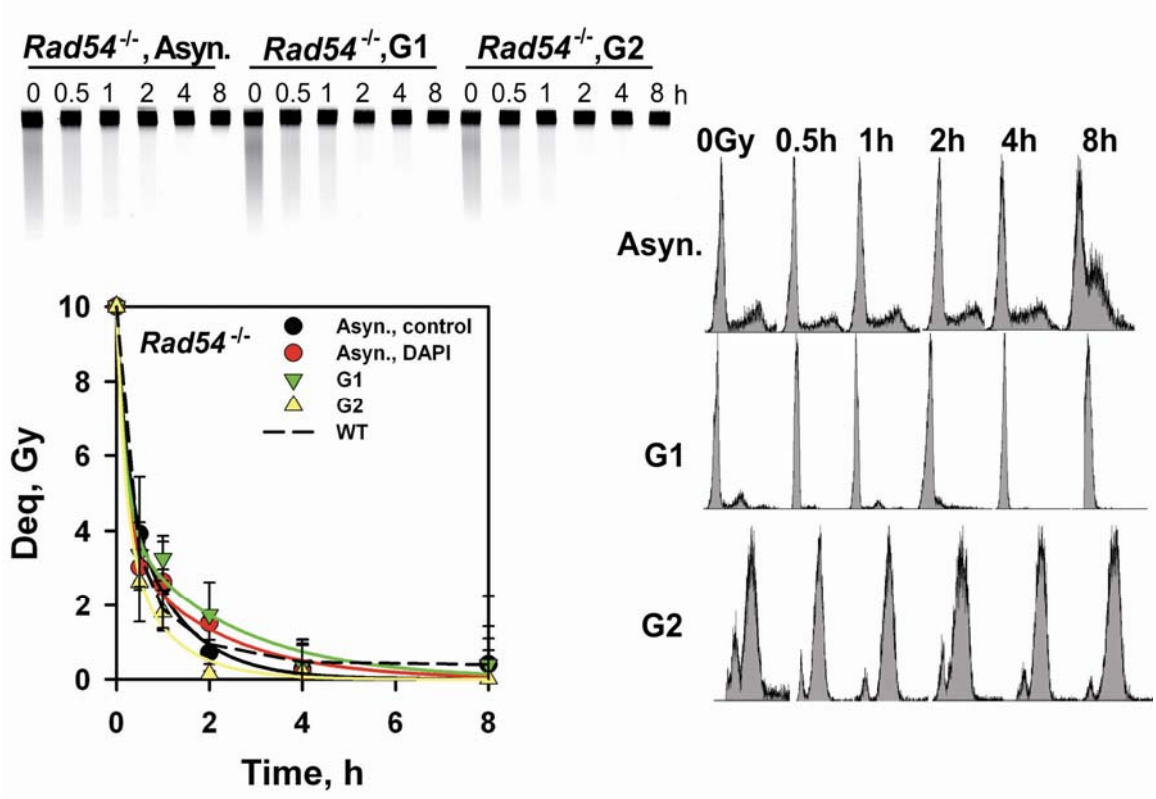

Figure 3.4: Rejoining of IR-induced DSBs in *Rad54*$^{-/-}$ MEFs. Results are obtained from two experiments and six determinations. Other details are as in Figure 3.2.

3.1.5. DSB rejoining throughout the cell cycle in HRR and D-NHEJ deficient MEFs

To investigate the possibility that defects in HRR have no measurable effect in the repair of DSBs in G2 because D-NHEJ complements for the defect associated with Rad54 mutation, we tested a double mutant of MEFs in which both *LIG4* and *Rad54* were knocked out. These cells were also deficient in p53. The repair ability of these cells was evaluated while growing asynchronously, as well as after sorting in G1 and G2 phases of the cell cycle. The results obtained are summarized in Figure 3.5.

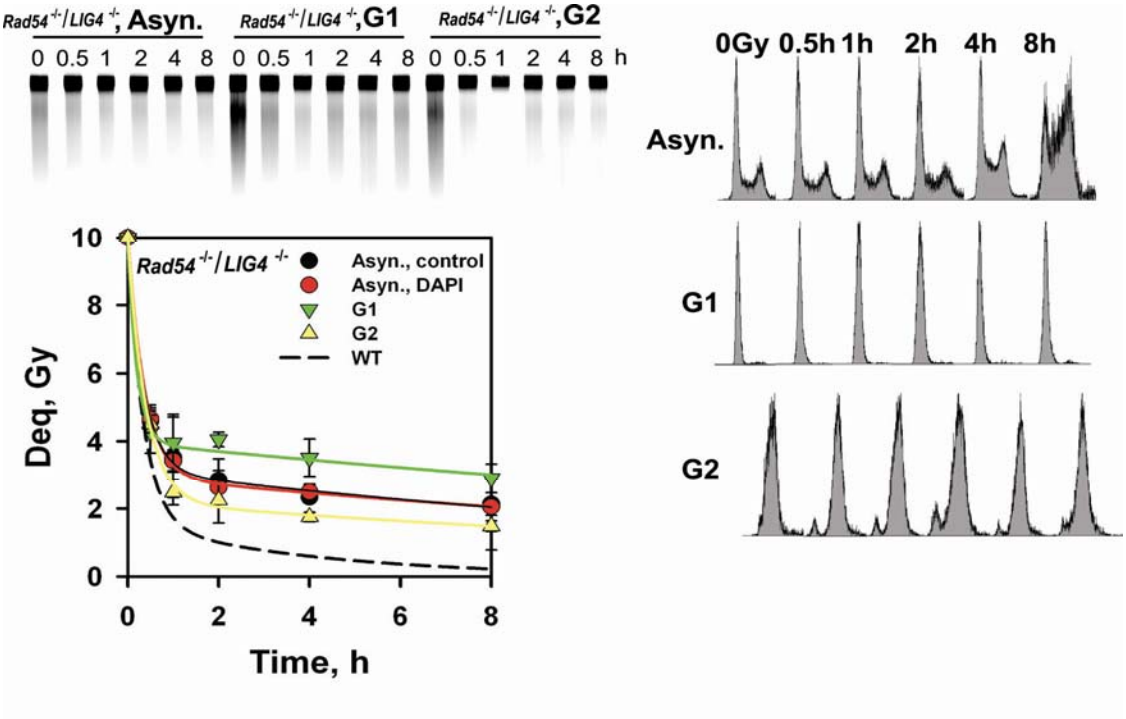

Figure 3.5: Rejoining of IR-induced DSBs in *Rad54*$^{-/-}$*/LIG4*$^{-/-}$ MEFs. Results are obtained from two experiments and six determinations. Other details are as in Figure 3.2.

AFIGE in asynchronous cells showed a defect in DSB repair reminiscent of the one observed in *LIG4*$^{-/-}$ cells. Furthermore, in these cells a G2 arrest was seen that was stronger than that observed either in *LIG4*$^{-/-}$ or in *Rad54*$^{-/-}$ cells. This suggests that a defect in HRR enhances cellular responses to DNA damage such as the checkpoint activated in G2. Asynchronous cells were sorted to obtain populations enriched in G1 and G2 phase cells with purity similar to that of the other mutants used.

Despite stronger G2 arrest in the double mutant, repair of DSBs was similar to that observed in *LIG4*$^{-/-}$ cells. This result was surprising as it indicated that even under conditions where D-NHEJ is compromised, a contribution of HRR cannot be established even in G2, where HRR is expected to be most active.

These observations together with results described in the previous section point to backup pathways of NHEJ as an important component of the overall DSB repair activity. This repair activity appears more pronounced during the G2-phase of cell cycle.

3.2. Marked dependence on growth state of the efficiency of B-NHEJ

D-NHEJ operates efficiently across all phases of the cell cycle (Kim et al., 2005; Metzger and Iliakis, 1991; Rothkamm et al., 2003) and shows only a minor dependence on cell growth state and growth factor signaling. B-NHEJ, on other hand, shows cell cycle dependence and operates more efficiently in the G2 phase of the cell cycle (see above). In addition, B-NHEJ shows a pronounced dependence on growth state (Windhofer et al., 2007). This dependence points to regulatory mechanism and processing determinants that require further elucidation.

The dependence of B-NHEJ on growth conditions has only been demonstrated for *LIG4*$^{-/-}$ MEFs. It was therefore unknown whether it reflects an isolated response, or a more general phenomenon that can be seen across species and in different D-NHEJ mutants. This is not a trivial inquiry as indicated by the observation that different D-NHEJ mutants show qualitatively and quantitatively distinct phenotypes (Bassing and Alt, 2004).

3.2.1. B-NHEJ is compromised in non-cycling D-NHEJ mutants across species

We have previously reported that when *LIG4*$^{-/-}$ cells move into plateau phase of growth, a strong defect in DSB repair capacity is observed. Typical growth curves of all the MEFs, CHO and human cell lines used in these experiments are shown in Figure 3.6. To examine whether the growth state effect on DSB repair is specific to the *LIG4*$^{-/-}$ phenotype, we examined MEFs from *KU70*$^{-/-}$ and *KU80*$^{-/-}$ deficient mice. The DSB repair characteristics of these cells, measured during exponential growth (day 2) and in the plateau-phase (day 4) are summarized in Figures 3.7A and B. Shown in the graphs as dotted line is the repair kinetics of exponentially growing wt MEFs. In addition to representative gels, the figures also include flow cytometry data of the distribution of cells throughout the cell cycle at day 2 and 4. Exponentially growing *KU70*$^{-/-}$ and *KU80*$^{-/-}$ MEFs repair DSBs by B-NHEJ more efficiently than their plateau-phase counterparts do, demonstrating that the growth state dependence of B-NHEJ is not a peculiarity of *LIG4*$^{-/-}$ MEFs.

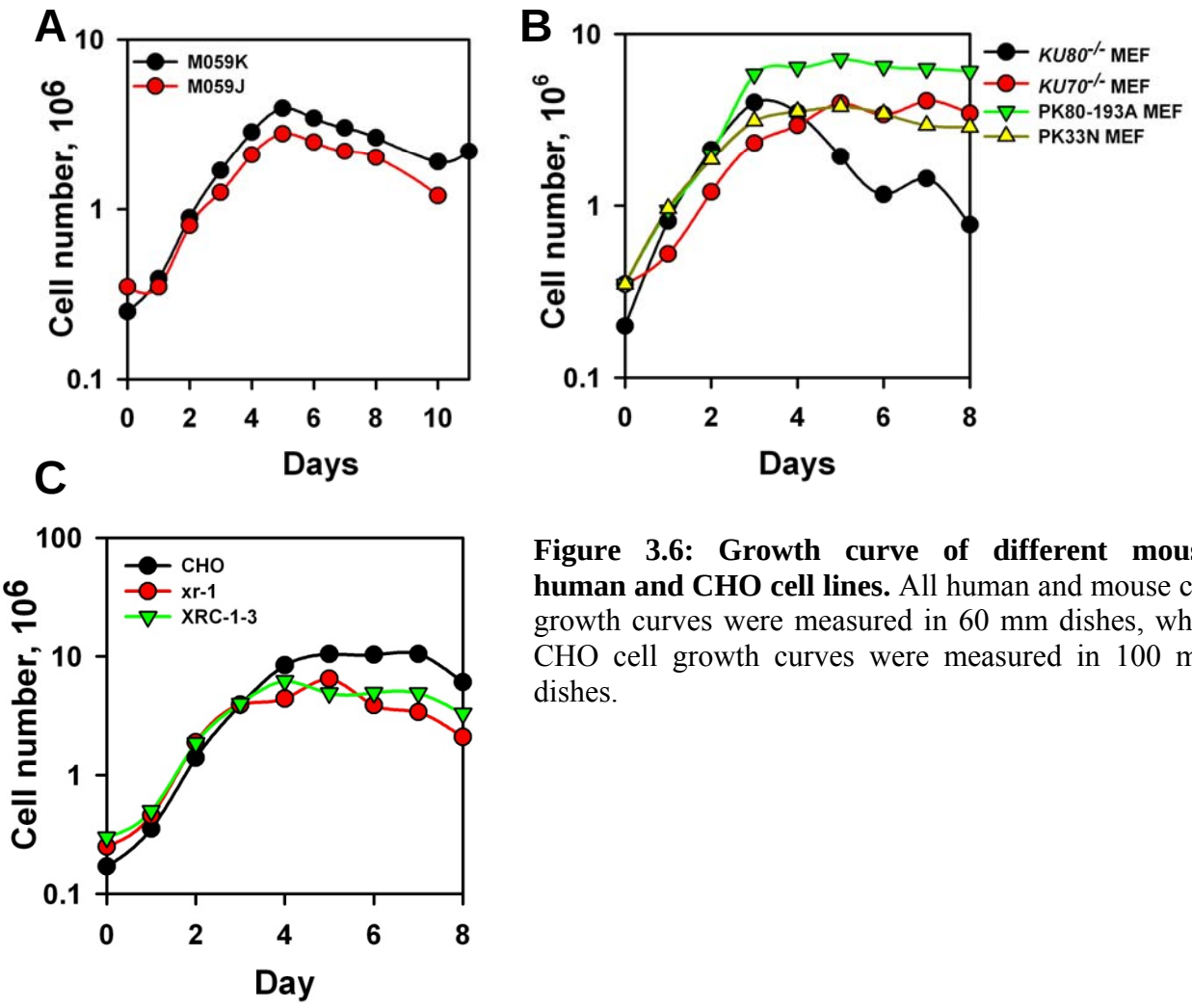

Figure 3.6: Growth curve of different mouse, human and CHO cell lines. All human and mouse cell growth curves were measured in 60 mm dishes, while CHO cell growth curves were measured in 100 mm dishes.

After confirming the persistence of this effect to all D-NHEJ mutants, we speculated the generality of this phenotype among different species. *XRCC4* mutants of Chinese hamster origin were investigated along with their wt counterpart. *XRCC4* mutant *xr1* cells showed a strong reduction in repair capacity in the plateau phase of growth, whereas the wt cells did not show any difference. (Figure 3.8)

Surprisingly, the DNA-PKcs mutant *XR-C1-3* shows similar DSB repair capacity when tested in the exponential or in the plateau-phase of growth (Figure 3.9). Since this response was unexpected, we investigated additional mutants of DNA-PKcs from Chinese hamster, mouse and human. All mutants were showing nearly the same phenotype like *XR-C1-3* cells. There was no

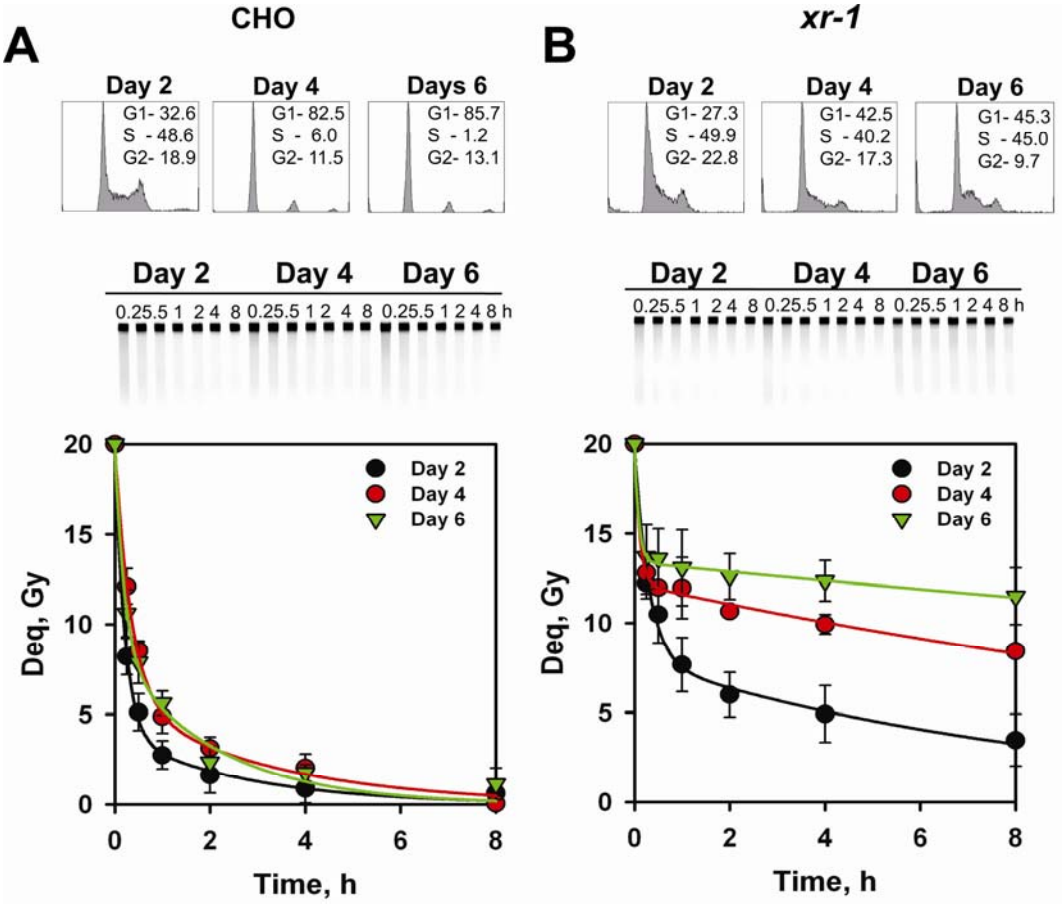

Figure 3.7: DSB repair capacity strongly depends on growth state in *Ku70*$^{-/-}$ and *Ku80*$^{-/-}$ MEFs. Cells were grown for the indicated times, were irradiated and incubated for repair. DSB repair kinetics was measured by PFGE. Results shown are the average of six determinations from two experiments. Flow cytometry histograms, typical gels and repair kinetics of *Ku70*$^{-/-}$ MEFs at day 2 and day 4. The broken line traces the kinetics of wt MEFs (A). As in A, but for *Ku80*$^{-/-}$ MEFs (B).

qualitative difference between DNA-PKcs mutant cell lines like *XR-C1-3, irs20*, M059J cells and DNA- PKcs knock out cell lines like PK33N and HCT116 *DNA-PKcs*$^{-/-}$ cells.

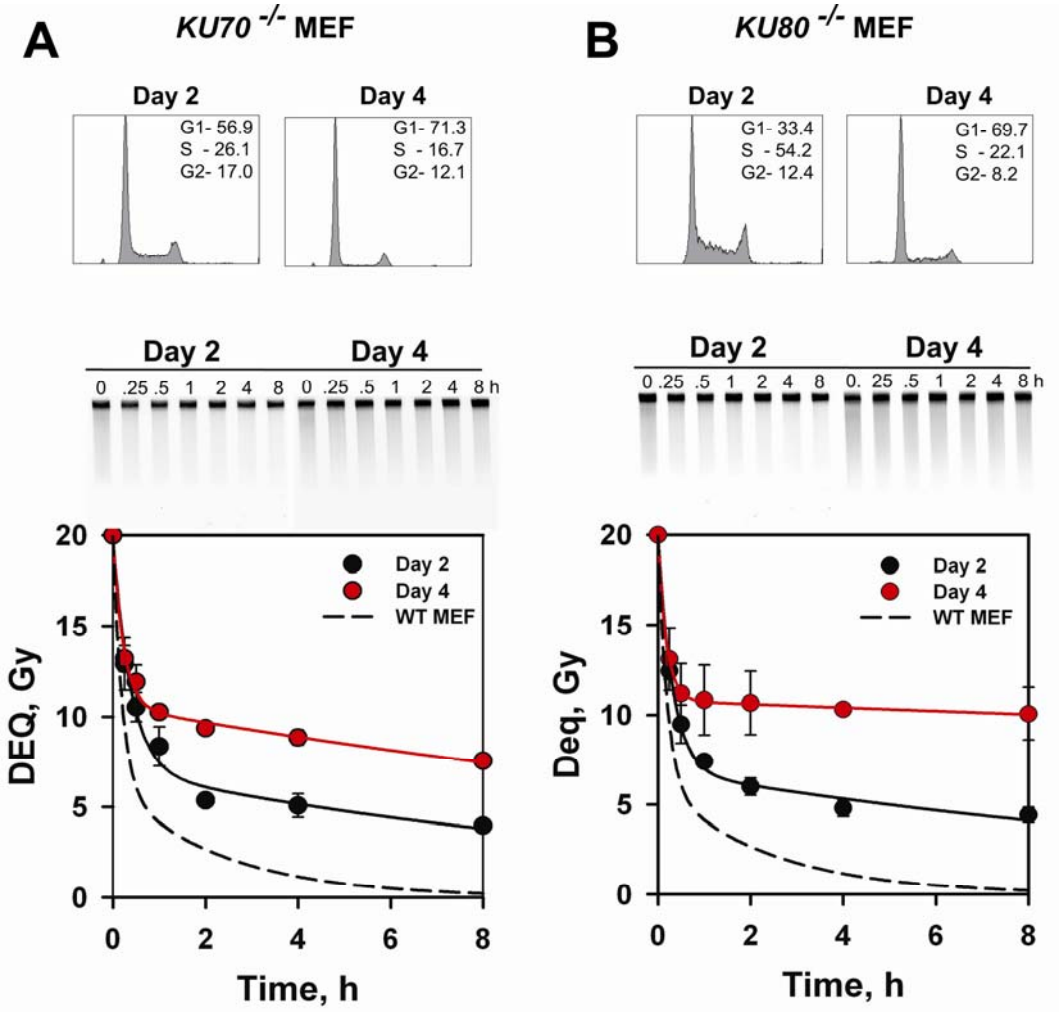

Figure 3.8: DSB repair capacity strongly depends on growth state in *XRCC4* deficient *xr-1* cells. Cells were grown for the indicated times, were irradiated and incubated for repair. DSB repair kinetics was measured by PFGE. Results shown are the average of six determinations from two experiments. The corresponding growth curves are shown in Figure 3.6C. DSB repair kinetics of wt cells at day 2, 4 and 6 along with representative gels (A), DSB repair kinetics of *xr-1* cells at day 2, 4, and 6 with representative gels (B).

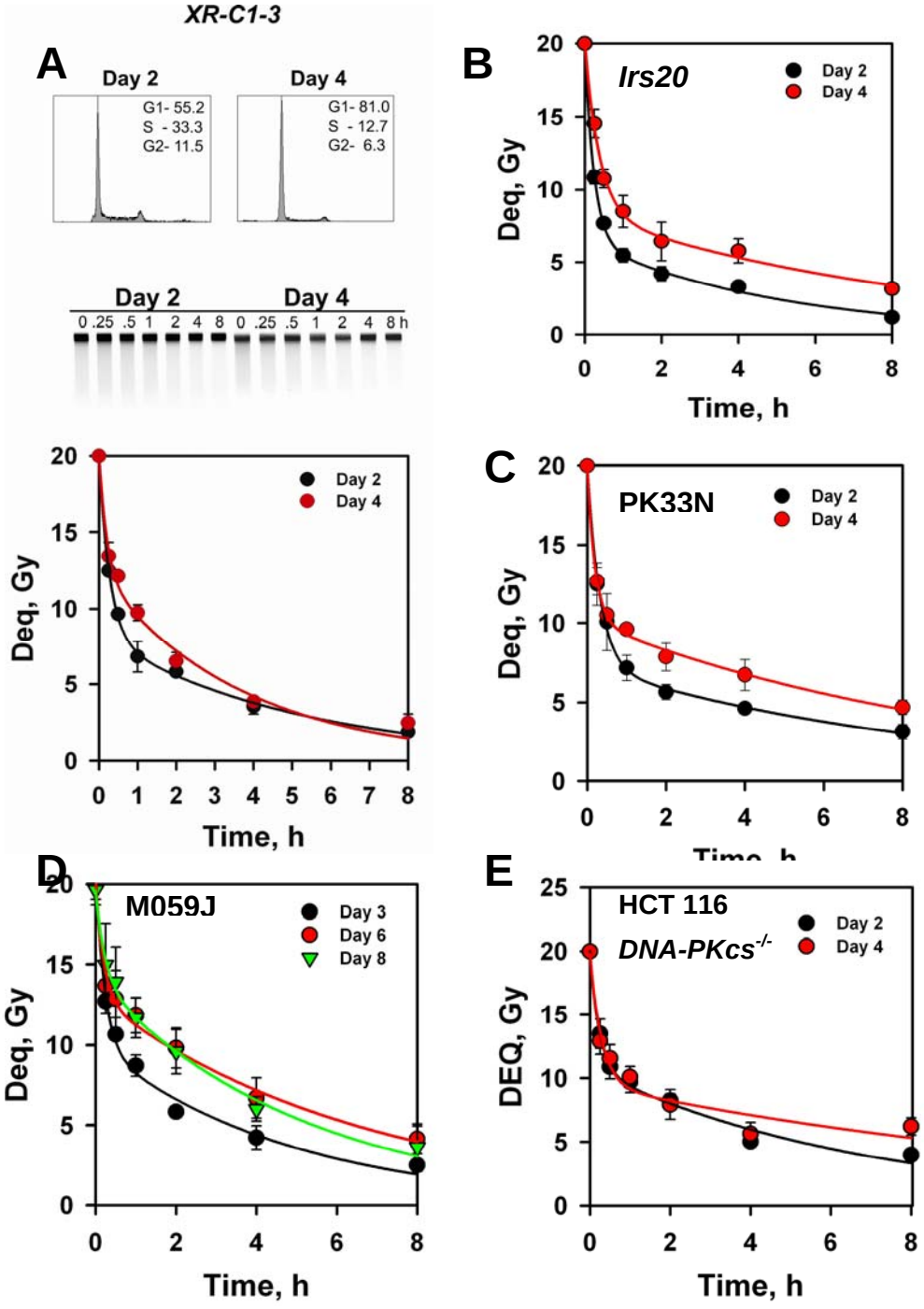

Figure 3.9: DSB repair capacity does not change during growth in DNA-PKcs deficient cells. Cells were grown for the indicated times, were irradiated and incubated for repair. DSB repair kinetics was measured by PFGE. Results shown are the average of six determinations from two experiments. The corresponding growth curves are shown in Figure 3.6. DSB repair kinetics results obtained with *XR-C1-3* cells (A). DSB repair kinetics results obtained with PK33N cells, *irs20*, M059J and HCT116 *DNA-PKcs*$^{-/-}$ cells respectively in panels B, C, D and E.

3.2.2. DNA-PKcs inhibitors are more efficient in plateau-phase

Tumors with mutations in D-NHEJ components are only rarely encountered in the clinic. On the other hand, there are efforts to introduce inhibitors targeting D-NHEJ in the radiation treatment of human tumors. It is relevant therefore, to investigate whether inhibition of D-NHEJ with such inhibitors will uncover B-NHEJ showing growth dependence similar to that of DNA-PKcs mutant that has minimum effect of growth state, or like to that of Ku and DNA Ligase IV/XRCC4 mutants that show maximum effect on growth state.

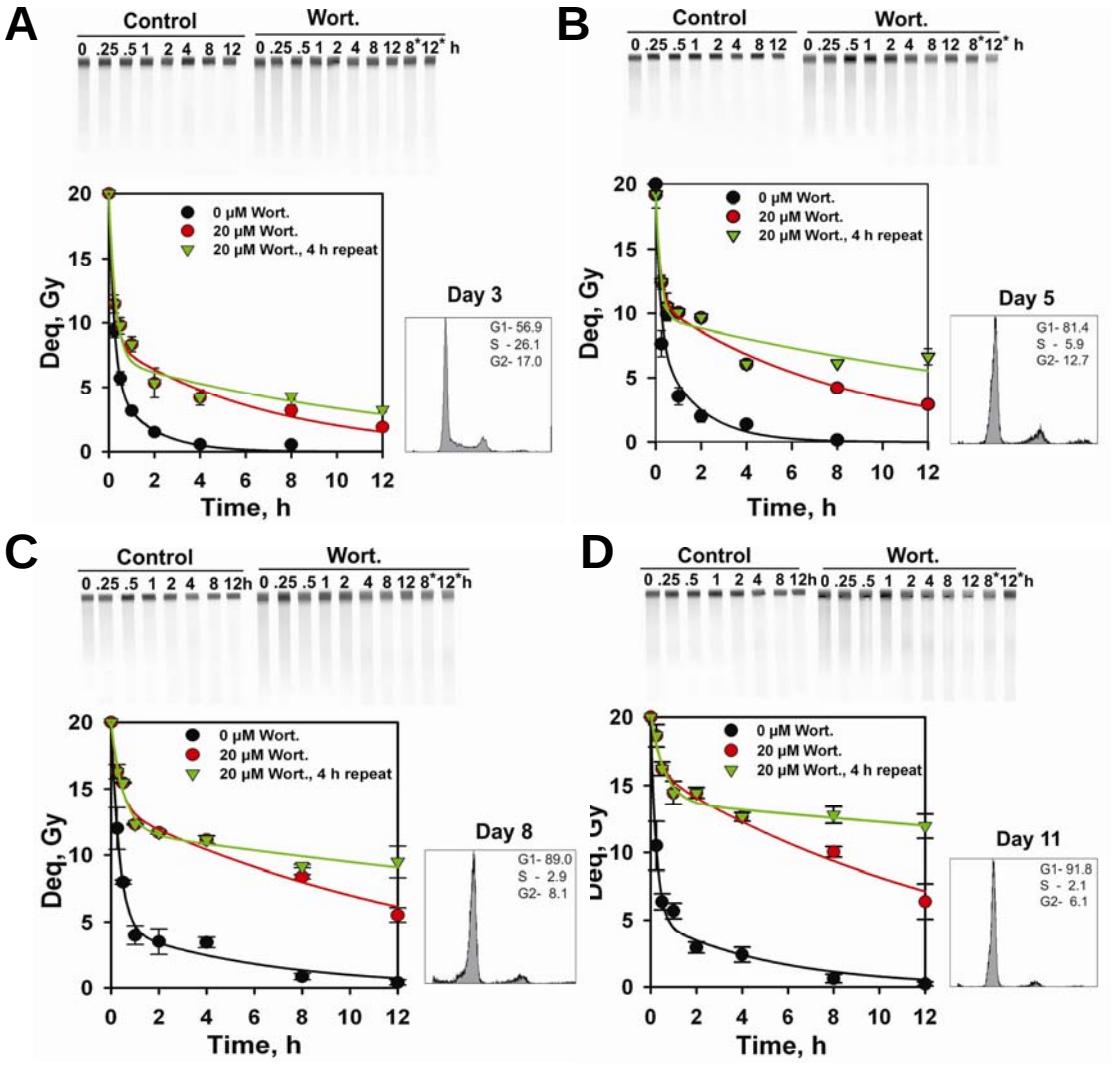

Figure 3.10: Wortmannin induced inhibition of DSB repair depends on growth state in human glioma M059K cells. M059K cells were grown for the indicated times, were irradiated and incubated for repair. Results shown are the average of six determinations from two experiments. (A) DSB repair kinetics at day 3 in the presence or absence of 20 µM wortmannin, given 1 h prior to irradiation. In one set wortmannin was added every 4 h, starting at 1 h before

irradiation, to counteract inactivation by hydrolysis in the growth medium. Shown are also typical gels, as well as the cell cycle distribution at different growth times measured by flow cytometry. (C) As in A but for cells at day 5. (D) As in A but for cells at day 8. (E) As in A but for cells at day 11.

For these experiments, we used repair proficient human glioma M059K cells. Growth curves for these cells are included in Figure 3.6. Cells were grown for different periods of time to reach different stages of growth and repair was followed in the presence or absence of wortmannin, a non-competitive and irreversible inhibitor of DNA-PKcs (Wipf and Halter, 2005). The results are summarized in Figure 3.10 and show the repair kinetics of day 3, 5, 8, and 11 cultures together with the corresponding flow cytometry. A substantial enhancement in the effect of wortmannin is observed as cells enter the plateau-phase reflecting the compromised function of B-NHEJ. Similar results are obtained in cultures where wortmannin is added once before irradiation and in cultures where wortmannin is first added 1 h before irradiation and in 4 h intervals thereafter. This rules out the possibility of incomplete inhibition of DNA-PK and explains role of B-NHEJ in the observed effect.

This result is completely opposite to the results obtained with the DNA-PKcs mutant cell lines that we have discussed above, where there was no difference between DSB repair measured in exponentially growing and plateau-phase cultures. This result indicates a dominant negative effect of the wortmannin inhibited kinase.

3.2.3. Kinase dead DNA-PKcs cells show dominant negative effect

As we have shown above that a DNA-PKcs inhibitor is more effective in plateau-phase cells than the inactivated enzyme we investigated the molecular basis of the suggested dominant negative action. It is likely that the wortmannin inhibited DNA-PKcs blocks the DSBs and inhibits the function of B-NHEJ. In addition, wortmannin at the concentrations used here also inhibits ATM and we wondered whether part of the effect derives from this associated action. To shed light in these questions, we examined different DNA-PKcs mutants with defects in specific essential regions of DNA-PKcs.

V3 is a DNA-PKcs deficient CHO mutant. This mutant was transfected in the laboratory of Dr. Kathy Meek with a wt human *DNA-PKcs* cDNA or mutant forms with specific defects as

indicated in the Figure 1.3. When a kinase dead but otherwise complete DNA-PKcs polypeptide was tested for effects in the exponential and the plateau-phase of growth, results similar to the chemically inhibited DNA-PKcs were obtained. These observations are in line with published studies suggesting that DNA-PKcs autophosphorylation is needed for detachment from the DSBs and their funneling to alternative repair pathways. For more information on this effect, we studied mutants of the autophosphorylation sites (Figure 3.11B).

3.2.4. Effect of DNA-PKcs autophosphorylation sites mutants on DSB repair

The ABCDE cluster and the PQR cluster mutants are having serines and threonines substituted with alanine, which cannot be phosphorylated. The ABCDE mutant is more radiosensitive than cells lacking DNA-PKcs. Because of this fact we wanted to study the role of DNA-PKcs autophosphorylation on DSB repair at different stages of growth. These mutants were used for PFGE experiment and the results are summarized in Figure 3.11C and D. The ABCDE cluster mutant shows only a small difference in DSB repair between exponentially growing and plateau-phase cells. No effect was observed with the PQR cluster mutant. As mentioned above these mutants retained kinase activity.

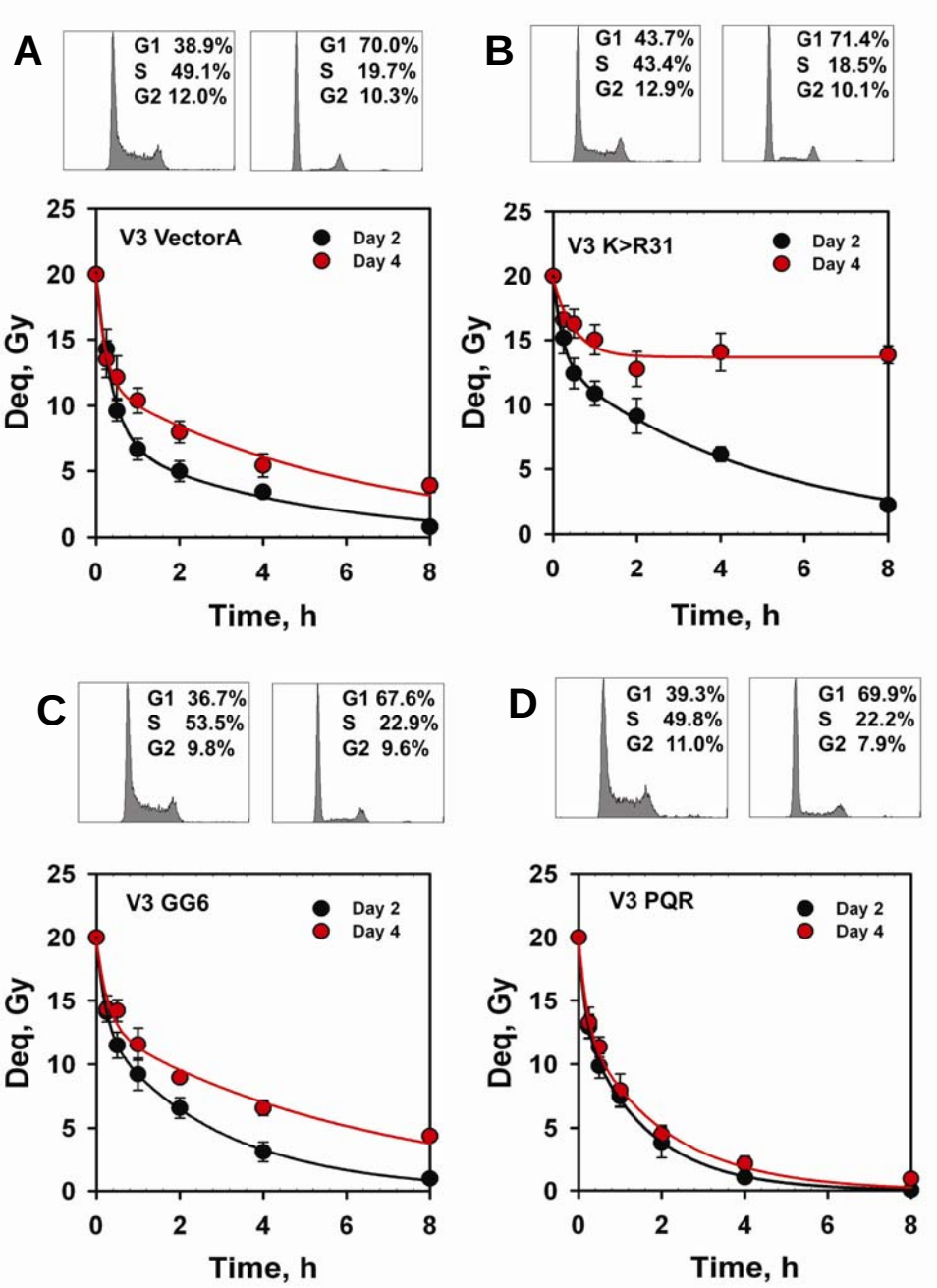

Figure 3.11: Repair kinetics of DNA-PKcs kinase dead and autophosphorylation mutants. V3 vector A is a control cell lines generated by transfection of the DNA-PKcs deficient V3 mutant with the empty vector used for the generation of the remaining DNA-PKcs mutants. Cells were irradiated as indicated and repair of DSBs analyzed by PFGE (A). V3 K>R31 is a kinase dead mutant; other details as in A (B). V3 GC6 is a mutant at the ABCDE site with all serine and threonine residues replaced by alanine. The mutant retains normal kinase activity; other details as in A (C). V3 PQR cells are mutated at the PQR domain with serine residues replaced by alanine. The mutant retains normal kinase activity; other details as in A (D).

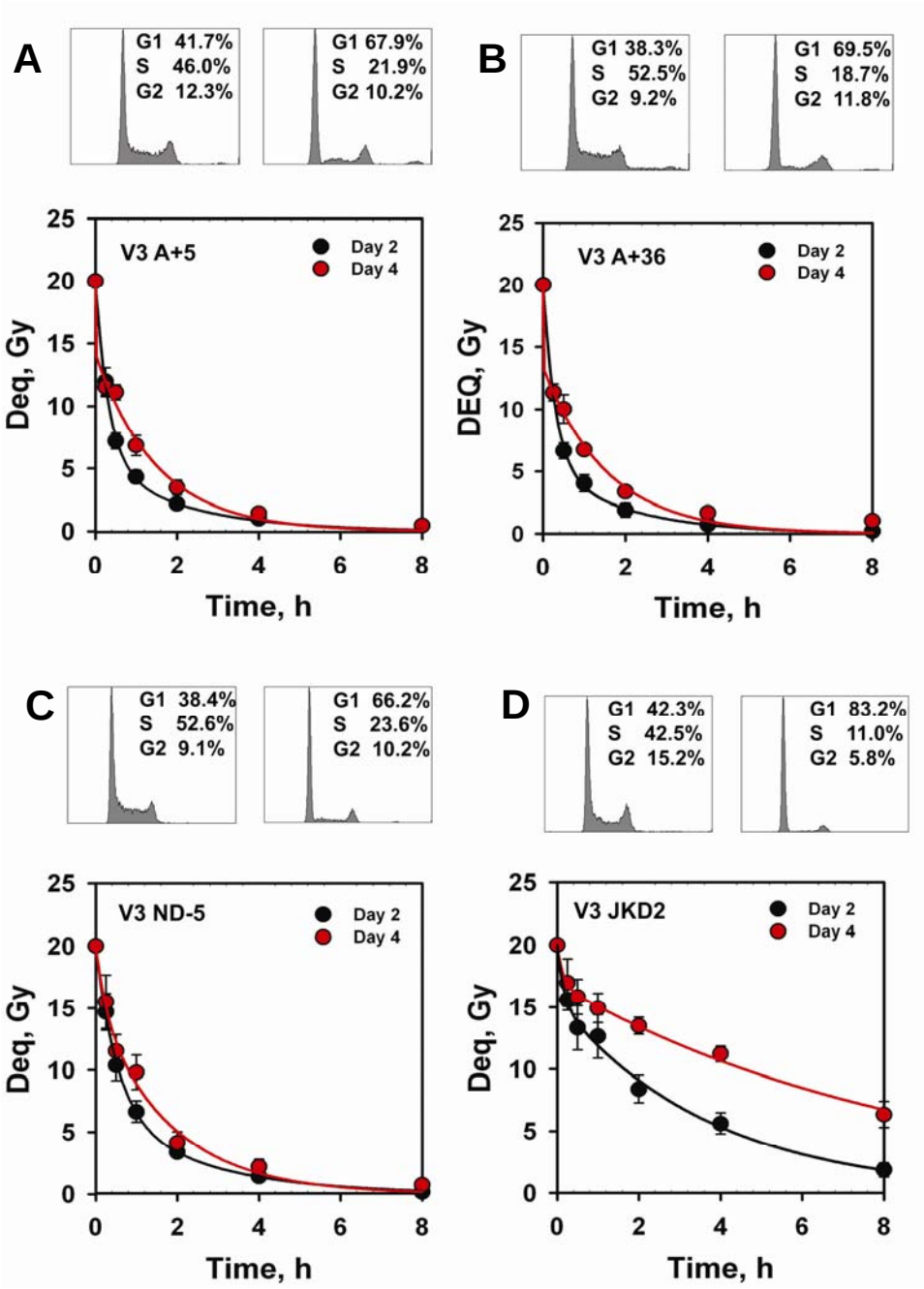

Figure 3.12: Repair kinetics of cells expressing different level of DNA-PKcs and phosphomimicking forms of DNA-PKcs. V3 A5 cells have DNA-PKcs levels similar to wt CHO cells. Cells were irradiated and DSB repair kinetics measured at different stages of growth using PFGE (A). V3 A36 cells have 20-fold higher DNA-PKcs level than wt CHO cells; other details as in A (B). V3 ND5 is a phosphomimicking mutant at two sites in the extreme N-terminal. Other details as in A (C). V3 JKD2 is a phosphomimicking mutant at two sites around 1000 amino acids from N-terminus. Other details are as in A (D).

3.2.5. Effect of phosphomimicking mutants of DNA-PKcs on DSB repair

The two phosphomimicking forms of DNA-PKcs, V3 ND-5 and V3 JKD2 were generated by replacing serine residues with aspartic acid. The ND-5 domain is in the region of the molecule that interacts with the death domain. This mutant interacts with Ku bound DNA but has very low kinase activity. The JKD2 domain contains two completely conserved serine phosphorylation sites around 1000 amino acids from N-terminus. Although this mutant retains wt kinase activity (Figure 3.12C and D).

In our PFGE experiment the ND-5 mutant repairs efficiently in both the exponential, as well as in the plateau-phase of growth. On the other hand, the JKD2 mutant behaves like the kinase dead mutant and shows strong inhibition of repair in the plateau phase of growth (Figure 3.12C and D)

3.2.6. Effect of different levels of DNA-PKcs on DSB repair

From V3 cells transfected with wt DNA-PKcs human cDNA, two clones were selected: one with nearly normal levels of DNA-PKcs for CHO cells that was named A+5, and a second having 20-fold higher levels, A36. We used these clones to investigate the effect of DNA-PKcs level on DSB repair. As expected, both mutants effectively repaired DSBs using D-NHEJ. In line with this observation, there was no significant difference in DSB repair kinetics between exponentially growing and plateau phase cells (see Figures 3.12A and B).

3.2.7. Repair kinetics of double knock out of D-NHEJ proteins

All the D-NHEJ mutants except DNA-PKcs show a strong reduction in DSB repair capacity when they reach plateau phase. These results indicate a regulatory role of DNA-PKcs in this effect. To address this question we studied the PK80-193A mutant that is double knock out for *Ku80* and *DNAPKcs*.

In this double knock out cell line we inquired whether the phenotype is as in $Ku80^{-/-}$ cells or like $DNAPKcs^{-/-}$ cells. Interestingly, this double knockout mutant showed DSBs repair kinetics similar to $DNAPKcs^{-/-}$ cells. The observation is an indication that the reduction observed in DSB rejoining activity in the plateau-phase of growth is a consequence of normal cellular activities occurring in cells as they transit to a non-growing state and that DNA-PKcs is needed for this

function. (see Figure 3.13).

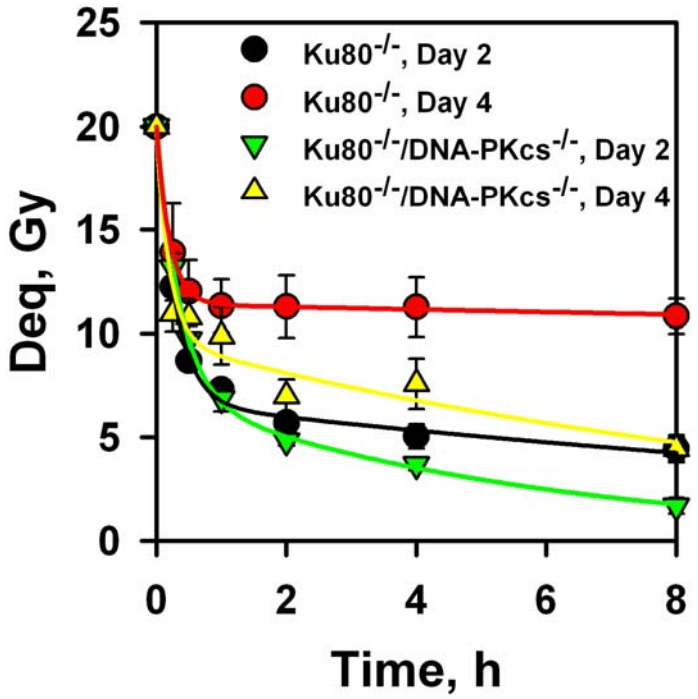

Figure 3.13: Repair kinetics of double D-NHEJ mutant (*Ku80*$^{-/-}$ and *DNA-PKcs*$^{-/-}$). DSB repair kinetics of the PK80-193A mutant in the exponential and the plateau-phase of growth measured by PFGE. Results represent the average of two experiments and six determinations.

3.3. Effect of EGFR signaling over DSB repair by B-NHEJ

3.3.1. B-NHEJ inhibition in plateau phase cells generated by serum deprivation

A plateau-phase in the growth of a culture is reached when essential nutrients or growth factors become limited, either due to depletion or due to cell overgrowth that generates diffusion limitations. The multitude of factors causing a culture to enter plateau phase make the system difficult to study. We therefore sought to develop a better defined system allowing the reproducible analysis of B-NHEJ response under conditions limiting cell growth. Therefore, we tested the generation of quasi plateau-phase cells by depriving from serum exponentially growing cells. Serum is known to provide growth factors and other substances that stimulate the progression of cells through the cell cycle. By removing serum from an exponentially growing

culture before reaching high cell densities, it is possible to produce non growing cells mainly depleted of growth factors but amply supplied with all other essential nutrients provided by the growth medium component.

The protocol optimized for MEFs was to allow cultures seeded in 60 mm tissue culture vessels at $4x10^5$ per dish to grow for 24 h. Subsequently, the standard growth medium was replaced with the same growth medium but prepared without serum. The response of these cells was then investigated at various times after medium change. In this way, cells optimally growing and well supplied with media are brought to a state of limited growth in a rapid way allowing the study of the dynamics of B-NHEJ.

The results in Figure 3.14 demonstrate that in *LIG4*$^{-/-}$ MEFs, soon after serum deprivation, DSB repair capacity starts decreasing reaching a minimum after 24 h at levels similar to those observed in late plateau phase cultures. Longer incubation times in serum-free medium did not further reduce the DSB repair capacity.

3.3.2. Inhibition of B-NHEJ by serum deprivation is reversible

We inquired whether the above inhibition in B-NHEJ observed upon serum deprivation was reversible. Therefore, we supplied with growth medium, supplemented with different amounts of serum, *LIG4*$^{-/-}$ MEFs that had been transferred to serum-free medium. Even incubation with 0.5% serum made a significant difference (Figure 3.15). The recovery in repair capacity depended on the duration of serum deprivation, as well as on the concentration of serum during re-incubation. If cells are serum deprived for 4 h, they regain repair capacity more readily than cultures deprived of serum for 24 h.

In the case of 8 h serum deprived *LIG4*$^{-/-}$ cells, 1 h incubation with different serum concentrations gives a serum concentration-dependent recovery in DSB repair capacity. Compared to cells treated with 0% serum that repaired only 40% of DSBs within 8 h, 0.5%, 1%, 2% 10% serum treated cells repaired 60%, 68%, 75% and 80% of DSBs within 8 h, respectively (Figure 3.15A).

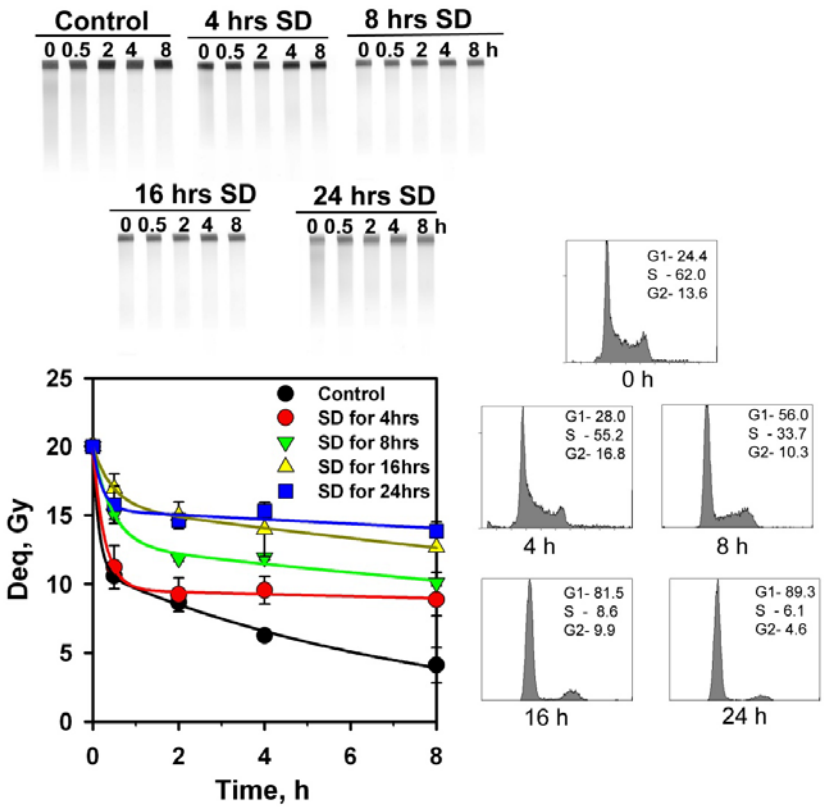

Figure 3.14: Repair kinetics of *LIG4*$^{-/-}$ cells after serum deprivation. *LIG4*$^{-/-}$ cells were grown in 10% serum for 24 h and then serum-deprived for 4, 8, 16, or 24 h before being exposed to IR to measure the kinetics of DSB repair. During repair, cells were kept in serum free media. Results shown are the average and standard deviation of six determinations from two experiments.

In another experiment, we looked for 4, 16 and 24 h serum deprivation in *LIG4*$^{-/-}$ cells, to monitor how duration of serum deprivation affects recovery of B-NHEJ after transfer to serum containing medium. In this experiment, repair activity was monitored up to 8 h but for convenience and simplicity we are presenting only 4 h repair time point (details are in appendix 1 and 2). The results show that there is no difference in the pattern of recovery after treatment with different concentrations of serum. However, for a given time point, the recovery of repair capacity is dependent on the serum concentration used after serum deprivation (Figure 3.15B).

3.3.3. Reversal in B-NHEJ is not a very fast process

The kinetics of recovery of B-NHEJ after replenishing serum is informative. When *LIG4*$^{-/-}$ cells deprived of serum for 24 h are returned to 10% serum for 1, 2, 4 and 8 h, a relatively prompt recovery in the repair capacity is observed. After 4 h incubation in serum containing medium the

cell cycle distribution of the cultures remains unchanged, but the repair capacity increases by about 50%. After 8 h of incubation, DSB repair proceeds as effectively as in exponentially growing cells albeit with slower kinetics (Figure 3.16).

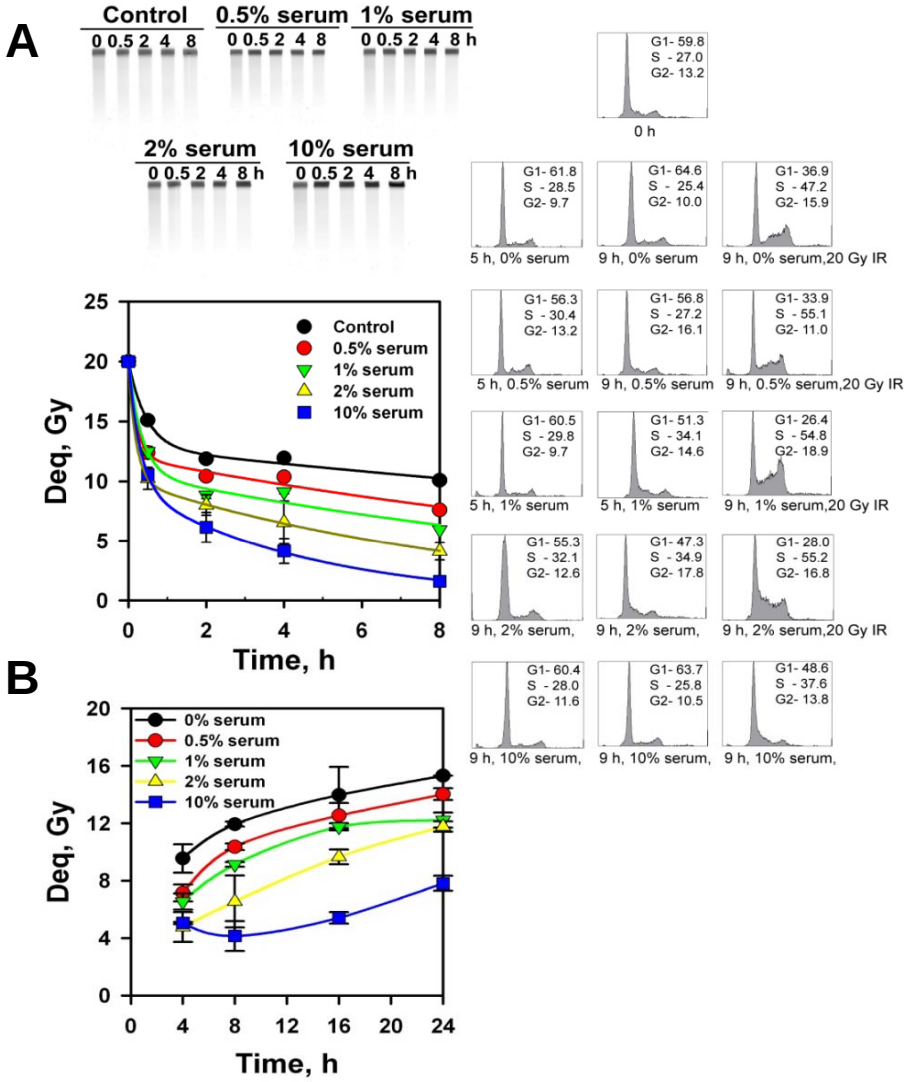

Figure 3.15: Recovery of repair capacity as a function of serum concentration applied immediately after the end of the serum deprivation period. *LIG4*$^{-/-}$ cells were serum deprived for 8 h and then returned to growth medium supplemented with the indicated amounts of serum. Serum deprived (SD) cells were treated with 0.5%, 1%, 2% and 10% serum just 1 h before IR and repair was followed by PFGE while incubating in the same media. Results shown are average and standard deviation of six determinations from two different experiments (A). Same experiment but with cells deprived from serum for 4, 16 and 24 h and treated subsequently for 1 h with media containing different concentrations of serum. Cells were irradiated and DSB repair followed by PFGE. For simplicity, we only show the 4 h time point from each curve (B).

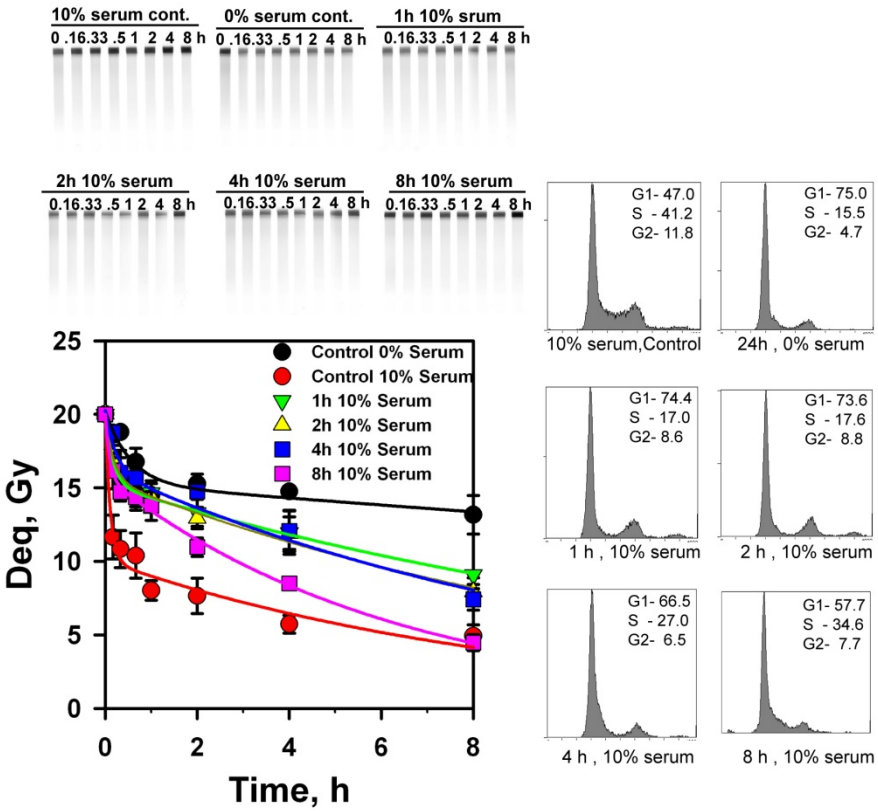

Figure 3.16: Recovery of repair capacity as function of time of incubation in growth medium supplemented with 10% serum. *LIG4*$^{-/-}$ cells serum deprived for 24 h were returned to growth medium supplemented with 10% serum for 1, 2, 4 and 8 h, irradiated and followed for DSB repair in the same media. Results shown are the average and standard deviation of six determinations from two experiments.

3.3.4. Relationships between time of incubation and serum concentration for B-NHEJ recovery

The recovery of B-NHEJ after serum deprivation was incubation time and serum concentration dependent. With increasing incubation time, at a given serum concentration, the DSB repair capacity improved. Similarly, DSB repair capacity improved for a given incubation time point as the serum concentration increased (Figure 3.17, 3.18, and 3.19).

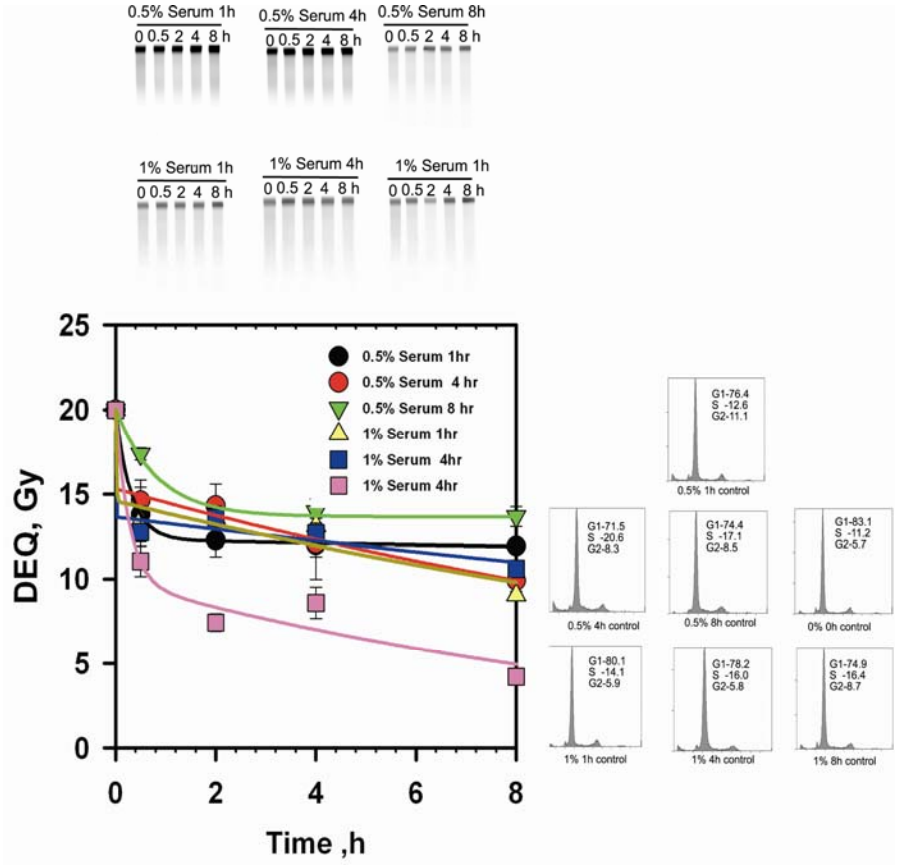

Figure 3.17: Relationship between time of incubation and serum concentration in the recovery of B-NHEJ. Repair kinetics of *LIG4*$^{-/-}$ cells after 24 h of serum deprivation and re-incubation in growth media containing different concentrations of serum. Repair of DSBs was followed at different times after re-incubation using PFGE. Other details are as in Figure 3.14.

3.3.5. Repair after chemical inhibition of EGFR

Results shown above show a clear effect of growth factor signaling in the efficiency of B-NHEJ. To address this question more precisely, a very specific and potent inhibitor of EGFR BIBX1382 was used in our experiments. Exponentially growing *LIG4*$^{-/-}$ cells were deprived from serum for 2, 4, 6, and 8 h with and without drug, and 4 h after IR cells were collect and tested. There was a clear inhibition in DSB repair after drug treatment as compare to DMSO treated controls (Figure 3.20).

.

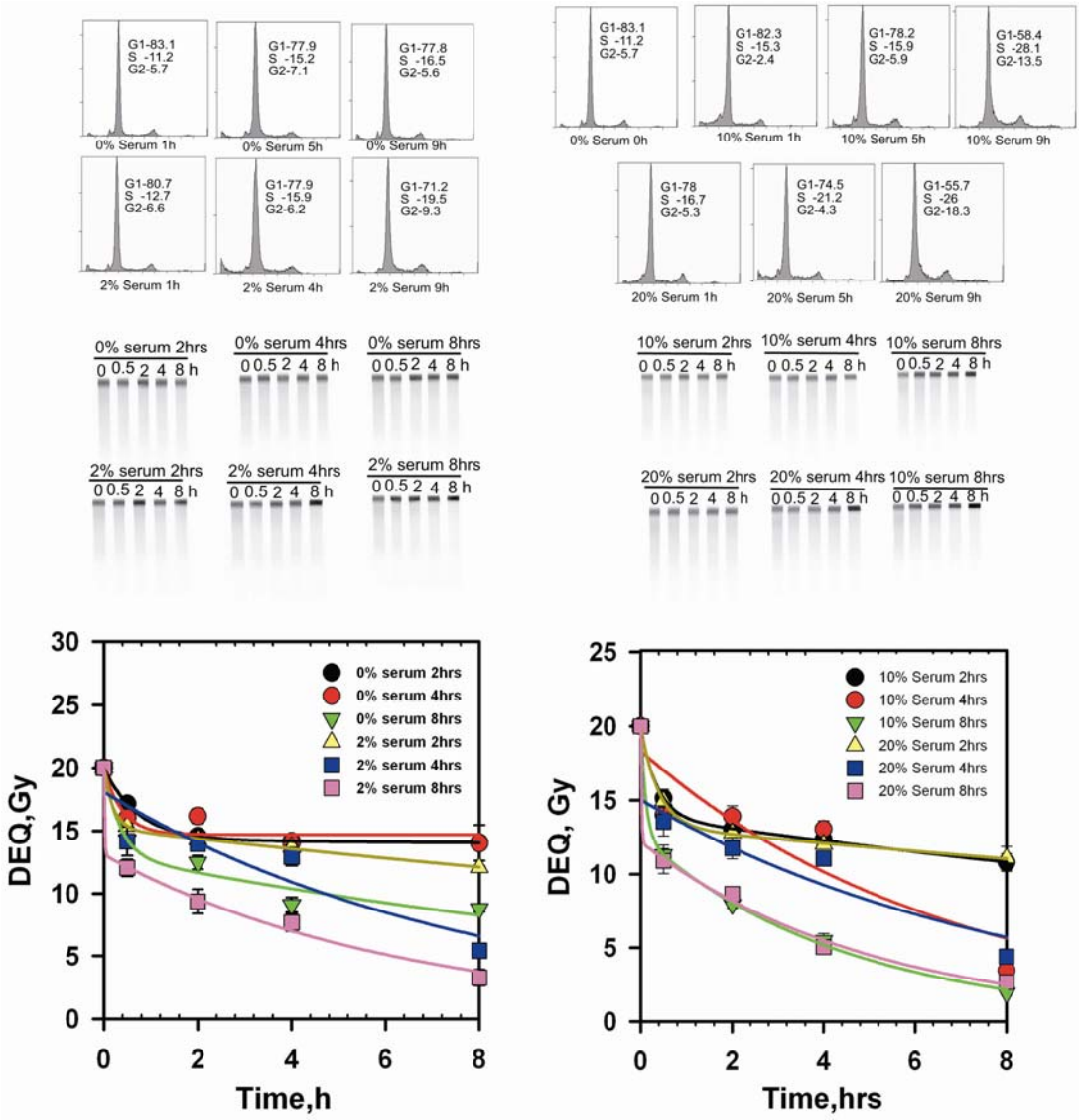

Figure 3.18: Relationships between time of incubation and serum concentration in B-NHEJ recovery. Repair kinetics of *Lig4*$^{-/-}$ cells after 24 h of serum deprivation and re-incubation with growth media containing different serum concentrations. Cells were exposed to IR at different times after re-incubation with serum and DSB repair kinetics was followed by PFGE. Other details are as in Figure 3.14.

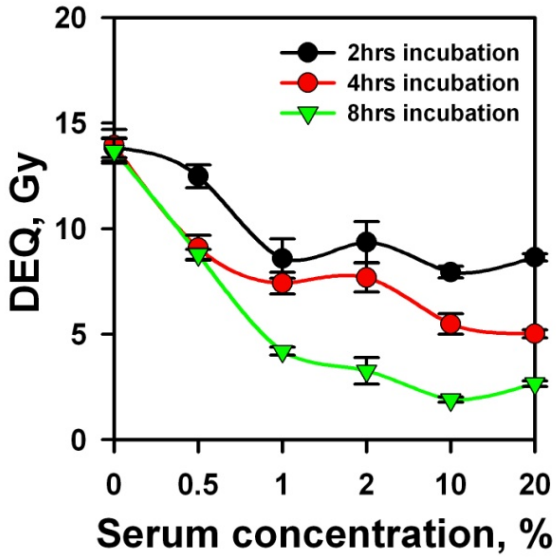

Figure 3.19: Relationships between time of incubation and serum concentration in the recovery of B-NHEJ. Data shown have been extracted from Figures 3.17 and 3.18 at the 8 h time point.

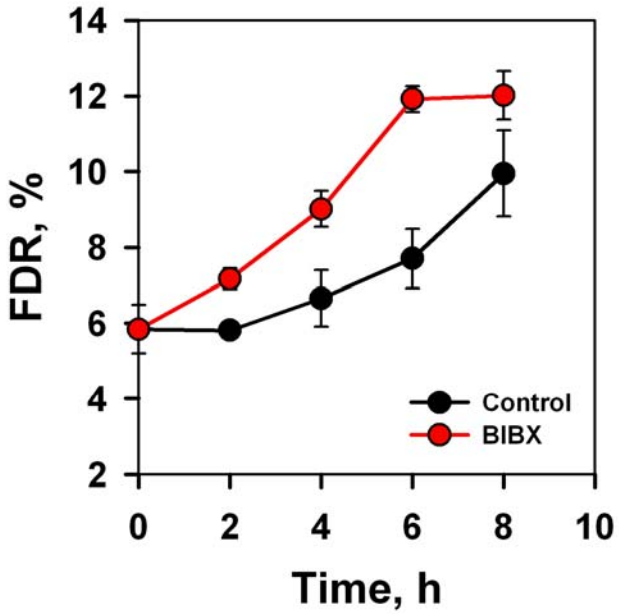

Figure 3.20: Effect of the EGFR inhibitor BIBX-1382 on repair of DSBs by B-NHEJ. *LIG4*$^{-/-}$ cells were serum deprived for a given period of time with 500 nM BIBX-1382 or without drug (DMSO as a control). Thereafter, cells were exposed to 20 Gy and residual DSBs measured 4 h later using PFGE.

3.3.6. Expression levels of proteins implicated in B-NHEJ

The above documented reduction in B-NHEJ capacity during the plateau phase of growth raises the possibility that it may derive from a reduction in the levels of participating proteins. We used therefore Western blotting to check the levels of proteins implicated in B-NHEJ like 53BP1, PARP1 and histone H1. The results in Figure 3.21 indicate that with the exception of 53BP1, there is no significant difference in the expression levels of proteins involved in B-NHEJ. Particularly relevant in this regard are the levels of DNA Ligase III and PARP1. The significance of the increase during the plateau phase of growth of the levels of 53BP1 needs further investigation (Figure 3.21).

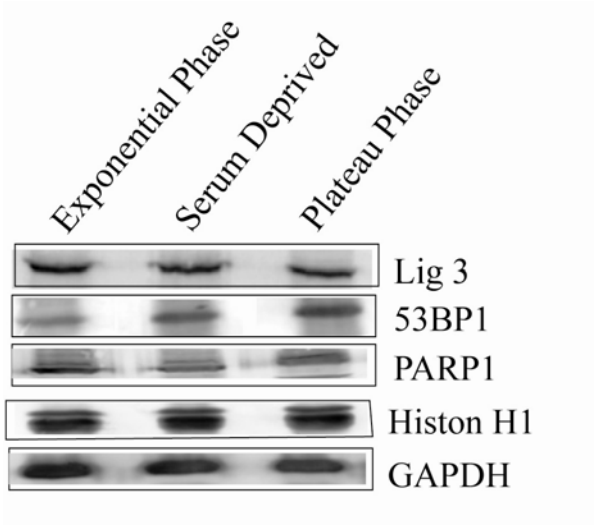

Figure 3.21: Expression levels of proteins implicated in B-NHEJ in the different stages of growth. Using Western blot analysis we tested DNA ligase III, 53BP1, PARP-1, and Histone H1. GAPDH is used a loading control.

3.4. B-NHEJ contributes to cell survival

When cells enter the plateau-phase of growth, B-NHEJ is compromised. If B-NHEJ contributes to the survival of irradiated cells, the compromised function of the pathway should reflect on cell radiosensitivity to killing. Figure 3.22 A summarizes results obtained with exponentially growing and plateau-phase *LIG4*$^{-/-}$ and wt MEFs. Plating efficiency (PE) for *LIG4*$^{-/-}$ was 67% and 58% in the exponential (day 2) and the plateau-phase (day 4), respectively. WT MEFs had a PE of 75% and 66% in the exponential and in the plateau-phase, respectively. Typical flow cytometry

histograms with the cell cycle distributions are shown in Figure 3.22A of the cells used in the survival experiments. It is evident that while wt cells show similar radiosensitivity in the exponential as well as in the plateau-phase of growth, *LIG4*$^{-/-}$ cells are much more radiosensitive when tested in the plateau-phase.

The increased radiosensitivity of plateau-phase *LIG4*$^{-/-}$ cells could be attributed to the disproportional distribution of cells in different phases of cell cycle. To examine this possibility we elutriated exponentially growing and plateau-phase populations to obtain fractions enriched in G1 or G2 cells. Centrifugal elutriation fractionates cells on the basis of their size. Highly enriched G1 and G2 populations obtained in this way were then exposed to radiation and plated to determine survival. Shown is the cell survival as a function of dose of cell populations enriched in G1 cells from exponentially growing (day 2), or plateau phase (day 4) cultures. The survival curves of the same cells before elutriation are also shown for comparison. PE was 47% and 43% for G1 cells obtained from exponentially growing and plateau-phase cultures, respectively. In cells that were not subject to elutriation, PE was 50% and 56% in the exponential and the plateau phase, respectively. Fraction 21.5 signifies a fraction collected at a flow rate of 25 ml/min and a rotor speed of 2150 rpm. Figure 3.22B summarizes results obtained with *LIG4*$^{-/-}$ MEFs. We also obtained G2 enriched cells on the basis of their larger size. A G2-cells-enriched fraction of *LIG4*$^{-/-}$ cells was irradiate and plated for survival assay. PE was 70% and 54% for exponential and plateau-phase cultures, respectively. In cells that were not subject to elutriation PE was 50% and 47% for exponentially growing and plateau phase, respectively (Figure 3.22C). Cells in G2 phase are more radioresistant than in G1 for either growth state, which reflects radiosensitivity of cells across the cell cycle. It is evident that G1 cells from plateau-phase cultures are more radiosensitive to killing than G1 cells from exponentially growing cultures. Furthermore, cells from plateau-phase cultures enriched by elutriation in G2 are significantly more radiosensitive than G2 cells obtained from exponentially growing cultures.

Figures 3.23 summarize similar results for wt MEFs. PE was 64% and 58% for G1 cells obtained from exponentially growing and plateau-phase cultures, respectively. In cells that were not subject to elutriation PE was 70% and 49% for the exponential and plateau phase, respectively (Figure 3.23A). It is evident that G1 cells from exponentially growing and plateau-phase cultures

show no detectable fluctuations in cell radiosensitivity to killing in line with observations on DSB repair. In case of G2 cells, PE was 40% and 52% for exponentially growing and plateau-phase cultures, respectively. In cells that were not subject to elutriation, PE was 70% and 49% for the exponential and plateau phase, respectively (Figure 3.23B). Notably, G2 cells from plateau-phase wt MEFs are significantly more radioresistant than those obtained from exponentially growing cultures, a result opposite to the observations with *LIG4*$^{-/-}$ MEFs and which greatly magnifies the observed relative radiosensitivity of plateau phase G2 *LIG4*$^{-/-}$ MEFs.

Together, these observations indicate that the reduction in repair capacity observed in non-cycling D-NHEJ deficient cells is also reflected in cell radiosensitivity to killing, and that it is not limited to G1 cells but can also be seen to an even greater extent in G2 cells.

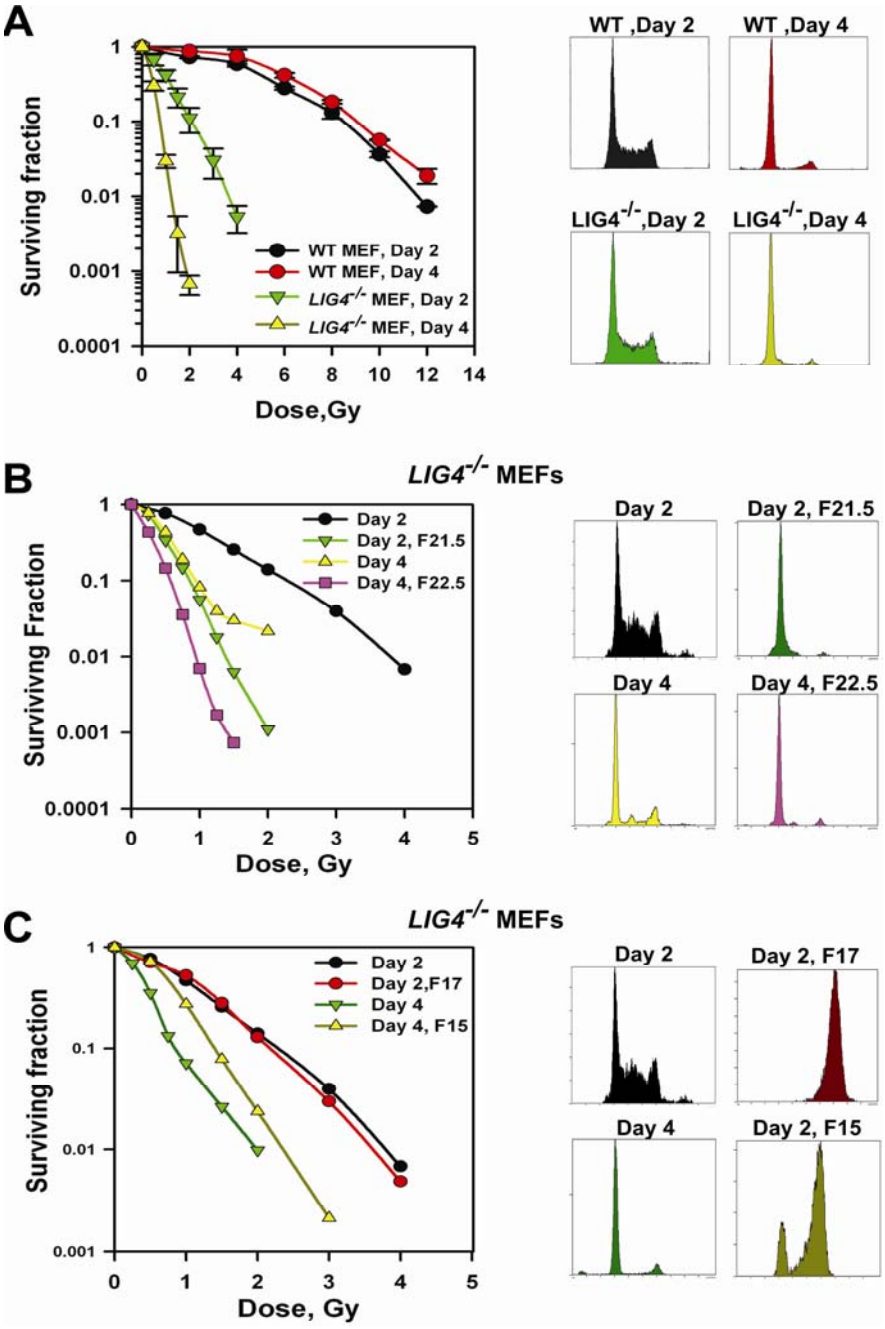

Figure 3.22: Survival of *LIG4*$^{-/-}$ and wt MEFs at different stages of growth and phases of the cell cycle. Cells were tested either in the exponential or in the plateau phase of growth. Populations enriched with cells in different phases of the cell cycle were obtained by centrifugal elutriation. (A) Cell survival after exposure to different doses of IR in *LIG4*$^{-/-}$ and wt MEFs examined either in the exponential or in the plateau-phase of growth. (B) Cell survival as a function of radiation dose of cell populations enriched in G1 cells by centrifugal elutriation from exponentially growing (day 2), or plateau phase (day 4) cultures. Fraction 21.5 signifies a fraction collected at a flow rate of 25 ml/min and a rotor speed of 2150 rpm. (C) Same as in B but for

cells enriched in G2. PE was 70% and 54% for G2 cells obtained from exponentially growing and plateau-phase cultures,

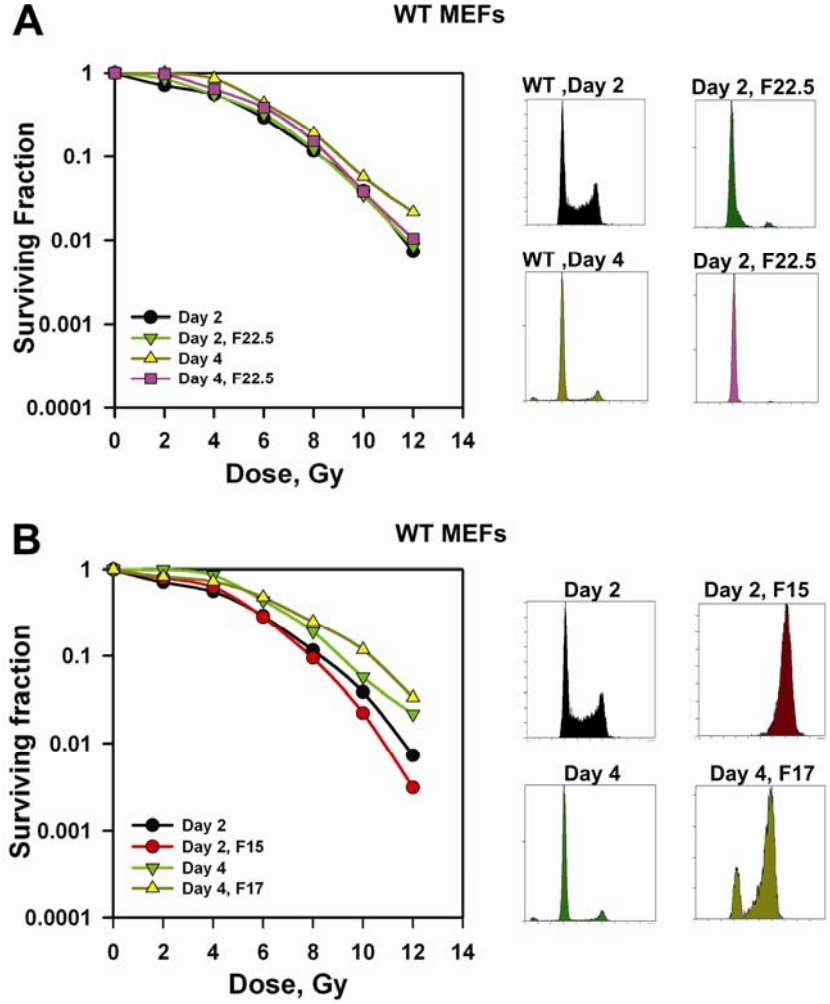

Figure 3.23: Survival of wt MEFs at different stages of growth and phases of the cell cycle. Survival curve of G1 cells obtained from exponentially growing and plateau-phase cultures, respectively. (A). Survival curve of G2 cells obtained from exponentially growing and plateau-phase cultures, respectively (B). Other details are as Figure 3.22.

3.5. Backup pathways of NHEJ after exclusion of heat labile site (HLSs)

PFGE is the most common technique used to assay DSB repair *in vivo*. However, it employs a step of lysis at 50°C and some reports indicate the induction at this temperature of additional DSBs from the transformation to SSBs of heat labile sites. The same reports suggest that B-NHEJ is an artifact of the induction and repair of such HLS and that B-NHEJ thus reflects the repair of non-DSB lesions. Since it was very important to clarify this essential aspect of B-NHEJ function,

we carried out an extensive set of experiments designed to investigate this topic. These experiments are briefly summarized below.

3.5.1. The function of B-NHEJ is demonstrated under low-temperature lysis (LTL)

To study the role of lysis conditions in the induction and rejoining of DSBs, particularly under conditions compromising D-NHEJ, we carried out experiments using M059K and M059J cells. These cell lines have been used extensively to study the effect of lysis temperature on DSB repair and several of the observations summarized in the Introduction refer to these results (Karlsson et al., 2008; Rydberg, 2000; Stenerlöw et al., 2003). Figure 3.24 summarizes experiments with M059K cells. Panel A shows images of typical ethidium bromide stained gels from dose response and repair measurements, while panels B-E summarize the quantification of such gels from repeat experiments. For dose response determinations, cells are first embedded in agarose, cooled to 4ºC, irradiated on ice and subsequently lysed using either HTL or LTL. For repair experiments, cells are embedded in agarose blocks after completion of the indicated repair incubation time at 37ºC, and are subsequently processed for lysis. These experimental procedures ensure the analysis of identical cell populations with the two lysis protocols.

Figure 3.24B depicts dose response curves obtained following either HTL or LTL. Under the experimental conditions employed and for the range of doses examined a linear increase of FDR with dose is observed, reflecting a linear induction of DSBs with dose. The signal generated after LTL is for the same radiation dose approximately 40% lower than that of HTL, suggesting that 40% of the DSBs measured under HTL derive from the transformation to DSBs of HLS.

Figure 3.24C summarizes the repair kinetics of M059K cells exposed to 20 Gy and incubated at 37ºC. Plotted is FDR as a function of repair time. Despite differences in the starting points, only a slight reduction in the half time of the initial fast repair component is observed when LTL lysis is utilized instead of HTL. There is no statistically significant difference in the final levels of FDR measured after 8 h of repair between HTL and LTL.

Figure 3.24D shows the repair results of Figure 3.24C after normalization to the initial (t = 0 h) FDR. This way of plotting allows a better visualization of relative differences in the kinetics and the extent of repair measured after HTL or LTL. The results reinforce the above conclusions and

suggest similar relative repair capacity with slightly slower kinetics for lesions assessed under LTL. Similar conclusions can also be drawn when repair results are plotted as Deq as a function of time (Figure 3.24E) suggesting that in repair proficient cells the two methods of normalization provide equivalent results.

Figure 3.25 summarizes results of experiments similar to those shown in Figure 3.24 but for the DNA-PKcs deficient cell line, M059J. The dose response curves shown in Figure 3.25B indicate an increase in DSB induction under HTL, as compared to LTL, by a magnitude similar to that measured in M059K cells. This observation suggests similar induction in the two cell lines of clustered damage sites containing HLS that are transformed to DSBs under HTL. The repair results after HTL in Figure 3.25C demonstrate the extensive potential of M059J cells to remove DSBs from their genome despite the defect in DNA-PKcs and are in line with previously published observations (DiBiase et al., 2000). Compared to HTL, the kinetics of DSB rejoining is in this repair deficient cell line markedly affected after LTL (Figure 3.25C), but a reduction in FDR is also evident suggesting repair. The relative repair activity under the two lysis protocols is clearly evident after normalization (Figure 3.25D) and is further reinforced when repair results are plotted as Deq versus dose (Figure 3.25E).

The normalized results allow two important conclusions. First, DSBs assayed under LTL display slower apparent repair than DSBs assayed under HTL, and the fast rejoining observed at early repair times under HTL is absent under LTL. Qualitatively, this is in line with results previously published with this cell line (Karlsson et al., 2008; Rydberg, 2000; Stenerlöw et al., 2003). Second, while DSB rejoining is more extensive under HTL, as compared to LTL, more than 50% of the DSB load initially measured under LTL is removed by 8 h. Since rejoining has not plateau at 8 h, further repair at later times will remove an even larger fraction of DSBs (see also below). Thus, while the results of Figures 3.24 and 3.25 confirm important aspects of earlier observations regarding the salient features of DSB repair under LTL (Karlsson et al., 2008; Rydberg, 2000; Stenerlöw et al., 2003), they also demonstrate that even after LTL ample repair attributable to B-NHEJ can be measured in a D-NHEJ deficient mutant.

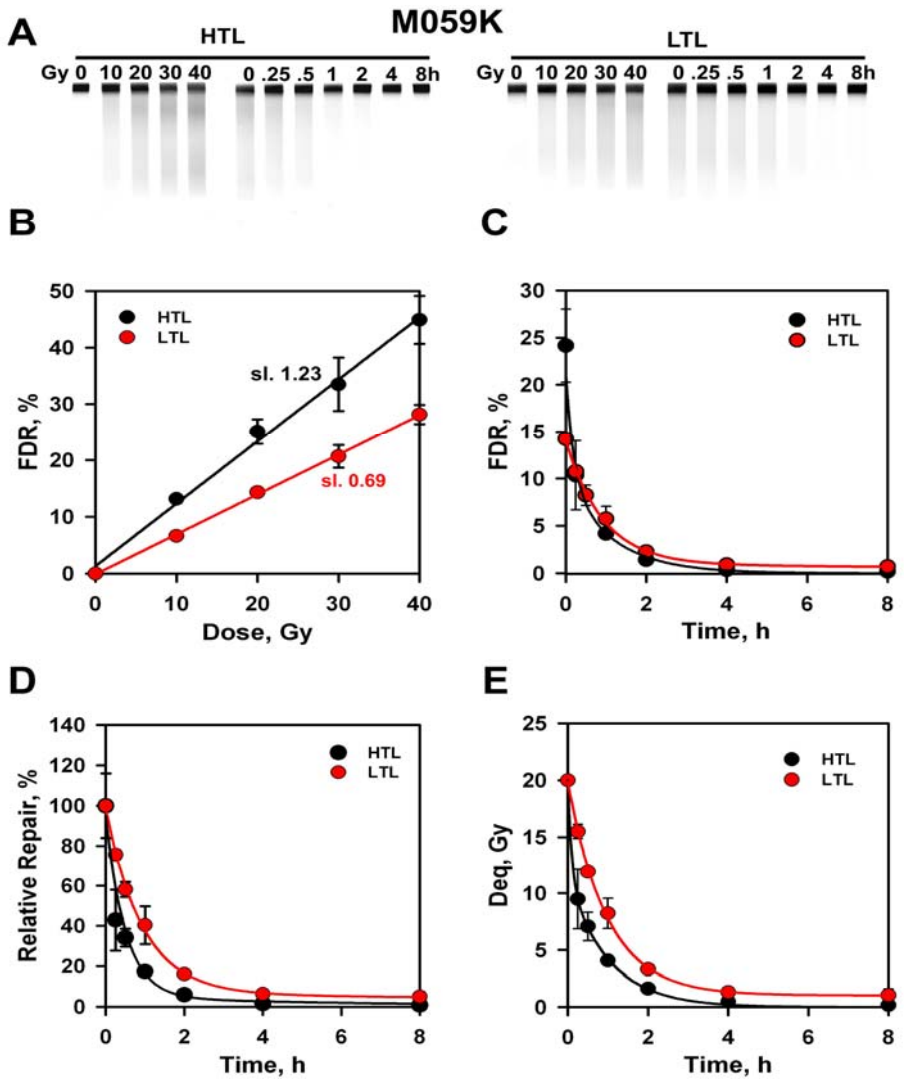

Figure 3.24: Dose response and repair kinetics of IR induced DSBs in human DNA-PKcs proficient M059K cells following high (HTL) and low (LTL) temperature lysis. A. Images of typical ethidium bromide stained gels from dose response and repair measurements obtained using AFIGE. Experiments were carried out with exponentially growing cells and were processed using either HTL or LTL. For dose response measurements cells were embedded in agarose, exposed to the indicated radiation doses and analyzed after HTL or LTL. Gels were scanned in a FluorImager and the fraction of DNA released from the well into the lane (FDR) was determined for different radiation doses and repair times. B. Dose response curves for M059K cells processed with either HTL or LTL. C. Repair kinetics plotted as FDR versus repair time for cells processed either with HTL or LTL. D. Normalized repair kinetics obtained by dividing the FDR values shown for different repair times in Figure C with that measured at t = 0 h and expressing the ratio as a percent value. E. Normalized repair kinetics expressed as Deq versus time. Deq is read from the FDR shown at each repair time point in Figure C using the dose response curves in Figure B (see Material and Methods for more details).

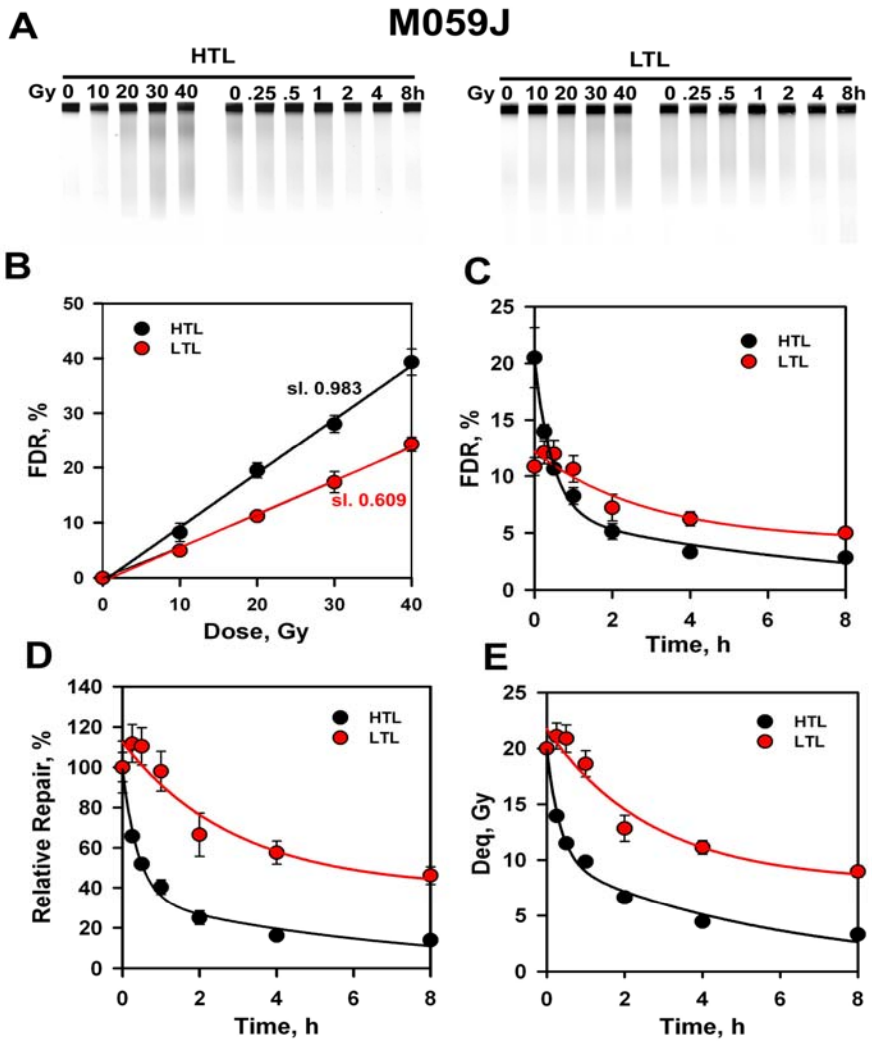

Figure 3.25: Dose response and repair kinetics of IR induced DSBs in human DNA-PKcs deficient M059J cells after HTL or LTL. Exponentially growing M059J cells were used for experiments. Other details are as in the legend of Figure 3.24.

To examine in other species the generality of the results obtained with the human M059J and M059K cells, we carried out experiments with the DNA-PKcs deficient Chinese hamster mutant, *irs20*, (Figure 3.28). It is evident from the dose response curves shown in Figure 2.28A that in these cells over 50% of the DSBs measured under HTL can be attributed to the transformation to breaks of HLS. This proportion is higher than in human cells implying species specificities in the relationship between prompt and total DSBs. Slower rejoining kinetics is observed in the *irs20*

mutant under LTL, but here again extensive rejoining removes nearly 75% of the initial DSB load 24 h after IR. These results confirm the observations of human cells in the Chinese hamster background and indicate a robust function of B-NHEJ even when repair is assayed by LTL.

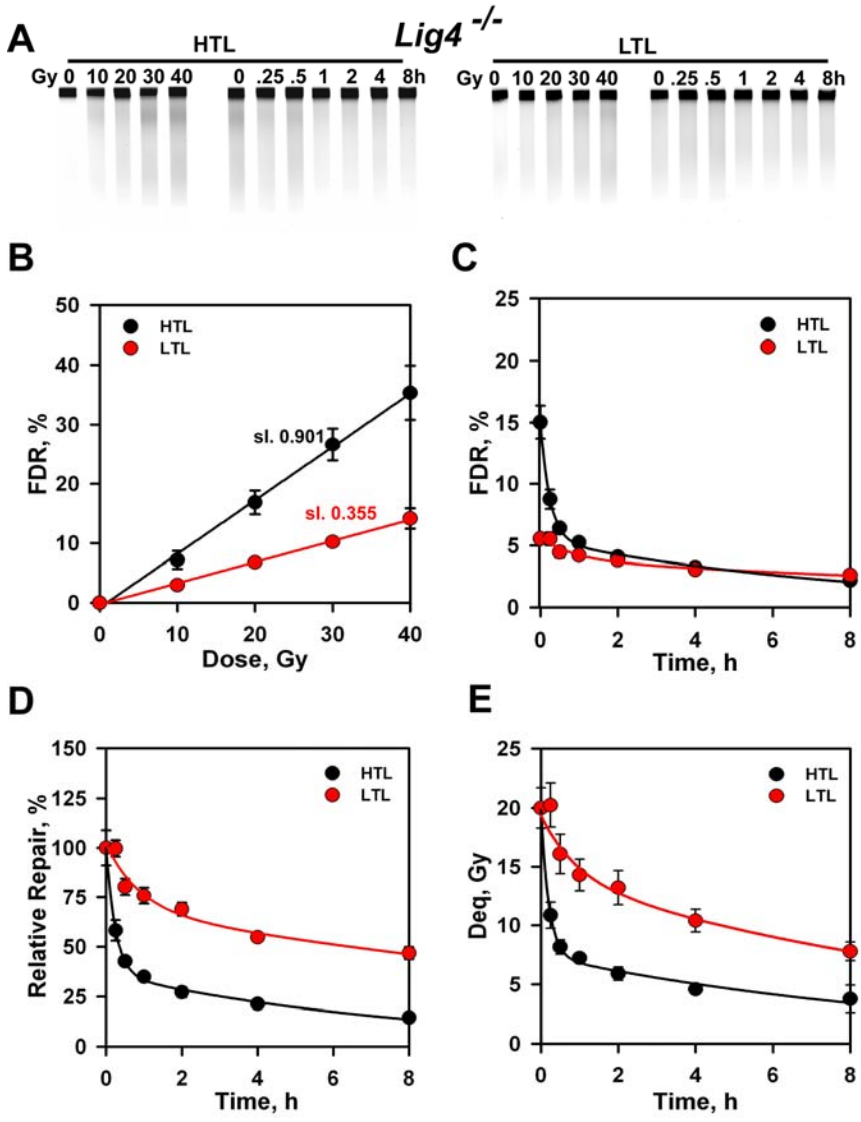

Figure 3.26: Dose response and repair kinetics of IR induced DSBs in *LIG4*$^{-/-}$ MEFs after HTL or LTL. Exponentially growing MEFs were used for experiments. Other details are as in the legend of Figure 3.24.

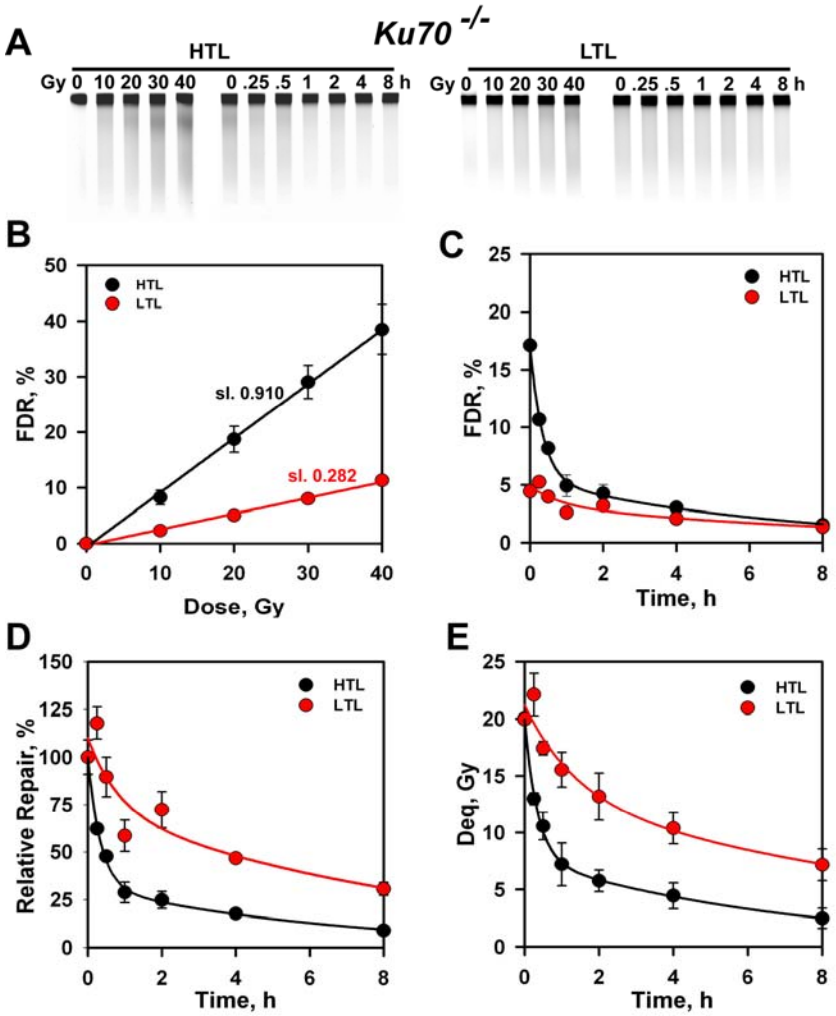

Figure 3.27: Dose response and repair kinetics of IR induced DSBs in Ku70$^{-/-}$ fibroblasts after HTL or LTL. Exponentially growing MEFs were used for experiments. Other details are as in the legend of Figure 3.24.

For a more comprehensive evaluation across species of the effect of lysis conditions on the induction and rejoining of IR-induced DSBs, we tested mouse cells with defects in components of D-NHEJ other than DNA-PKcs. Figure 3.27 summarizes results obtained with *Ku70*$^{-/-}$ MEFs. The dose response results shown in Figure 3.27B indicate a surprising 75% contribution of HLS to the DSB load measured under HTL. This species specific contribution of HLS to the DSB load points to species specific parameters in the induction of HLS and their transformation to DSBs. Similar to observations with other D-NHEJ deficient mutants, rejoining of DSBs is reduced under LTL in *Ku70*$^{-/-}$ cells. However, here again extensive rejoining is observed removing nearly 75%

of the initial DSB load within 8 h. Qualitatively and quantitatively similar results are also obtained with *LIG4*$^{-/-}$ MEFs and are summarized in Figure 3.26. Collectively, the above results point to markedly altered kinetics of DSB rejoining in D-NHEJ deficient cells under LTL, but demonstrate for all examined cases extensive DSB rejoining, which is compatible with DSB processing by B-NHEJ.

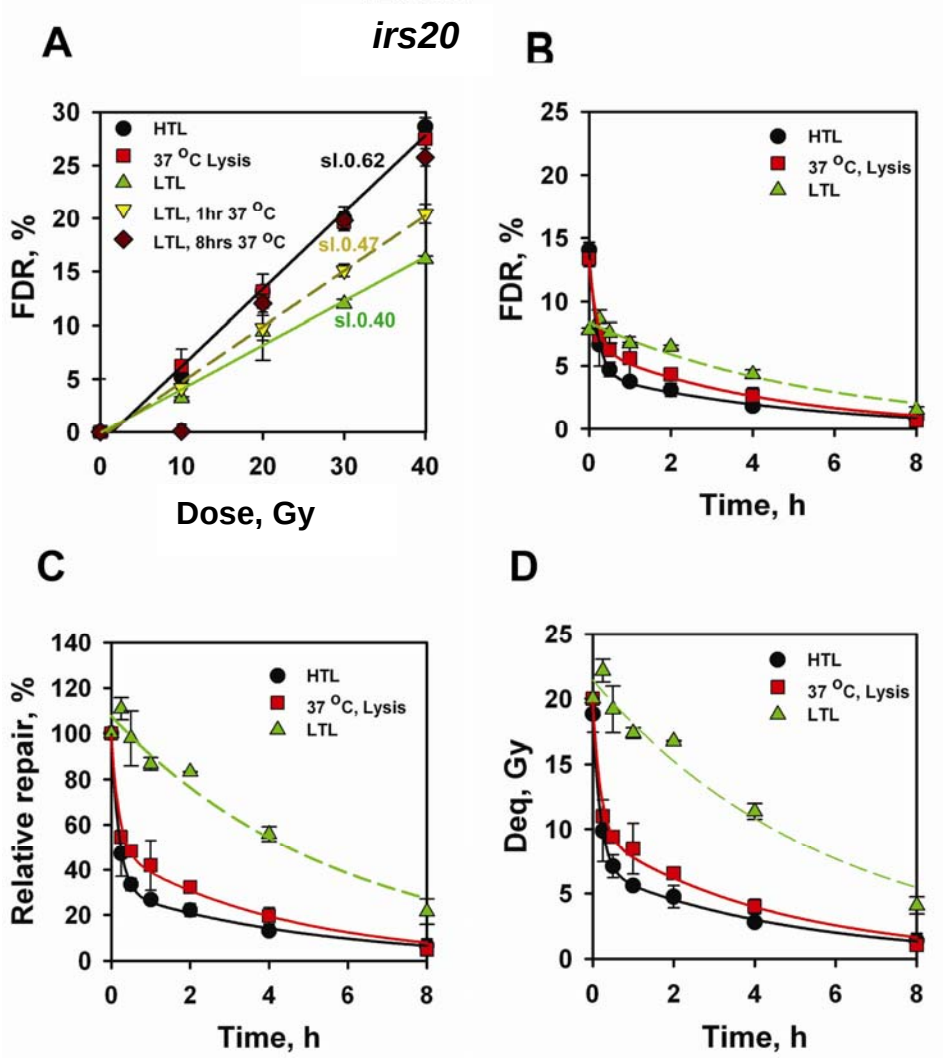

Figure 3.28: Dose response and repair kinetics of radiation induced DSBs in DNA-PKcs deficient Chinese hamster mutant *irs20* cells after lysis at 37°C. Exponentially growing *irs20* cells were treated using a lysis protocol as during low-temperature lysis that included incubation at 37°C for different periods after exposure to 20 Gy. Results obtained with high-temperature lysis are also shown. Other details are like in the legend of Figure 3.24. Results from seven determinantions in two experiments are shown.

3.5.2. Lysis at 37°C is equivalent to HTL

The arguments presented on HLS and their contribution to the DSB signal are formulated on the premise that the transformation of HLS to breaks only occurs during incubation at 50°C and that therefore the DSBs they indirectly generate are artifact in the sense that they will not form in a cell growing under physiological conditions (Rydberg, 2000; Stenerlöw et al., 2003). However, early work using plasmid DNA suggests a substantial sensitivity of HLS to 37°C or even to 20°C (Jones, Bowell, and Ward, 1994). Since the normal growth temperature of the cell lines used here is 37ºC, we inquired on the effect of lysis at this physiological temperature on the induction and rejoining of DSBs. Figure 3.28 summarizes results obtained with the *irs20* mutant. It is notable that the dose response curves measured after lysis at 37ºC are indistinguishable from those measured after HTL. This observation suggests that full transformation of HLS to breaks takes place during incubation for lysis at the physiological temperature of 37ºC, and that this transformation is not the specific characteristic of 50ºC lysis. Also the repair kinetics measured after lysis at 37ºC is indistinguishable from that seen after HTL, again pointing to the fact that HTL is not detecting artifacts of high temperature events, but rather events that may also occur at 37ºC, the standard temperature of cell growth.

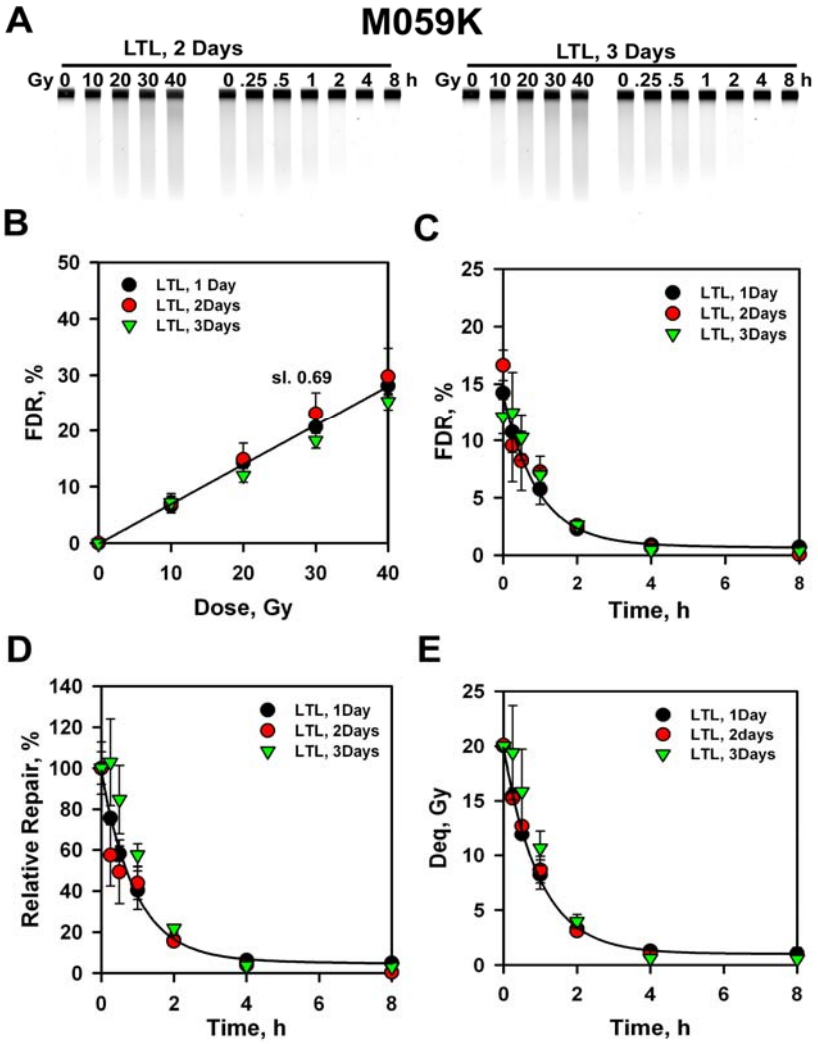

Figure 3.29: Dose response and repair kinetics of IR induced DSBs in human DNA-PKcs proficient M059K after LTL for different duration. Exponentially growing M059K cells were treated using the LTL protocol that was modified to prolong the first lysis step with non-ionic detergent and protease from one to two or even to three days. Other details are as in the legend of Figure 3.24.

3.5.2.1. Effect of lysis on dose response and repair kinetics

One could argue that some of the differences seen in the dose response and the DSB rejoining kinetics under LTL derive from incomplete lysis. Although this aspect has been extensively studied by the investigators who developed the LTL protocol (Stenerlöw et al., 2003) we wished to ensure that incomplete lysis does not present a problem in our experimental systems. Experiments carried out with M059K and M059J cells, respectively, in which the initial step of

incubation with detergent and protease was prolonged from one to two and even to three days, showed that extending this initial lysis step confers no further improvement. This result confirms that incomplete lysis is unlikely to contribute significantly to the differences in response seen after LTL and HTL. (Figure 3.29 and 3.30)

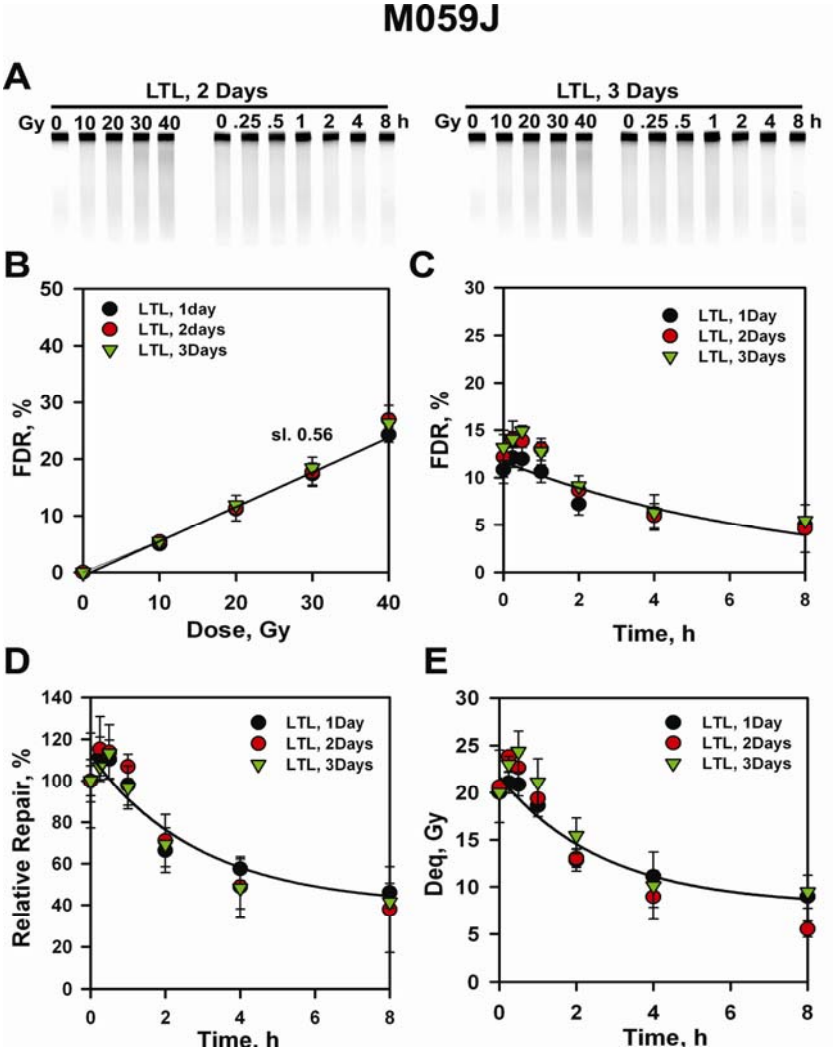

Figure 3.30: Dose response and repair kinetics of IR induced DSBs in human DNA-PKcs proficient M059K after LTL for different duration. Exponentially growing M059K cells were treated using the LTL protocol that was modified to prolong the first lysis step with non-ionic detergent and protease from one to two or even to three days. Other details are as in the legend of Figure 3.24

3.5.3. Estimation of HLSs induction at 37°C in naked DNA and in intact cells during repair

IR induces a variety of sugar adducts (SAs), one class (termed for convenience here SA-1) is associated with the relatively prompt disruption of the sugar phosphate backbone and leads to the formation of a single strand break (SSB). However, there is also evidence that IR induces a second class of SAs (to be termed here SA-2s), that are not immediately disrupting the sugar-phosphate backbone but which display increased chemical lability manifest as thermal lability. As a result of this thermal lability, SA-2s can lead to the formation of delayed SSBs in a manner that depends upon the post-irradiation incubation temperature and possibly also the chemical environment in the vicinity of the lesion.

SA-1s and SA-2s can be induced in random combinations within the clustered damage sites (CDS) induced by clusters of ionizations and the simultaneous presence of the resulting SSBs in opposite DNA strands will lead to the formation of DNA double strand breaks (DSBs).

3.5.4. Conversion of HLSs induced in intact cells into DSBs *in vitro*

We sought to develop protocols allowing studies of the thermal stability of SA-2s under in vitro conditions to ensure optimal control of the experimental conditions. We reasoned that SA-2s induced in irradiated cells that have been processed using LTL, should remain in the naked DNA after completion of lysis. First, we inquired whether such SA-2s retain their lability to an in vitro exposure to 50ºC. The results obtained with *LIG4*$^{-/-}$ cells are summarized in Figure 3.31. When cells embedded in agarose blocks are irradiated, subject to LTL and exposed subsequently to 50ºC in TEN buffer an increase in FDR is observed with time that reaches a plateau at about 8 h. This result demonstrates that SA-2s are preserved under LTL and can be converted to DSBs after exposure of the naked DNA to high temperature (Figure 3.31). The FDR levels reached at the plateau are only 20% lower than those measured after HTL (broken line in the figure) suggesting that over 80% of SA-2s contributing to DSBs under HTL are also converted to DSBs under the experimental conditions employed. The increase in FDR is radiation specific, as it is not observed in non-irradiated cells that have been similarly treated. These observations demonstrate that LTL preserves SA-2s at a chemical state still amenable to thermal conversion to DSBs by incubation

in vitro, and validate conditions to investigate SA-2 lability at different temperatures.

We next inquired whether SA-2s preserved in the DNA by LTL can cause DSBs after incubation at 37ºC. Notably, incubation of irradiated, protein-free DNA at 37ºC also causes a substantial increase in FDR, although the kinetics are slower and the final levels reached slightly lower than those measured after incubation at 50ºC. Here again, the increase in FDR is radiation specific, as it is not observed in non-irradiated cells.

3.5.5. Thermally unstable sugar adducts are induced after irradiation of naked DNA

Damage induced by IR is modulated by the packaging of DNA into chromatin with the help of histone and non-histone proteins. We inquired whether the induction and thermal sensitivity of SA-2s is altered when protein-free DNA obtained by LTL of non-irradiated *LIG4*$^{-/-}$ cells is exposed to IR and subsequently tested at different temperatures. Figure 3.32 summarizes the results obtained. It is evident that in non-irradiated cells incubation at different temperatures has no detectable effect on the integrity of the DNA. IR induces in naked DNA DSBs more effectively that in DNA packaged in chromatin as indicated by the higher FDR values measured at half the dose of IR. Direct comparison with the results shown in Figure 3.31 suggests that under these conditions about five times more DSBs are induced per unit of radiation dose.

There is no increase in FDR when DNA is maintained after irradiation either at 4ºC, 10ºC, or 20ºC. Incubation, on the other hand, of irradiated DNA at 50ºC causes a pronounced increase in FDR that reaches a plateau at 24 h. This result clearly demonstrates the induction of SA-2s by IR in naked DNA and confirms their thermal conversion to DSBs at 50ºC. Notably, here again, incubation at 37ºC causes an increase in FDR only slightly slower and only about 20% lower than that observed at 50ºC. Thus, large changes in DNA organization, which confer dramatic increases in the yield of DSBs, have no pronounced influence on the spectrum and the thermal stability of the induced SA-2s. Results similar to those obtained with *LIG4*$^{-/-}$ cells were also derived with M059K cells supporting the generality of the observation (data not shown).

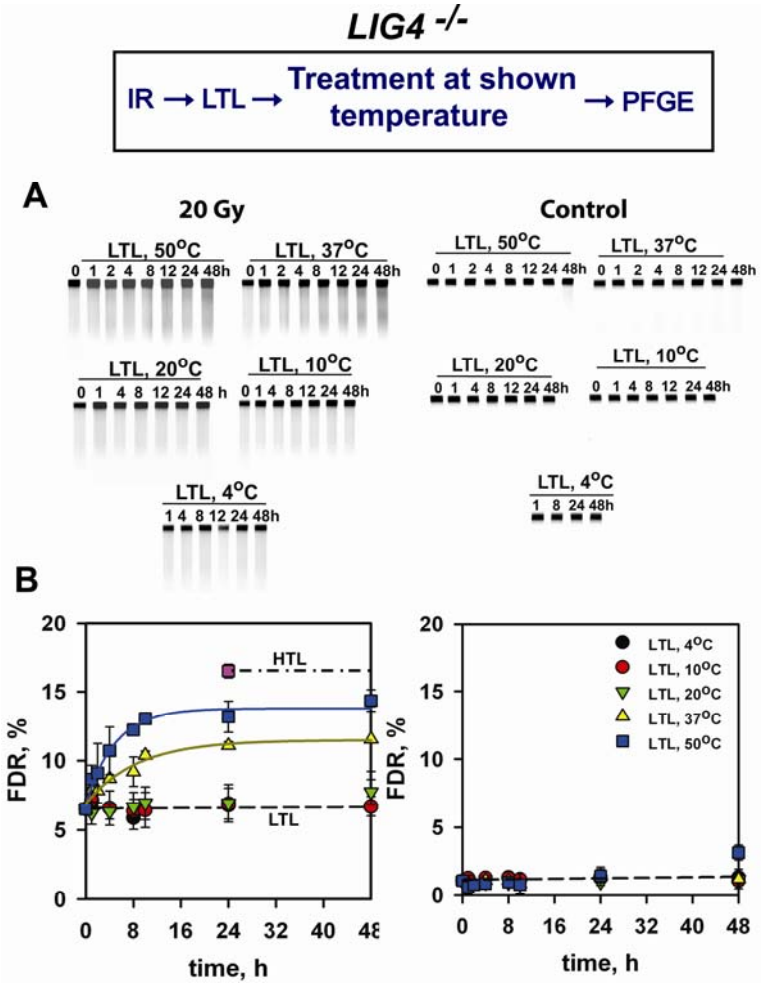

Figure 3.31: Conversion of HLSs induced in irradiated cells to DSBs by incubation of lysed DNA at elevated temperatures. *LIG4*$^{-/-}$ cells were embedded into agarose, irradiated at 20 Gy and lysed using the LTL protocol. Subsequently, they were treated at the indicated temperatures and times in TEN buffer and analyzed by PFGE. Result represents the average from six determinations in two experiments.

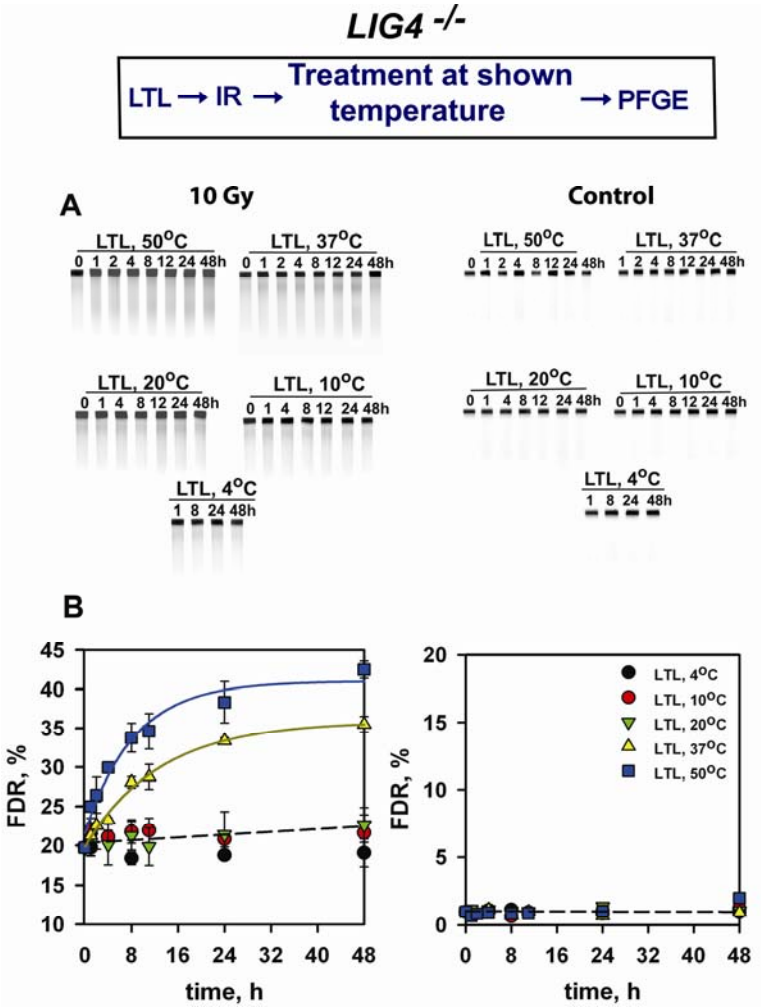

Figure 3.32: Induction of HLSs in irradiated lysed DNA. *LIG4*$^{-/-}$ cells were embedded in agarose, lysed using LTL, and irradiated. Thereafter agarose blocks were incubated at different temperatures and times in TEN buffer and analyzed by PFGE. Result represents the average from six determinations in two experiments.

3.5.6. Protein during incubation at elevated temperatures accelerates SA-2 conversion

The above results clearly demonstrate that SA-2s are converted to DSBs at 37ºC, which suggests that the same should happen in the repairing cell. However, the 5-10 h half times for chemical transformation of SA-2 lesions to SSBs indicated in the above experiments, would suggest a rather slow production of DSBs in the repairing cell. Yet, the changes in the kinetics of DSB removal observed in D-NHEJ deficient cells are compatible with kinetics of conversion occurring much faster. Is it possible that the intracellular conversion of SA-2s to DSBs is more efficient

than that measured in naked DNA?

We inquired first whether the presence of protein accelerates this response. For this purpose we prepared cells using a protocol previously developed for cell sorting. Cells are incubated in solution with triton X-100 that stops all biological functions in the cell, such as DNA repair etc., but retains the form and DNA integrity of the cells, which can still be sorted as independent entities and analyzed for DNA damage. In this experiment irradiated agarose blocks were incubated in TEN + 0.2% triton X-100 for given period of time at the indicated temperature and after completion of incubation, blocks were lysed by standard low temperature lysis protocol. Figure 3.33 summarizes the results obtained in TEN with triton X-100 buffer and indicates a conversion of SA-2s to DSBs that appears nearly complete in about 2 h. Thus, conversion of SA-2s to DSBs is strongly dependent on the presence of proteins in the vicinity of the DNA, which alter the chemical environment of the lesion.

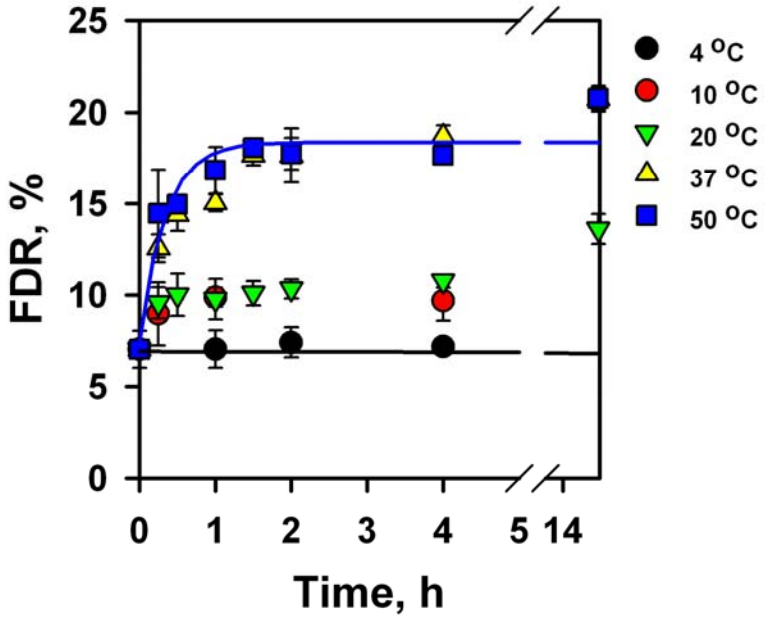

Figure 3.33: Conversion of HLSs in chromatin bound DNA. *LIG4*$^{-/-}$ cells were embedded in agarose after exposure to 20 Gy and were subsequently treated in TEN buffer containing 0.2% tritonX-100. Agarose blocks were incubated at different temperatures and times, lysed by LTL and analyzed by PFGE. Result represents the average of six determinations in two experiments.

3.6. Effect of high LET radiation on the repair of DSBs by B-NHEJ

3.6.1. Induction of HLSs by heavy ions

When charged Fe or Ni ions of energy of 1 GeV pass through cells they create locally multiply damaged sites (LMDS) in DNA. Because of the high LET of about 150 keV/µm, heavy ions deposit a large amount of energy in a much more localized area of chromatin. We addressed therefore the question as to what happens to HLSs with increase in LET. (Figure 3.24, 3.25, 3.26)

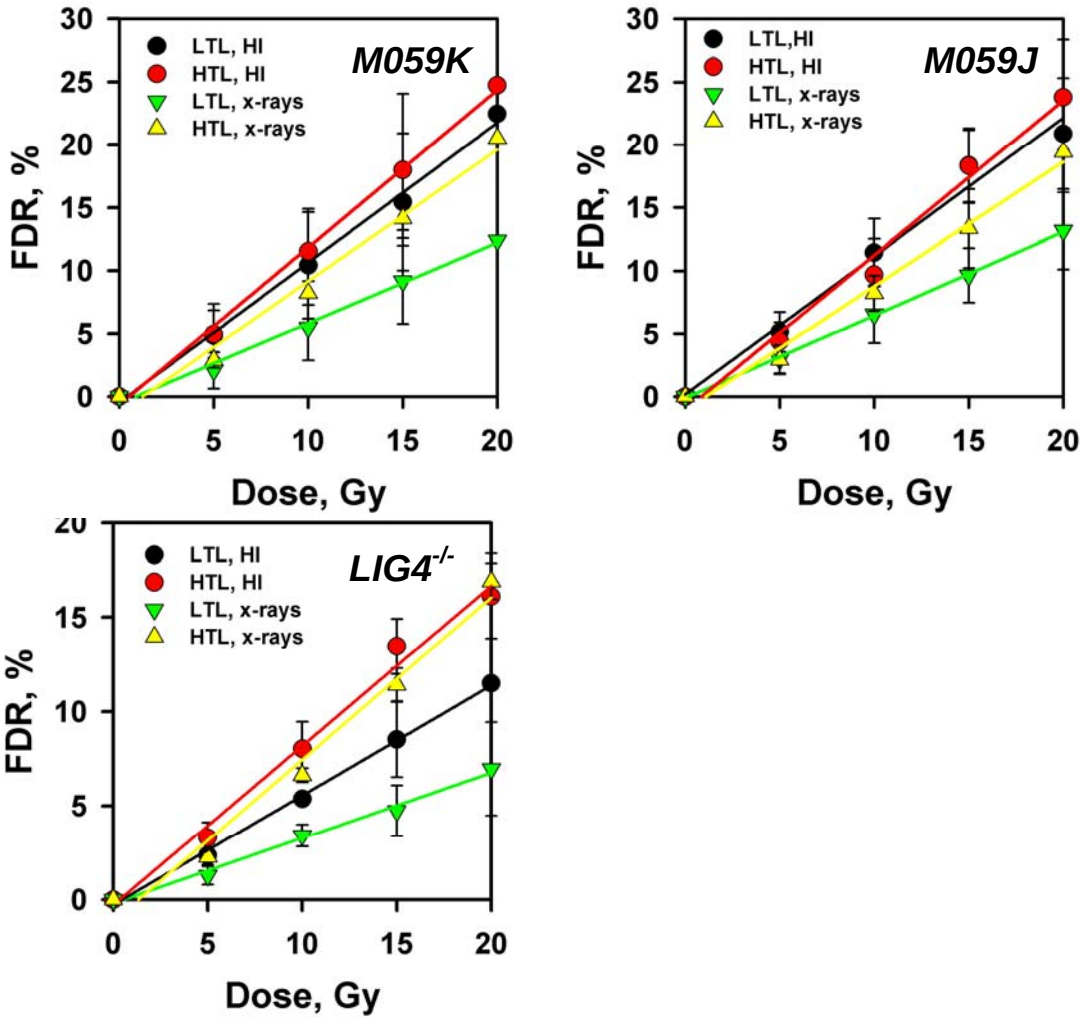

Figure 3.34: **Dose response curves for DSB induction in different cell lines after exposure to heavy ions.** Agarose blocks were prepared from exponentially growing cells and irradiated with heavy ions of 1GeV energy (Fe ions). Irradiated agarose blocks were lysed by HTL or LTL and analyzed by PFGE. Results presented are the average of six determinations in two experiments.

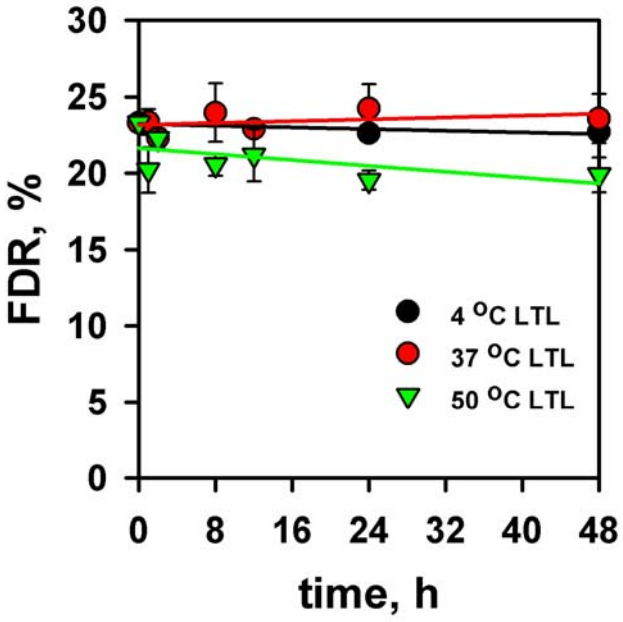

Figure 3.35: Conversion of HLSs at different temperatures after heavy ion irradiation. Agarose blocks were prepared from exponentially growing M059K cells and exposed to 15 Gy of heavy ions. Blocks were lysed by LTL and incubated at different temperatures as indicated. Results shown are the average and standard deviation from four determinations in one experiment.

We used exponentially growing cells for agarose block preparation and irradiated them with heavy ion of 1 GeV (Fe and Ni ions) at different doses. After irradiation, blocks were lysed by LTL or HTL and FDR was measured by PFGE. The difference between HTL and LTL was much smaller in the case of heavy ions as compared to X-rays. This can be explained by the complexity of DNA lesions generated by heavy ions that make more localized breaks that mask the effects of HLSs (Figure 3.32).

Similarly, when M059K cells were irradiated in agarose, lysed by LTL and treated at different temperatures for the indicated periods of time, there was no extra formation of DSBs by conversion of HLS in the case of heavy ion irradiation, even at 50^{o}C. In contrast, after exposure to X-rays a significant generation of DSBs by HLSs conversion was observed at elevated temperatures (Figure 3.29 and 3.32).

3.6.2. Effect of lesion complexity on B-NHEJ efficiency

Heavy ions generate extensive localized damage in the DNA possibly even disrupting chromatin locally. It is possible that this affects the efficiency of B-NHEJ. Therefore, we examined *LIG4*$^{-/-}$ and wt MEFs, for repair by B-NHEJ after heavy ion irradiation. Repair was slow after heavy ion irradiation (15Gy). The effect of high LET on repair was stronger for B-NHEJ as compared to D-NHEJ. Whereas in case of LTL where we used relative repair compare to 0 h time point, because dose response curve does not represent real *in vivo* induction of DSBs. The effect of high LET on repair was stronger for *LIG4*$^{-/-}$ cells as compared to wt cells. The repair kinetics of *LIG4*$^{-/-}$ cells after LTL did not show the typical kink at early time points (see results in Figure 3.24 and 3.26). This observation is in line with the above reported lack of DSB generation by HLS conversion after exposure to heavy ions (Figure 3.35).

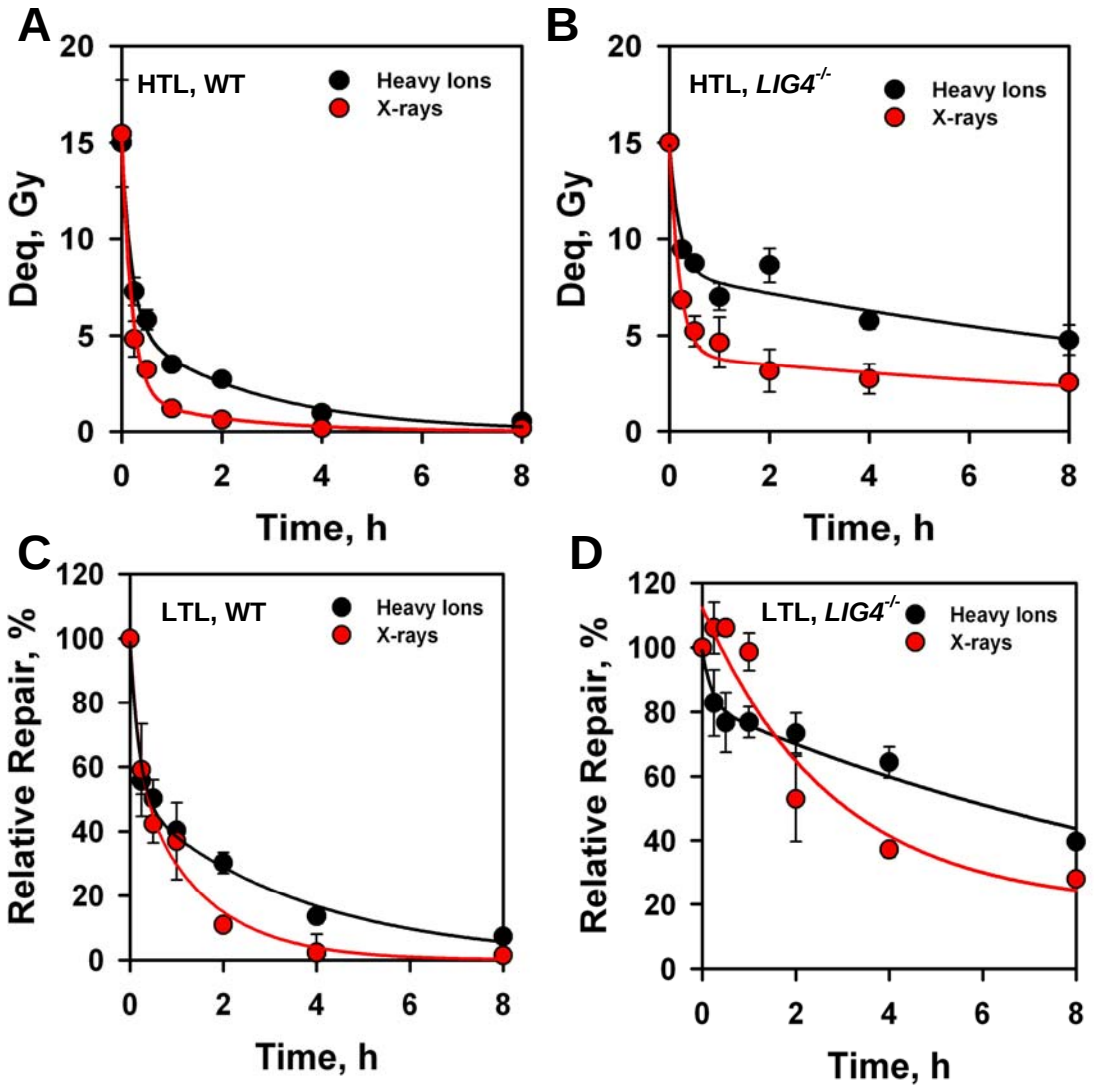

Figure 3.36: Effect of lesion complexity on B-NHEJ efficiency. Exponentially growing wt, *LIG4*$^{-/-}$ MEFs cells were irradiated with 15 Gy heavy ions (1 GeV, Ni) and X-rays. After irradiation samples were processed by HTL (A and B) or LTL (C and D) protocol and analyzed by PFGE. Figure A and show dose equivalent where as Figure D, E and F show relative repair compare to 0 h time point. Results represent the average and the standard deviation from 4 determinations in one experiment.

4. Discussion

4.1. The function of B-NHEJ is enhanced in G2

4.1.1. Background

Double strand breaks (DSBs) in DNA are severe lesions which if unrepaired or misrepaired can lead to cell death, mutation or transformation. Cells have therefore (Hendrickson et al., 1991; van Gent, Hoeijmakers, and Kanaar, 2001b) developed efficient mechanisms to repair this type of lesion and restore genomic integrity. Molecular processes with the potential of repairing DNA DSBs include homologous recombination repair (HRR) and non-homologous endjoining (NHEJ). Details about these two repair mechanism were described in detail in the introduction.

While bacteria and lower eukaryotes utilize almost exclusively HRR for the removal of DSBs, higher eukaryotes use extensively NHEJ. Although the function of NHEJ is well documented in all model systems examined, the function of HRR remains poorly defined. However, its involvement is indicated by a series of observations including the radiation sensitivity of the mutants with defect in proteins implicated in this repair pathway (Hoeijmakers, 2001; Rothkamm et al., 2003), by abundance and regulation of these proteins throughout the cell cycle, as well as loss of S-phase dependent radioresistance in cells with defects in this repair pathway (Cheong et al., 1994; Rothkamm et al., 2003). A common assumption is that cells in higher eukaryotes utilize NHEJ throughout the cell cycle, but HRR only occurs during S and G2-phase where the sister chromatid can serve as the homologous template (Lee et al., 1997).

Despite the opportunity for HRR in S and G2-phase, mutants with defects in HRR, such as those with defect in Rad54, Xrcc2, Xrcc3, Brca1 and Brca2, show nearly normal kinetics of DSB repair in the exponential phase (Cheong et al., 1992; Jones, Stewart, and Thompson, 1990; Wu et al., 2008). However, it remained possible that the HRR contribution remains undetectable because it is confined in S and G2-phase of the cell cycle. To address this question, results are required on the repair kinetics in specific phases of the cell cycle. This work, specifically address this important issue.

The question of the relative involvement of HRR and NHEJ in the repair of IR induced DNA DSBs has been the focus of our laboratory during the last several years and a significant amount

of work has been carried out along these lines. Since the repair kinetics of IR induced DSBs is biphasic with a fast and slow component (Wang et al., 2003; Wang et al., 2001a), and because defects in NHEJ mainly compromise the fast component (DiBiase et al., 2000; Nevaldine, Longo, and Hahn, 1997; Wang et al., 2001a; Wang et al., 2001b), it was speculated that the slow component reflects HRR. This was in line with the slow kinetics of DSB rejoining observed in yeast, which mainly utilize HRR to remove DSBs from their genome. Nevertheless, an extensive study utilizing mutants of DT40 cells with defects in various genes involved in HRR, failed to demonstrate an obvious defect in the rejoining of DSBs using PFGE. This was the case even under condition where NHEJ was also compromised by a mutation in Ku. The results of these genetic studies led us to propose that the slow component of the kinetics of DSB rejoining does not reflect HRR, but rather yet another form of NHEJ that acts as a backup to the main DNA-PK dependent pathway of end joining. We termed the DNA-PK dependent pathway of end joining D-NHEJ and the backup pathway B-NHEJ.

Recent work from our laboratory implicates DNA ligase III in B-NHEJ and suggests that PARP-1 may also play a role in the process. Proteins consisting of PARP-1/DNA ligase III /Xrcc1 are also known to be involved in the repair of single strand breaks (Audebert, Salles, and Calsou, 2004; Caldecott et al., 1994; Wang et al., 2005) , as well as of base damages. Hence, these observations suggest that the cell recruits to rejoin DSBs repair components primarily used for the processing of other forms of DNA damage.

Taking this into consideration, it was important to establish that the lack of phenotype was not due to the phase of the cell cycle the cells were tested. Therefore it became essential to develop methodology that allowed evaluation of DSB repair in specific phases of the cell cycle.

4.1.2. Methodology

There are several ways to synchronize cells in different phases of cell cycle like Mitotic shake-off (Hill et al., 1999), use of DNA synthesis inhibitors that are applied once or twice to obtain cell populations synchronized at the beginning of the S-phase, and centrifugal elutriation. Each of these techniques has their own limitations.

Considering the limitations of cell synchronization methods, we introduced cell sorting in our studies to obtain results from cells after minimum disturbance and in the absence of any treatment

with chemicals that perturb normal cell cycle progression. As a first step we sorted cells in G1 and G2 phase of cell cycle. We confirmed that the method required for cell staining and subsequent sorting did not induce DNA damage in non-irradiated cells, but stopped repair of DSBs in irradiated cells. These characteristics were essential for the success of proposed experiments.

For experiments described here the following aspects should be considered. After exposure to high dose of IR a strong arrest in G2 will almost completely stop cell division for the entire duration of the experiment. As a result, there will be no new arrivals in the G1 cell population, and sorted G1 cells at all time points will be cells irradiated in G1 phase. The situation is more complex for cells sorted in G2. Cells sorted in G2 will be blocked in G2 by the activation of the G2 checkpoint. However, because the S-phase delay is short, cell irradiated in late S-phase will start entering G2 with progressing repair time. As a result, G2 populations analyzed for repair after 2-4 h will contain both cells irradiated in G2 as well as cells irradiated in late S-phase. For late time points (8 h), it is even possible that cells irradiated in early S and even G1 will have reached G2 phase. This progression of cells from earlier phases of the cell cycle to G2 is one of the reasons why repair was followed only up to 8 h in our experiments.

Interpretation of the results obtained is further facilitated by the fact that PFGE allows for a reliable estimate of DSB rejoining. This is because the method assays for the physical rejoining and not for events indirectly associated with DSB processing, such as for example the phosphorylation of H2AX. Since, gel electrophoresis is complicated when secondary structures such as replication forks and bubbles are present, we avoided analyzing S-phase cells.

4.1.3. HRR throughout the cell cycle

The results of the experiment described in figure 3.2 suggest a marginal, at best, contribution of HRR to the removal of IR induced DSBs from the genome of vertebrate cells and therefore, to the slow component of rejoining in asynchronous cells, as well as in cells sorted in G1 and G2 phase of the cell cycle. First, rejoining of DSBs occurs with wild-type kinetics in the *Rad54*$^{-/-}$ mutant despite the fact that the *Rad54* gene is an important component of the *Rad52* epistasis group of genes (Takata et al., 1998), Indeed its mutation leads to increased radiosensitivity in S and G2-phases of the cell cycle (Essers et al., 2000; Takata et al., 1998), *Rad54*$^{-/-}$ MEFs are defective in telomere maintenance (Jaco et al., 2003), and *Rad54*$^{-/-}$ stem cell are defective in gene

conversion (Dronkert et al., 2000). Despite all this, cells repair IR induced DSBs essentially completely and show no measurable difference when compared to wild type cells. It is relevant to point out that this is true not only when repair is measured in asynchronous cell populations but also when measured in the G1 or G2 phase. These results are consistent with results reported with *Xrcc2* and *Xrcc3* cells, which show similar repair kinetics to their wild type counterpart (Asaad et al., 2000).

Of course, the above results could be interpreted as indicating that HRR cannot be involved in a significant way in the repair of IR induced DSBs in the presence of an active D-NHEJ system. Therefore, we examined the double mutant that carries defects both in the *Rad54,* as well as in the *LIG4* genes. The observation that the repair kinetics of the double mutant is very similar to that of the single mutant *LIG4*$^{-/-}$, suggests that a measurable contribution of HRR cannot be found even when D-NHEJ is compromised.

The lack of a detectable role for HRR in the repair of IR-induced DSBs is in apparent contradiction with genetic studies indicating a contribution of HRR in cell radiosensitivity to killing (Hoeijmakers, 2001; Rothkamm et al., 2003). Combination of these observations to those presented here leads us to propose that HRR either handles a very small subset of highly lethal DSBs, or, that it is recruited after initial stage of rejoining.

4.1.4. Enhanced function of B-NHEJ in G2

D-NHEJ is known to proceed with fast ($t_{1/2}$: 10-30 min) repair kinetics, and to require among other factors DNA-PK, Ku, DNA Ligase IV and XRCC4 (Wang et al., 2003; Wang et al., 2001a). In IR-induced cell killing experiments D-NHEJ deficient cells showed pronounced radiosensitivity throughout the cell cycle but were relatively more radioresistant in late S/G2 than in G1(Lee et al., 1997; Rothkamm et al., 2003). Therefore, D-NHEJ is thought to be the predominant repair pathway in the G1 phase of the cell cycle (Metzger and Iliakis, 1991). Results presented in previous section (figure 3.3) confirmed this expectation by showing that D-NHEJ mutants tested in G1 show a clear defect in DSB rejoining. It should be emphasized, however, that this defect is not associated with a complete deficiency in DSB repair, but rather with a reduction in the contribution of the fast component of end joining. Indeed, despite this defect, cells remove a substantial proportion of IR-induced DSBs utilizing backup pathways (B-NHEJ) that remain unaffected by mutation in these proteins (Wang et al., 2003; Wang et al., 2001a) .

It is particularly interesting that D-NHEJ mutants showed, specifically in G2 phase, a greater ability to repair DSBs than in G1. This observation suggests that backup pathways are more active in G2. This possibility is in line with the reduced radiosensitivity of *LIG4*$^{-/-}$ mutants in G2 phase of the cell cycle.

Although other studies (Lee et al., 1997) have reported similar repair kinetics for DSBs in G1 and G2, it should be noted that these studies employed synchronization methods that do not allow high level of homogeneity during G2 phase. The observations discussed here and those presented above for HRR suggest that D-NHEJ is important throughout the cell cycle. However, when it becomes compromised, backup pathways rather than HRR take over and operate more efficiently in the G2 phase of the cell cycle.

4.2. Marked dependence on growth state of B-NHEJ

Our earlier work has shown a marked reduction in the efficiency of DSB rejoining in *LIG4*$^{-/-}$ cells after transition from the exponential phase to the plateau phase of growth. Since a difference in the ability of wt cells to repair DSBs is not detectable under similar conditions, we concluded that the dependence of B-NHEJ on growth state is stronger than that of D-NHEJ. The reduction in DSB repair efficiency after transition into the plateau-phase of growth may derive from the accumulation of cells in G1 phase, from the reduction in growth factor signaling in plateau-phase cultures, or both. To answer this question, we centrifugally elutriated populations of G1 cells from exponential and plateau phase culture and tested them using PFGE. Interestingly, we found that G1 populations derived from plateau-phase cultures are less efficient in DSB rejoining compared to exponentially growing populations (Windhofer et al., 2007). These results implicate reduction in growth signaling as the major determinant of the observed effect.

4.2.1. Growth state as a determinant of B-NHEJ efficiency

The results presented here extend our previous investigations on the subject in a number of important ways. Firstly, *Ku70*$^{-/-}$ and *Ku80*$^{-/-}$ MEFs, as well as *XRCC4* deficient CHO cells show compromised function of B-NHEJ under conditions of reduced growth. This phenotype indicates the general character of the response regardless of the mutation in D-NHEJ and documents the extensive contribution of B-NHEJ under normal conditions. The conspicuous and quite puzzling exception with DNA-PKcs mutants suggests important regulatory components of the response.

Secondly, D-NHEJ mutants of CHO, MEF and humans showing similar response demonstrated that the effect is not species specific. Thirdly, it interesting that B-NHEJ uncovered in repair proficient cells treated with chemical inhibitors of D-NHEJ responds to growth conditions as B-NHEJ functioning in D-NHEJ mutants. This aspect shows a direct relevance to the clinical application of these inhibitors. This is because previous studies have failed to implicate HRR in the removal of DSBs under conditions that compromise D-NHEJ (Wang et al., 2001a). Since a difference in the ability of wt cells to repair DSBs is not detectable under the conditions employed here (see below for further discussion of this topic), we concluded that the dependence of backup pathways of NHEJ on growth state is larger than that of D-NHEJ.

It was observed that the fraction of DSBs rejoining in *LIG4*$^{-/-}$ MEFs is reduced when tested at high radiation doses (e.g. 80 Gy) in the plateau phase of growth. These results confirmed earlier reports of severely limited DSB repair activity in *LIG4*$^{-/-}$ (Riballo et al., 2004) cells that would otherwise have been incompatible with our results at lower radiation doses (in the range of 20 Gy) in actively growing cells.

4.2.2. Dependence of D-NHEJ on growth state

The resolution of our measurements here was not sufficient to detect effects on D-NHEJ as wt cells enter into the plateau-phase of growth. However, earlier work indicates a measurable reduction in the half times of DSB rejoining in repair proficient cells studied in the plateau phase of growth, as compared to exponentially growing cells, or cells irradiated in various phases of the cell cycle (Metzger and Iliakis, 1991). The difference between our previous study and the present results may reflect differences in the cells used, but it can also be due to the lower resolution in the repair kinetics of the experiments presented here.

More recent work directly links growth factor signaling with DSB repair in repair proficient cells, which also provides a connection to D-NHEJ. Thus, cells overexpressing EGFR or showing a constitutive activation of this growth factor receptor are frequently radiation resistant (Baumann and Krause, 2004; Schmidt-Ullrich et al., 2003), which indirectly suggests a higher capacity for DSB repair. Additional work provides clues into some of the underlying mechanisms by showing a reduction in the ability of cells to repair DSBs when signaling through the EGFR receptor is blocked in a *k*-Ras mutant. The intriguing explanation for the latter effect is that, inhibition is mediated by a direct interference with the function of DNA-PK, the central component of D-

NHEJ (Dittmann et al., 2005; Dittmann, Mayer, and Rodemann, 2005; Toulany et al., 2006; Toulany et al., 2008). Radiation induced PI3K/Akt signaling promotes DNAPKcs activity and consequently enhances repair of DSBs (Toulany et al., 2006). These observations suggest multiple connections between growth signaling and various pathways of DSB rejoining that are likely to have important implications for cells radiosensitivity to killing.

4.2.3. B-NHEJ is not compromised in DNA-PKcs$^{-/-}$ cells at plateau phase of growth

As results from Figure 3.9 have clearly shown that DNAPKcs mutants repair DSBs efficiently even in the plateau phase of growth. We have shown this effect in CHO DNAPKcs mutant cells like XRC1-3 and human glioma M059J cells. Both cell lines have mutant nonfunctional DNAPKcs with no kinase activity. M059J cells have a frameshift mutation and protein cannot be detected by Western blotting (Galloway et al., 1999; Lees-Miller et al., 1995). It is possible that this DNAPKcs mutant does not bind to DSBs and allows factors of B-NHEJ to be recruited at the DSB and take over its processing.

DNAPKcs interacts directly with Xrcc1 after IR. IR induced Xrcc1 expression in these cell lines depends on EGFR/MAPK/ERK pathway (Hagan, Yacoub, and Dent, 2004a; Toulany et al., 2006; Yacoub et al., 2001). The Xrcc1 level is lower in DNAPKcs mutants compared to WT and gets elevated after IR. However, Xrcc1 levels are strongly upregulated after IR in tumor cell lines like DU145 and LNCaP. IR induced *XRCC1* expression in these cell lines was described to be dependent on EGFR/MAPK/ERK pathway (Hagan, Yacoub, and Dent, 2004b; Yacoub et al., 2003; Yacoub et al., 2001).

4.2.4. Effect of growth factor signaling in double knockout of DNA-PKcs and Ku80

Existing data suggests that IR causes EGFR to migrate into the nucleus along with DNA-PKcs and with time DNA-PKcs concentration in the nucleus increases. But in absence of EGFR signaling, or following its blockage by a chemical inhibitor, an antibody, or a mutation in EGFR, DNA-PKcs fails to migrate into the nucleus and this causes mild radiosensitivity to killing. Our data indicate that this DNA-PKcs dependent effect is even stronger in the absence of D-NHEJ, but it is puzzling that *DNA-PKcs* is the exception in this rule. Indeed, in the absence of DNA ligase IV, XRCC4, Ku70 and Ku80 the effect of growth factor signaling is much stronger than in DNA-PKcs mutants. This suggests that even in the absence of all other components of D-NHEJ, DNA-PKcs somehow regulates the growth dependence of B-NHEJ.

In order to address this issue in greater depth, we tested the repair kinetics of double knockout cells i.e. *Ku80*$^{-/-}$*/DNA-PKcs*$^{-/-}$ MEFs. Comparison of the repair kinetics of *Ku80*$^{-/-}$ and *Ku80*$^{-/-}$*/DNA-PKcs*$^{-/-}$ cells in the exponential and plateau phase of growth, clearly showed the contribution of DNA-PKcs in the response as the double mutant was repairing better than Ku80$^{-/-}$ cells. Since in this study cells were mainly in the G1 phase of cell cycle where HRR cannot function, DNA-PKcs should somehow regulate B-NHEJ during growth.

4.2.5. Inhibition of D-NHEJ with inhibitor of DNA-PKcs allows the function of B-NHEJ in repair proficient cells

Next, we wanted to investigate the response of wt cells after chemical inhibition of D-NHEJ. For this purpose, we used wortmannin, a competitive inhibitor of DNA-PKcs that binds covalently at active site of the protein. We took human glioma cells, M059K and treated them with 20 µM wortmannin, a concentration that has been shown to impair DNA-PK activity (Sarkaria et al., 1998). Inhibition of DNA-PK by wortmannin allows the function of B-NHEJ and under these conditions B-NHEJ showed a growth state dependence similar to that of B-NHEJ functioning in D-NHEJ mutants. We confirmed this observation in CHO wt cells (data not shown). These observations are relevant for the clinical application of agents with a similar spectrum of activity in combination with radiation for the treatment of cancer.

Tumors, beyond a certain size, have a significant number of non-cycling cells, and it has been proposed that plateau-phase cultures, such as those tested here, are a useful model for tumors *in vivo* (Hahn and Little, 1972; Iliakis, 1988). In addition, recent strategies for improvement of tumor response to radiation consider the use of inhibitors and antisense oligonucleotides inhibiting the function of DNA-PK (Sak et al., 2002; Salles et al., 2006). Under conditions of inhibited DNA-PK, B-NHEJ is expected to gain influence and to remove radiation induced DSBs. The results presented here (Figure 3.10) with M059K cells showed an apparent increase in drug efficiency during the plateau-phase of growth that directly derives from the reduced function of B-NHEJ. Such response modulations could be exploited for the optimal application of drug and radiation in the clinical settings.

4.2.6. DNA-PKcs act as regulator of B-NHEJ in plateau phase of growth

By analyzing the above apparent discrepancies in the results from DNAPKcs mutants and wortmannin treated wt cells, mechanistic insights can be gained. Indeed, the results suggest a dominant negative effect of chemically inhibited DNA-PKcs (Allen, Halbrook, and Nickoloff, 2003; Calsou et al., 1999). Chemically inhibited DNAPKcs at the DSB can block further processing by alternative repair pathways. DNA-PKcs autophosphorylates itself to achieve detachment from the site of the DSB (Cui et al., 2005) after completion of the repair process. Interestingly, a kinase dead DNA-PKcs mutant showed the same phenotype as chemically inhibited DNA-PKcs in the plateau-phase of growth.

This experiment clearly shows a dominant negative effect of DNA-PKcs that affects B-NHEJ. To analyze this response further we tested mutants with defects in the DNA-PKcs autophosphorylation clusters ABCDE and PQR (Cui et al., 2005), These sites have been reported earlier to be involved in DSB repair regulation and DNA-PKcs with mutations at these sites are interesting as the mutant protein retains otherwise normal kinase activity. These mutants were suitable to test a function of autophosphorylation in B-NHEJ regulation during growth. The GG6 mutant shows slow repair kinetics in the exponential phase compared to wt, which reflects the role of this autophosphorylation in DSB repair. Repair of DSBs was compromised in GG6 cells in the plateau phase of growth but not to the extent seen in the kinase dead mutant. The PQR showed repair kinetics as wt cells with no difference in the kinetics between exponential and plateau phase of growth.

The ND-5 and JKD2 mutants have phosphomimicing forms of DNA-PKcs at their extreme N-terminal region and around 1000 amino acids from the N-terminus, respectively. The ND-5 mutant has very low kinase activity and robustly inhibits HRR but is absolutely dead in NHEJ assays. Interestingly in our DSB rejoining assay these cells repaired like wild type. In both growth states there was no difference in DSB repair capacity. The JKD2 mutant has wt kinase activity, but is unable to correct radiosensitivity to killing or V(D)J recombination. Alanine substitutions at these sites have a modest effect on NHEJ. In our PFGE experiments, the phosphomimicing JKD2 mutant shows repair kinetics similar to the kinase dead mutant. But, in the plateau-phase, these cells displayed stronger inhibition than the kinase dead mutant.

These data suggest that these DNA-PKcs domains are contributing functions that affect the handing over of DSBs to B-NHEJ. However, in none of the mutants, we found inhibition comparable to that of the kinase dead mutant in the plateau phase of growth. Thus, we need to speculate that additional regulatory modifications are required to the overall effect. Indeed, there are more than 30 autophosphorylation sites on DNA-PKcs and more work is required to elucidate their function.

4.2.7. D-NHEJ deficient cells show enhanced radiosensitivity in the plateau-phase of growth

We have shown before that when *LIG4*$^{-/-}$ cells reach the plateau phase of growth they become compromised in their ability to repair DSBs by B-NHEJ. Here we have shown that this growth-state dependent reduction in B-NHEJ efficiency leads to reduced cell survival. D-NHEJ deficient cells became radiosensitive as they moved into the plateau phase of growth. In order to evaluate the possibility that this effect is not due to the loss of radioresistant S-phase cells from plateau phase cultures we tested cell populations selected in different phases of the cell cycle. Highly enriched G1 and G2 cell populations from exponentially growing exponential and plateau phase cultures were generated by centrifugal elutriation and tested for radiosensitivity to killing. Interestingly, not only G1 but also G2 cells were also radiosensitive to killing when obtained from plateau phase cultures.

These results are in line with PFGE data showing that D-NHEJ deficient cells have reduced efficiency for B-NHEJ in the plateau phase of growth. There was no effect on the survival of wt cells when tested in the plateau phase of growth. However, there are reports that DNAPKcs interacts with EGFR after IR and that a small sensitization takes place when growth factor signaling is inhibited (Dittmann, Mayer, and Rodemann, 2005) Our results show for the first time a strong effect of growth factor signaling on B-NHEJ and the associated radiosensitivity to killing. Additional aspects of this response are discussed next.

4.2.8. Growth factor signaling and its effect on B-NHEJ

We have shown earlier that when *LIG4*$^{-/-}$ MEF cells move into plateau phase of growth they become compromised in B-NHEJ (Windhofer et al., 2007). We have shown earlier that when *LIG4*$^{-/-}$ MEF cells move into plateau phase of growth they become compromised in B-NHEJ

(Windhofer et al., 2007). In these experiments we used simple entry into plateau phase as a method of generating non cycling cells, which is not well defined. We tested here therefore serum deprivation as a more specific tool for generating non-cycling cells to study the dynamics of B-NHEJ in dependence to growth state. By specifically removing serum from exponentially growing cells for different periods of time is possible to inhibit cell growth by solely depriving cells from growth factors. Adding serum back, growth growth factor signaling pathways get activated. In a large set of experiments we observed that with increasing duration of serum deprivation in *LIG4*$^{-/-}$ cells, B-NHEJ efficiency was decreased. This decrease was initially proportional to the duration of serum deprivation, but reached a plateau at 24 h. Serum deprivation for up to 24 h has no effect on apoptosis via p38 MAPK signaling (Lu et al., 2008). Although the G1 fraction increased with increasing time of serum deprivation, we have shown earlier that this redistribution is not solely responsible for the effect observed (Windhofer et al., 2007).

The reduced efficiency of B-NHEJ generated upon serum deprivation is reversible. Upon re-incubation of cells with serum the ability of cells to repair DSBs by B-NHEJ recovers. This reversal of B-NHEJ efficiency was dependent on the duration of incubation with serum and the concentration of serum used. One hour incubation enhanced significantly the repair kinetics by B-NHEJ. Even incubation with 1% serum for 1 h, had a measurable effect in this regard.

There was no difference in the levels of all proteins that were involved in B-NHEJ between exponential and plateau phase of growth. Proteins like DNA ligase III, PARP1 and Histone H1 remained at similar levels (Figure 3.21). Growth factors like EGF, bFGF and IGF-1 affect PARP1 activity in aged cells and PARP1 ribosylates DNA ligase III, Histone H1and some other proteins involved in DSB repair (Spina Purrello et al., 2002). It is therefore possible that for post translational modifications of B-NHEJ repair enzymes are induced by growth factor activated signaling and regulate B-NHEJ. Histone H1 is a specific inhibitor of core histone acetylation in chromatin (Herrera et al., 2000). As gene expression of Xrcc1 is regulated by EGFR signaling, and inhibition of EGFR signaling drastically down regulates Xrcc1 (Yacoub et al., 2003; Yacoub et al., 2001), down regulation of B-NHEJ is possible.

Several lines of evidence suggest a correlation between growth factor signaling and DNA-PK dependent NHEJ (Das et al., 2007; Dittmann et al., 2005; Dittmann, Mayer, and Rodemann,

2005; Friedmann et al., 2006). EGFR activation leads to the activation of several downstream signaling cascades including the phosphoinositol 3-kinase (PI3K) pathway, the signal transducer and activator of transcription (STAT-1, STAT-3, STAT-5) pathway, the Ras-MAPK (mitogen-activated protein kinase) pathway. More work will be required to establish which of these signaling cascades is associated with B-NHEJ regulation.

4.3. Prompt and temperature dependent DSBs

Although a number of reports in the last decades have pointed out the temperature sensitivity of radiation induced DNA lesions, particularly with reference to the production of DSBs (e.g.(Henle et al., 1995; Jones, Bowell, and Ward, 1994)), the ramifications and potential complications of this sensitivity in DSB analysis have largely been ignored. For mammalian cells, the issue was resurrected by Rydberg et al (Karlsson et al., 2008; Karlsson and Stenerlöw, 2007; Rydberg, 2000; Stenerlöw et al., 2003) who described potential problems in the analysis of DSB induction and repair when using pulsed-field gel electrophoresis protocols including 50°C lysis. In several reports, these authors demonstrated that high temperature lysis transforms HLS to DSBs, which may not be present in intact cells at the moment of sampling for quantification. Indeed, in human cells nearly 40% of DSBs measured immediately after irradiation using HTL are generated from HLS during lysis and are not actually present in the cell at the moment taken for quantification.

The dose response curves presented here (Figures 3.24, 3.25, 3.26, 3.27, and 3.28) and data published by other investigators (Gulston et al., 2004) quantitatively and qualitatively confirm these observations. Indeed, in human cells analyzed immediately after IR 40% of the DSBs are generated during HTL and are not detectable after LTL. The proportion of DSBs generated through HLS during HTL appears to be species specific and higher in rodent than in human cells; it increases from 40% in human to 50% and 60% in Chinese hamster and mouse cells, respectively. This observation points to biological determinants in the transformation of HLS to DSBs.

Despite the fact that combinations of lesions are required to generate DSBs, either under HTL or under LTL conditions, the dose response curves remain linear. Linear induction with dose of DSBs is indicative of single particle track production of the underlying clustered DNA damage (Gulston et al., 2004). The bp distance between the lesions in each of the DNA strands that combine to form a DSB has not been determined conclusively. However, it is likely to depend on

the organizational state of the DNA and is estimated to be less than 10 bp in the case of naked DNA.

4.3.1. Robust B-NHEJ activity detectable after LTL

The generation by high temperature lysis protocols of DSBs, which may actually not be present in the tested cells, raise questions regarding the validity of the repair kinetics measured using these protocols. Indeed results reported earlier, as well as the results presented here, indicate clear modifications in the repair kinetics when LTL is employed instead of HTL (Gulston et al., 2004; Karlsson, 2007; Karlsson et al., 2008; Rydberg, 2000; Stenerlöw et al., 2003). Although, the changes in repair kinetics are modest in repair proficient cells, cells with defects in components of D-NHEJ show significantly reduced repair half times up to an apparent complete halt of DSB repair. Such observations led to the postulate that the DSB repair deficiency of D-NHEJ deficient cells is complete (Rydberg, 2000; Stenerlöw et al., 2003). The repair activity detected after HTL was considered artifactual and reflecting repair by non-DSB repair pathways of HLS and SSBs leading to these DSBs, rather than repair of frank DSBs.

The results generated clearly demonstrate extensive end joining even under conditions of LTL suggesting robust B-NHEJ activity in all D-NHEJ deficient mutants tested. Although, the results of LTL suggest a lower efficacy of B-NHEJ than that estimated after HTL, this difference may be more apparent than real. First, in all experiments where kinetics was measured for relatively long periods of time, B-NHEJ removed nearly 75% of the DSBs detected under LTL. Second, the fate of HLS inside the cell remains unknown, and as we will discuss later it is likely that they actually transform to DSBs in a time dependent manner. Such delayed generation of DSBs will alter the repair kinetics and thus also the levels of damage reached at all time points prior to the completion of DSBs processing by B-NHEJ.

4.3.2. Independent lines of investigation provide strong evidence for a robust function of alternative pathways of NHEJ in D-NHEJ deficient cells

The existence of B-NHEJ would not be conclusive without additional independent evidence obtained using alternative methodologies and endpoints. Several lines of investigation converge and support the robust function of alternative pathways of NHEJ when D-NHEJ is defective and these are briefly summarized below.

As already mentioned above, biochemical evidence provides strong support for DNA Ligase IV independent end joining in extracts of repair proficient as well as of D-NHEJ deficient cells (Audebert, Salles, and Calsou, 2004; Wang et al., 2005; Wang et al., 2006). The major contributor to this end joining activity is DNA Ligase III, which also implicates PARP-1 and Xrcc1 in this function (Audebert, Salles, and Calsou, 2004; Wang et al., 2005; Wang et al., 2006). Robust end joining in D-NHEJ deficient cells is also observed using assays based on the rejoining of transfected plasmid substrates (Verkaik et al., 2002; Wang et al., 2005). Frequently, these assays do not detect measurable reduction in end joining efficiency between D-NHEJ proficient and deficient cells and show instead the frequent use of a form of end joining that utilizes microhomologies (Verkaik et al., 2002).

Further support for a robust function of B-NHEJ is obtained from cytogenetic studies carried out with D-NHEJ deficient cells. Analysis of chromosome aberrations in human and mouse cells deficient in DNA-PKcs demonstrate extensive end joining leading to substantially increased formation of exchange type aberrations (Martin et al., 2005; Virsik-Köpp et al., 2005; Virsik-Köpp et al., 2003). Direct support for the end joining activity at the chromosome level in cells with compromised DNA-PK is also reported in human lymphocytes using the technique of premature chromosome condensation (Terzoudi et al., 2008). This technique allows the direct visualization of interphase chromosome breaks in G0 or G1 cells immediately after IR, as well as different times thereafter. These experiments show nearly complete, albeit slow rejoining of chromosome breaks under conditions where DNA-PK activity is inhibited by wortmannin (Terzoudi et al., 2008). This cytogenetic result is also corroborated by results obtained with DNA-PKcs MEFs where nearly complete decay of γ-H2AX foci is observed after long periods of repair incubation (Riballo et al., 2004).

Perhaps the most conclusive evidence for the robust function of alternative pathways of NHEJ is obtained from the field of immunology that also contributed substantially to the delineation of D-NHEJ function. Two key processes initiated by DSBs and required for the maturation of B-cells for antibody production is V(D)J and class switch recombination, with both normally utilizing practically exclusively D-NHEJ. During V(D)J recombination, the products of the RAG genes generate DSBs within the V, D, and J gene clusters which are then processed by D-NHEJ. V(D)J recombination is barely detectable in D-NHEJ deficient cells, a result that led to the assumption that other pathways cannot substitute for D-NHEJ in this function. However, recent work

(Corneo et al., 2007) nicely demonstrates that the low levels of V(D)J recombination in D-NHEJ deficient cells is not due to the lack of alternative pathways capable of processing the generated DSBs, but rather to the strong binding to the DNA ends of the RAG proteins that prevents shunting to alternative pathways. Indeed, when RAG mutants with reduced affinity for DNA ends are examined, nearly 70% restoration of V(D)J recombination is observed despite the defects in D-NHEJ (Corneo et al., 2007). Class switch recombination utilizes a different mechanism than V(D)J recombination for generating the initiating DSBs that leaves them available for processing by alternative pathways. As a result, robust class switch recombination (over 50%) is observed in D-NHEJ deficient cells (Boboila et al., 2010b; Yan et al., 2007).

4.3.3. Why does DSB repair appear slow after LTL?

While the above outline provides strong support for the existence and robust function of B-NHEJ, it leaves unanswered why DSB rejoining detected under LTL appears much slower than after HTL, and why the initial fast component is undetectable after LTL. A plausible interpretation is that fast repair after HTL does not reflect repair of DSBs but rather repair of SSBs and HLS within the clustered lesions that form DSBs only after exposure to the high lysis temperatures (Gulston et al., 2004; Karlsson, 2007; Karlsson et al., 2008; Rydberg, 2000; Stenerlöw et al., 2003). Removal of these lesions by fast operating non-DSB repair pathways will appear in the HTL assay as repair of DSBs. An anticipated consequence of this interpretation is that inhibition of pathways implicated in the repair of SSBs or base damages should inhibit the initial fast rejoining after HTL. However, no effect was found when PARP-1 or Xrcc1, two components of repair pathways processing such lesions, were chemically or genetically compromised (Karlsson et al., 2008). Furthermore, the assumption that repair of SSBs and HLS within a clustered damage site will be as fast as in isolated lesions is unlikely to hold. Indeed, there is evidence that repair pathways highly efficient when processing isolated lesions, are compromised when processing the same lesion within the clustered damage site (Gulston et al., 2004). Finally, repair of base damage and thus probably also of HLS is a relatively slow process with half times much longer than a few minutes (Friedberg et al., 2006).

What other explanations can then be offered? The observation that lysis at 37ºC, or even at 20°C (results not shown), leads to repair kinetics practically indistinguishable from those of 50°C lysis, allows an alternative interpretation. We propose that transformation of HLS to SSBs is not an

artifact of the 50°C lysis protocol but a reality the cell faces immediately after its incubation for repair at 37°C. Thus, new DSBs are formed in the repairing cell. As a result, the observed kinetics is the net result of DSB removal by repair processing and of DSB production by the chemical transformation of HLS to SSBs (SSBs produced by processing of base damage within a clustered lesion may further add to this load). In repair proficient cells this balance remains tilted towards repair since it occurs efficiently and removes not only the initial DSBs but also those subsequently produced through the transformation of HLS. In D-NHEJ deficient cells, on the other hand, the production of new DSBs after IR cancels or even takes over repair giving the impression of a complete repair defect.

While the production of DNA lesions by IR with pronounced instability at 20°C or 37°C is demonstrated for plasmid DNA (Jones, Bowell, and Ward, 1994), it remains to be conclusively demonstrated for the complexly organized genome of mammalian cells. The results of 37°C lysis provide indirect support along these lines, but certainly more work is required to convincingly explore this important issue.

4.3.4. Induction and repair of DNA DSBs after heavy ion irradiation

Radiosensitivity to killing after heavy ion irradiation is much higher than after exposure to sparsely ionizing radiation like x-rays and γ-rays. Heavy ions are having high LET compared to x-rays, which effects a higher energy deposition in a localized area and a higher probability for the generation of locally multiply damaged sites (LMDS). As we have shown before that x-rays induce HLSs that is converted to DSBs at 37^{o}C, we tested here the production of HLSs after heavy ion irradiation. PFGE was used to analyze the induction of DSBs using LTL and HTL protocols.

Interestingly, after heavy ion irradiation the difference between HTL and LTL becomes negligible in the case of M059K and M059J cells, and significantly smaller in *LIG4*$^{-/-}$ MEFs (Figure 44). These results suggest qualitative differences in the induction of DNA lesions by these two types of radiation. The most likely explanation for the observed difference in the induction of DSBs through the transformation of HLSs to SSBs after high LET radiation is that the complexity of the initial lesion masks their transformation to DSBs. In other words, in the complex lesions generated after high LET radiation, there are enough prompt SSBs to generate the DSB and transformation of HLSs to SSBs is not required for this purpose. The kinetics of

DSB rejoining after LTL that lack the initial small increase observed after x-rays, provide further support to the conclusion that transformation of HLSs into SSBs does not measurably contribute to DSB generation after exposure to high LET radiation.

4.3.5. Efficiency of B-NHEJ after heavy ion irradiation

We inquired on the efficiency of B-NHEJ and D-NHEJ after heavy ion irradiation using PFGE. We used wt and *LIG4*$^{-/-}$ MEFs cells in these experiments. The repair kinetics of exponentially growing wt cells showed not significant difference after exposure to heavy ions and x-rays. On the other hand, D-NHEJ mutants showed slower processing of DSBs after exposure to heavy ions as compared to x-rays. This suggests a stronger dependence on lesion complexity of B-NHEJ than D-NHEJ.

B-NHEJ is a slow process whereas D-NHEJ is fast. It is possible that the slow kinetics of B-NHEJ interfere more severely with the complexity of high LET induced highly complex DSBs

5. Summary

DNA double strand breaks are highly cytotoxic lesions, induced by several endogenous and exogenous processes. DSBs are repaired by either homologous recombination (HR) or non-homologous end joining (NHEJ) and impairment in either pathway leads to mutations, chromosomal aberrations, or cell death. Cells mutated in any component of D-NHEJ repair nearly all DNA DSBs albeit with slower kinetics. We termed this slower pathway B-NHEJ and showed that it is distinct from HRR.

In present study we used cell sorting methods to select cells in specific phases of the cell cycle and monitored the efficiency of B-NHEJ. A range of radiation doses was used including comparatively lower dose (10 Gy) for PFGE. We found that B-NHEJ function is enhanced in the G2 phase of cell cycle, where HRR is also known to operate efficiently. Interestingly, in our assay, HRR mutants did not show any phenotype even in the G2 phase of cell cycle raising interesting question regarding the contribution of this pathway to the repair of DSBs.

B-NHEJ showed a strong dependency on cell growth state. D-NHEJ mutants tested in the plateau phase of growth showed a strong reduction in their capacity to repair DSBs. This inhibition is not a species specific phenomenon and mutants of all components of D-NHEJ show this phenotype except for DNA-PKcs mutants. Chemically inhibited or kinase dead DNA-PKcs mutants showed a similar strong inhibition in the plateau phase of growth, but DNA-PKcs mutants without residual kinase activity fail to show inhibition in DSB repair as they entered the plateau phase of growth. These results point to important regulatory function of DNA-PKcs in DNA DSBs repair that require further investigations.

In a survival assay, D-NHEJ mutants showed increased radiosensitivity in the plateau phase of growth even when tested specifically in the G1 and G2 phases of the cell cycle. Enhanced radiosensitivity of D-NHEJ deficient cells in G2 as they enter plateau phase is in line with our observations of enhanced function of B-NHEJ in this phase of the cell cycle.

LIG4$^{-/-}$ cells after serum deprivation show a response similar to that seen in cells entering the plateau phase of growth. A strong reduction in B-NHEJ capacity is observed that correlates growth factor signaling with B-NHEJ. In support of this conclusion, after treatment with a specific EGFR inhibitor, D-NHEJ mutants showed a marked reduction in their capacity to repair

DSBs. This inhibition observed in B-NHEJ upon serum deprivation was reversible and repair capacity returned to normal levels 24 h after incubating cells with serum again.

The above work was carried out by PFGE, which includes a lysis step at elevated temperatures. Since incubation of irradiated DNA at elevated temperatures transforms HLS into SSBs that contribute to the generation of DSBs that may not be present in the living cell we tested the potential complications of this phenomenon to our conclusions. We found a robust function of B-NHEJ even after exclusion of HLS. In continuation of this work, we have further showed that transformation of HLS to DSBs does not only occur at 50^{o}C but it also takes place at 37^{o}C. This result changes the status of HLSs from an alleged artifact to a fact the cell faces at all times.

Finally we investigated the role of DSB complexity in the function of D-NHEJ, B-NHEJ, as well as in the role of HLS to the yield of DSBs. In general increased DSB complexity is associated with reduced repair efficiency and a reduction in the contribution of HLSs to the generation of additional DSBs.

Overall the above results significantly enhance our understanding of the cellular mechanisms managing and processing DSBs and point to important characteristics of the underlying lesions that require further investigation. A number of in depth further studies will result from this work.

6. Reference List

Akimoto, T., Hunter, N. R., Buchmiller, L., Mason, K., Ang, K. K., and Milas, L. (1999). Inverse Relationship between Epidermal Growth Factor Receptor Expression and Radiocurability of Murine Carcinomas. *Clinical Cancer Research* **5**(10)**,** 2884-2890.

Allalunis-Turner, M. J., Zia, P. K. Y., Barron, G. M., Mirzayans, R., and Day, R. S., III (1995). Radiation-Induced DNA Damage and Repair in Cells of a Radiosensitive Human Malignant Glioma Cell Line. *Radiation Research* **144,** 288-293.

Allen, C., Halbrook, J., and Nickoloff, J. A. (2003). Interactive Competition between Homologous Recombination and Non-Homologous End Joining. *Molecular Cancer Research* **1**(12)**,** 913-920.

Allen, C., Kurimasa, A., Brenneman, M. A., Chen, D. J., and Nickoloff, J. A. (2002). DNA-dependent protein kinase suppresses double-strand break-induced and spontaneous homologous recombination. *Proceedings of the National Academy of Sciences of the United States of America* **99,** 3758-3763.

Almeida, K. H., and Sobol, R. W. (2007). A unified view of base excision repair: Lesion-dependent protein complexes regulated by post-translational modification. *DNA Repair* **6**(6)**,** 695-711.

Asaad, N. A., Zeng, Z.-C., Guan, J., Thacker, J., and Iliakis, G. (2000). Homologous recombination as a potential target for caffeine radiosensitization in mammalian cells: Reduced caffeine radiosensitization in *XRCC2* and *XRCC3* mutants. *Oncogene* **19,** 5788-5800.

Audebert, M., Salles, B., and Calsou, P. (2004). Involvement of Poly(ADP-ribose) Polymerase-1 and XRCC1/DNA Ligase III in an Alternative Route for DNA Double-strand Breaks Rejoining. *Journal of Biological Chemistry* **279,** 55117-55126.

Bandyopadhyay, D., Mandal, M., Adam, L., Mendelsohn, J., and Kumar, R. (1998). Physical Interaction between Epidermal Growth Factor Receptor and DNA-dependent Protein Kinase in Mammalian Cells. *Journal of Biological Chemistry* **273**(3)**,** 1568-1573.

Bassing, C. H., and Alt, F. W. (2004). The cellular response to general and programmed DNA double strand breaks. *DNA Repair* **3,** 781-796.

Baumann, M., and Krause, M. (2004). Targeting the epidermal growth factor receptor in radiotherapy: radiobiological mechanisms, preclinical and clinical results. *Radiotherapy and Oncology* **72,** 257-266.

Bekker-Jensen, S., Fugger, K., Danielsen, J. R., Gromova, I., Sehested, M., Celis, J., Bartek, J., Lukas, J., and Mailand, N. (2007). Human Xip1 (C2orf13) Is a Novel Regulator of Cellular Responses to DNA Strand Breaks. *Journal of Biological Chemistry* **282**(27)**,** 19638-19643.

Bennardo, N., Cheng, A., Huang, N., and Stark, J. M. (2008). Alternative-NHEJ Is a Mechanistically Distinct Pathway of Mammalian Chromosome Break Repair. *PLoS Genetics* **4**(6)**,** e1000110.

Bezzubova, O., Silbergleit, A., Yamaguchi-Iwai, Y., Takeda, S., and Buerstedde, J.-M. (1997). Reduced X-ray resistance and homologous recombination frequencies in a *RAD54* $^{-/-}$ mutant of the chicken DT40 cell line. *Cell* **89,** 185-193.

Blöcher, D., and Kunhi, M. (1990). DNA double-strand break analysis by CHEF electrophoresis. *International Journal of Radiation Biology* **58**(1)**,** 23-34.

Block, W. D., Yu, Y., Merkle, D., Fifford, J. L., Ding, Q., Meek, K., and Lees-Miller, S. P. (2004). Autophosphorylation-dependent remodeling of the DNA-dependent protein kinase catalytic subunit regulates ligation of DNA ends. *Nucleic Acids Research* **32**(14)**,** 4351-4357.

Boboila, C., Jankovic, M., Yan, C. T., Wang, J. H., Wesemann, D. R., Zhang, T., Fazeli, A., Feldman, L., Nussenzweig, A., Nussenzweig, M., and Alt, F. W. (2010a). Alternative end-joining catalyzes robust IgH locus deletions and translocations in the combined absence of ligase 4 and Ku70. *Proceedings of the National Academy of Sciences of the United States of America* **107**(7)**,** 3034-3039.

Boboila, C., Yan, C., Wesemann, D. R., Jankovic, M., Wang, J. H., Manis, J., Nussenzweig, A., Nussenzweig, M., and Alt, F. W. (2010b). Alternative end-joining catalyzes class switch recombination in the absence of both Ku70 and DNA ligase 4. *Journal of Experimental Medicine* **207**(2)**,** 417-427.

Bonner, J. A., Harari, P. M., Giralt, J., Azarnia, N., Shin, D. M., Cohen, R. B., Jones, C. U., Sur, R., Raben, D., Jassem, J., Ove, R., Kies, M. S., Baselga, J., Youssoufian, H., Amellal, N., Rowinsky, E. K., and Ang, K. K. (2006). Radiotherapy plus Cetuximab for Squamous-Cell Carcinoma of the Head and Neck. *New England Journal of Medicine* **354**(6)**,** 567-578.

Bothmer, A., Robbiani, D. F., Feldhahn, N., Gazumyan, A., Nussenzweig, A., and Nussenzweig, M. C. (2010). 53BP1 regulates DNA resection and the choice between classical and alternative end joining during class switch recombination. *Journal of Experimental Medicine* **207**(4)**,** 855-865.

Bowers, G., Reardon, D. B., Hewitt, T., Dent, P., Mikkelsen, R. B., Valerie, K., Lammering, G., Amir, C., and Schmidt-Ullrich, R. K. (2001). The relative role of ErB1-4 receptor tyrosine kinases in radiation signal transduction responses of human carcinoma cells. *Oncogene* **20,** 1388-1397.

Buis, J., Wu, Y., Deng, Y., Leddon, J., Westfield, G., Eckersdorff, M., Sekiguchi, J. M., Chang, S., and Ferguson, D. O. (2008). Mre11 Nuclease Activity Has Essential Roles in DNA Repair and Genomic Stability Distinct from ATM Activation. *Cell* **135**(1)**,** 85-96.

Busuttil, R. A., Munoz, D. P., Garcia, A. M., Rodier, F., Kim, W. H., Suh, Y., Hasty, P., Campisi, J., and Vijg, J. (2008). Effect of Ku80 Deficiency on Mutation Frequencies and Spectra at a LacZ Reporter Locus in Mouse Tissues and Cells. *PLoS ONE* **3**(10)**,** e3458.

Caldecott, K. W. (2001). Mammalian DNA single-strand break repair: an X-ra(y)ted affair. *BioEssays* **23,** 447-455.

Caldecott, K. W., McKeown, C. K., Tucker, J. D., Ljungquist, S., and Thompson, L. H. (1994). An Interaction between the Mammalian DNA Repair Protein XRCC1 and DNA Ligase III. *Molecular and Cellular Biology* **14,** 68-76.

Calsou, P., Frit, P., Humbert, O., Muller, C., Chen, D. J., and Salles, B. (1999). The DNA-dependent protein kinase catalytic activity regulates DNA end processing by means of Ku entry into DNA. *Journal of Biological Chemistry* **274**(12)**,** 7848-7856.

Chan, D. W., Chen, B. P.-C., Prithivirajsingh, S., Kurimasa, A., Story, M. D., Qin, J., and Chen, D. J. (2002). Autophosphorylation of the DNA-dependent protein kinase catalytic subunit is required for rejoining of DNA double-strand breaks. *Genes & Development* **16,** 2333-2338.

Chan, D. W., Ye, R., Veillette, C. J., and Lees-Miller, S. P. (1999). DNA-dependent protein kinase phosphorylation sites in Ku 70/80 heterodimer. *Biochemistry* **38,** 1819-1828.

Chen, B. P. C., Chan, D. W., Kobayashi, J., Burma, S., Asaithamby, A., Morotomi-Yano, K., Botvinick, E., Qin, J., and Chen, D. J. (2005). Cell Cycle Dependence of DNA-dependent Protein Kinase Phosphorylation in Response to DNA Double Strand Breaks. *Journal of Biological Chemistry* **280**(15)**,** 14709-14715.

Chen, B. P. C., Uematsu, N., Kobayashi, J., Lerenthal, Y., Krempler, A., Yajima, H., Löbrich, M., Shiloh, Y., and Chen, D. J. (2007). Ataxia Telangiectasia Mutated (ATM) Is Essential for DNA-PKcs Phosphorylations at the Thr-2609 Cluster upon DNA Double Strand Break. *Journal of Biological Chemistry* **282**(9)**,** 6582-6587.

Chen, D. J., and Nirodi, C. S. (2007). The Epidermal Growth Factor Receptor: A Role in Repair of Radiation-Induced DNA Damage. *Clinical Cancer Research* **13**(22)**,** 6555-6560.

Cheong, N., Wang, X., Wang, Y., and Iliakis, G. (1994). Loss of S-phase dependent radioresistance in irs-1 cells exposed to x-rays. *Mutation Research* **314,** 77-85.

Cheong, N., Wang, Y., Jackson, M., and Iliakis, G. (1992). Radiation-sensitive *irs* mutants rejoin DNA double strand breaks with efficiency similar to that of parental V79 Cells but show altered response to radiation induced G2-delay. *Mutation Research* **274,** 111-122.

Convery, E., Shin, E. K., Ding, Q., Wang, W., Douglas, P., Davis, L. S., Nickoloff, J. A., Lees-Miller, S. P., and Meek, K. (2005). Inhibition of homologous recombination by variants of the catalytic subunit of the DNA-dependent protein kinase (DNA-PKcs). *Proceedings of the National Academy of Sciences of the United States of America* **102**(5)**,** 1345-1350.

Conway, A. B., Lynch, T. W., Zhang, Y., Fortin, G. S., Fung, C. W., Symington, L. S., and Rice, P. A. (2004). Crystal structure of a Rad51 filament. *Nature Structural & Molecular Biology* **11,** 791-796.

Cooper, M. P., Machwe, A., Orren, D. K., Brosh, R. M., Ramsden, D., and Bohr, V. A. (2000). Ku complex interacts with and stimulates the Werner protein. *Genes & Development* **14**(8)**,** 907-912.

Corneo, B., Wendland, R. L., Deriano, L., Cui, X., Klein, I. A., Wong, S.-Y., Arnal, S., Holub, A. J., Weller, G. R., Pancake, B. A., Shah, S., Brandt, V. L., Meek, K., and Roth, D. B. (2007). Rag mutations reveal robust alternative end joining. *Nature* **449,** 483-486.

Costantini, S., Woodbine, L., Andreoli, L., Jeggo, P. A., and Vindigni, A. (2007). Interaction of the Ku heterodimer with the DNA ligase IV/Xrcc4 complex and its regulation by DNA-PK. *DNA Repair* **6**(6)**,** 712-722.

Critchlow, S. E., Bowater, R. P., and Jackson, S. P. (1997). Mammalian DNA double-strand break repair protein XRCC4 interacts with DNA ligase IV. *Current Biology* **7,** 588-598.

Cui, X., Brenneman, M., Meyne, J., Oshimura, M., Goodwin, E. H., and Chen, D. J. (1999). The *XRCC2* and *XRCC3* repair genes are required for chromosome stability in mammalian cells. *Mutation Research* **434,** 75-88.

Cui, X., Yu, Y., Gupta, S., Cho, Y.-M., Lees-Miller, S. P., and Meek, K. (2005). Autophosphorylation of DNA-Dependent Protein Kinase Regulates DNA End Processing and May Also Alter Double-Strand Break Repair Pathway Choice. *Molecular and Cellular Biology* **25**(24)**,** 10842-10852.

Das, A. K., Chen, B. P., Story, M. D., Sato, M., Minna, J. D., Chen, D. J., and Nirodi, C. S. (2007). Somatic Mutations in the Tyrosine Kinase Domain of Epidermal Growth Factor Receptor (EGFR) Abrogate EGFR-Mediated Radioprotection in Non-Small Cell Lung Carcinoma. *Cancer Research* **67**(11)**,** 5267-5274.

Deriano, L., Stracker, T. H., Baker, A., Petrini, J. H. J., and Roth, D. B. (2009). Roles for NBS1 in Alternative Nonhomologous End-Joining of V(D)J Recombination Intermediates. *Molecular Cell* **34**(1)**,** 13-25.

Dianov, G. L., and Parsons, J. L. (2007). Co-ordination of DNA single strand break repair. *DNA Repair* **6**(4)**,** 454-460.

DiBiase, S. J., Zeng, Z.-C., Chen, R., Hyslop, T., Curran, W. J., Jr., and Iliakis, G. (2000). DNA-dependent protein kinase stimulates an independently active, nonhomologous, end-joining apparatus. *Cancer Research* **60,** 1245-1253.

Ding, Q., Reddy, Y. V. R., Wang, W., Woods, T., Douglas, P., Ramsden, D. A., Lees-Miller, S. P., and Meek, K. (2003). Autophosphorylation of the Catalytic Subunit of the DNA-Dependent Protein Kinase Is Required for Efficient End Procesing during DNA Double-Strand Break Repair. *Molecular and Cellular Biology* **23,** 5836-5848.

Dinkelmann, M., Spehalski, E., Stoneham, T., Buis, J., Wu, Y., Sekiguchi, J. M., and Ferguson, D. O. (2009). Multiple functions of MRN in end-joining pathways during isotype class switching. *Nature Structural & Molecular Biology* **16**(8)**,** 808-813.

Dittmann, K., Mayer, C., Fehrenbacher, B., Schaller, M., Raju, U., Milas, L., Chen, D. J., Kehlbach, R., and Rodemann, H. P. (2005). Radiation-induced Epidermal Growth Factor Receptor Nuclear Import Is Linked to Activation of DNA-dependent Protein **Kinase. *Journal of Biological Chemistry* 280(35), 31182-31189.**

Dittmann, K., Mayer, C., and Rodemann, H.-P. (2005). Inhibition of radiation-induced EGFR nuclear import by C225 (Cetuximab) suppresses DNA-PK activity. *Radiotherapy and Oncology* **76**(2)**,** 157-161.

Douglas, P., Sapkota, G. P., Morrice, N., Yu, Y., Goodarzi, A. A., Merkle, D., Meek, K., Alessi, D. R., and Lees-Miller, S. P. (2002). Identification of in vitro and in vivo phosphorylation sites in the catalytic subunit of the DNA-dependent protein kinase. *Biochemical Journal* **368,** 243-251.

Dronkert, M. L., Beverloo, H. B., Johnson, R. D., Hoeijmakers, J. H., Jasin, M., and Kanaar, R. (2000). Mouse *RAD54* affects DNA double-strand break repair and sister chromatid exchange. *Molecular and Cellular Biology* **20,** 3147-3156.

Drouet, J., Delteil, C., Lefrancois, J., Concannon, P., Salles, B., and Calsou, P. (2005). DNA-dependent Protein Kinase and XRCC4-DNA Ligase IV Mobilization in the Cell in Response to DNA Double Strand Breaks. *Journal of Biological Chemistry* **280**(8)**,** 7060-7069.

Du, L., van der Burg, M., Popov, S. W., Kotnis, A., van Dongen, J. J. M., Gennery, A. R., and Pan-Hammarstrom, Q. (2008). Involvement of Artemis in nonhomologous end-joining during immunoglobulin class switch recombination. *Journal of Experimental Medicine* **205**(13)**,** 3031-3040.

Essers, J., Hendriks, R. W., Swagemakers, S. M. A., Troelstra, C., de Wit, J., Bootsma, D., Hoeijmakers, J. H. J., and Kanaar, R. (1997). Disruption of mouse *RAD54* reduces ionizing radiation resistance and homologous recombination. *Cell* **89,** 195-204.

Essers, J., van Steeg, H., de Wit, J., Swagemakers, S. M., Vermeij, M., Hoeijmakers, J. H., and Kanaar, R. (2000). Homologous and non-homologous recombination differentially affect DNA damage repair in mice. *EMBO Journal* **19,** 1703-1710.

Fattah, F., Lee, E. H., Weisensel, N., Wang, Y., Lichter, N., and Hendrickson, E. A. (2010). Ku Regulates the Non-Homologous End Joining Pathway Choice of DNA Double-Strand Break Repair in Human Somatic Cells. *PLoS Genetics* **6**(2)**,** e1000855.

Frank, K. M., Sharpless, N. E., Gao, Y., Sekiguchi, J. M., Fergson, D. O., Zhu, C., Manis, J. P., Horner, J., DePinho, R. A., and Alt, F. W. (2000). DNA ligase IV deficiency in mice leads to defective neurogenesis and embryonic lethality via the p53 pathway. *Molecular Cell* **5,** 993-1002.

Friedberg, E. C., Walker, G. C., Siede, W., Wood, R. D., Schultz, R. A., and Ellenberger, T. (2006). "DNA Repair and Mutagenesis." Second Edition ed. ASM Press, Washington, D.C.

Friedmann, B. J., Caplin, M., Savic, B., Shah, T., Lord, C. J., Ashworth, A., Hartley, J. A., and Hochhauser, D. (2006). Interaction of the epidermal growth fractor receptor and the DNA-dependent protein kinase pathway following gefitinib treatment. *Molecular Cancer Therapeutics* **5**(2)**,** 209-218.

Fujimori, A., Tachiiri, S., Sonoda, E., Thompson, L. H., Kumar Dhar, P., Hiraoka, M., Takeda, S., Zhang, Y., Reth, M., and Takata, M. (2001). Rad52 partially substitutes for the Rad51 paralog XRCC3 in maintaining chromosomal integrity in vertebrate cells. *EMBO Journal* **20,** 5513-5520.

Funayama, R., Saito, M., Tanobe, H., and Ishikawa, F. (2006). Loss of linker histone H1 in cellular senescence. *Journal of Cell Biology* **175**(6)**,** 869-880.

Galloway, A. M., Spencer, C. A., Anderson, C. W., and Allalunis-Turner, M. J. (1999). Differential stability of the DNA-activated protein kinase catalytic subunit mRNA in human glioma cells. *Oncogene* **18,** 1361-1368.

Georgakilas, A. G. (2008). Processing of DNA damage clusters in human cells: current status of knowledge. *Molecular BioSystems* **4**(1)**,** 30-35.

Georgakilas, A. G., Bennett, P. V., and Sutherland, B. M. (2002). High efficiency detection of bi-stranded abasic clusters in gamma-irradiated DNA by putrescine. *Nucleic Acids Res* **30**(13)**,** 2800-8.

Goettlich, B., Reichenberger, S., Feldmann, E., and Pfeiffer, P. (1998). Rejoining of DNA double-strand breaks *in vitro* by single-strand annealing. *European Journal of Biochemistry* **258,** 387-395.

Grawunder, U., Wilm, M., Wu, X., Kulesza, P., Wilson, T. E., Mann, M., and Lieber, M. R. (1997). Activity of DNA ligase IV stimulated by complex formation with XRCC4 protein in mammalian cells. *Nature* **388,** 492-495.

Grawunder, U., Zimmer, D., Fugmann, S., Schwarz, K., and Lieber, M. R. (1998). DNA ligase IV is essential for V(D)J recombination and DNA double-strand break repair in human precursor lymphocytes. *Molecular Cell* **2,** 477-484.

Gu, J., Lu, H., Tippin, B., Shimazaki, N., Goodman, M. F., and Lieber, M. R. (2007). XRCC4: DNA ligase IV can ligate incompatible DNA ends and can ligate across gaps. *EMBO Journal* **26,** 1010-1023.

Gulston, M., de Lara, C., Jenner, T., Davis, E., and O'Neill, P. (2004). Processing of clustered DNA damage generates additional double-strand breaks in mammalian cells post-irradiation. *Nucleic Acids Research* **32**(4)**,** 1602-1609.

Gupta, S., and Meek, K. (2005). The leucine rich region of DNA-PKcs contributes to its innate DNA affinity. *Nucleic Acids Research* **33**(22)**,** 6972-6981.

Hada, M., and Georgakilas, A. G. (2008). Formation of Clustered DNA Damage after High-LET Irradiation: A Review. *Journal of Radiation Research* **49**(3)**,** 203-210.

Hagan, M., Yacoub, A., and Dent, P. (2004a). Ionizing radiation causes a dose-dependent release of transforming growth factor alpha in vitro from irradiated xenografts and during palliative treatment of hormone-refractory prostate carcinoma. *Clin Cancer Res* **10**(17)**,** 5724-31.

Hagan, M., Yacoub, A., and Dent, P. (2004b). Ionizing Radiation Causes a Dose-Dependent Release of Transforming Growth Factor Î± In vitro from Irradiated Xenografts and during

Palliative Treatment of Hormone-Refractory Prostate Carcinoma. *Clinical Cancer Research* **10**(17)**,** 5724-5731.

Hahn, G. M., and Little, J. B. (1972). Plateau-phase cultures of mammalian cells: an in vitro model for human cancer. *Current Topics in Radiation Research Quarterly* **8,** 39-83.

Hammel, M., Yu, Y., Mahaney, B. L., Cai, B., Ye, R., Phipps, B. M., Rambo, R. P., Hura, G. L., Pelikan, M., So, S., Abolfath, R. M., Chen, D. J., Lees-Miller, S. P., and Tainer, J. A. (2010). Ku and DNA-dependent Protein Kinase Dynamic Conformations and Assembly Regulate DNA Binding and the Initial Non-homologous End Joining Complex. *Journal of Biological Chemistry* **285**(2)**,** 1414-1423.

Harris, R., Esposito, D., Sankar, A., Maman, J. D., Hinks, J. A., Pearl, L. H., and Driscoll, P. C. (2004). The 3D Solution Structure of the C-terminal Region of Ku86 (Ku86CTR). *Journal of Molecular Biology* **335**(2)**,** 573-582.

Hayes, J. J., and Hansen, J. C. (2001). Nucleosomes and the chromatin fiber. *Current Opinion in Genetics & Development* **11,** 124-129.

Helleday, T., Bryant, H. E., and Schultz, N. (2005). Poly(ADP-ribose) Polymerase (PARP-1) in Homologous Recombination and as a Target for Cancer Therapy. *Cell Cycle* **4**(9)**,** 1176-1178.

Helleday, T., Lo, J., van Gent, D. C., and Engelward, B. P. (2007). DNA double-strand break repair: From mechanistic understanding to cancer treatment. *DNA Repair* **6**(7)**,** 923-935.

Hendrickson, E. A., Qin, X.-Q., Bump, E. A., Schatz, D. G., Oettinger, M., and Weaver, D. T. (1991). A link between double-strand break-related repair and V(D)J recombination: The *scid* mutation. *Proceedings of the National Academy of Sciences of the United States of America* **88,** 4061-4065.

Henle, E. S., Roots, R., Holley, W. R., and Chatterjee, A. (1995). DNA Strand Breakage Is Correlated with Unaltered Base Release after Gamma Irradiation. *Radiation Research* **143,** 144-150.

Herrera, J. E., West, K. L., Schiltz, R. L., Nakatani, Y., and Bustin, M. (2000). Histone H1 is a specific repressor of core histone acetylation in chromatin. *Mol Cell Biol* **20**(2)**,** 523-9.

Heyer, W.-D., Li, X., Rolfsmeier, M., and Zhang, X.-P. (2006). Rad54: the Swiss Army knife of homologous recombination? *Nucleic Acids Research* **34**(15)**,** 4115-4125.

Hill, A. A., Wan, F., Acheson, D. K., and Skarsgard, L. D. (1999). Lack of correlation between G_1 arrest and radiation age-response in three synchronized human tumour cell lines. *International Journal of Radiation Biology* **75,** 1395-1408.

Hoeijmakers, J. H. J. (2001). Genome maintenance mechanisms for preventing cancer. *Nature* **411,** 366-374.

Huang, S.-M., and Harari, P. M. (2000). Modulation of Radiation Response after Epidermal Growth Factor Receptor Blockade in Squamous Cell Carcinomas: Inhibition of Damage Repair, Cell Cycle Kinetics, and Tumor Angiogenesis. *Clinical Cancer Research* **6**(6)**,** 2166-2174.

Iliakis, G. (1988). Radiation induced potentially lethal damage: DNA lesions susceptible to fixation. (Review Article). *International Journal of Radiation Biology* **53,** 541-584.

Iliakis, G., Metzger, L., Denko, N., and Stamato, T. D. (1991). Detection of DNA double strand breaks in synchronous cultures of CHO cells by means of asymmetric field inversion gel electrophoresis. *International Journal of Radiation Biology* **59,** 321-341.

Iliakis, G., Wang, H., Perrault, A. R., Boecker, W., Rosidi, B., Windhofer, F., Wu, W., Guan, J., Terzoudi, G., and Pantelias, G. (2004). Mechanisms of DNA double strand break repair and chromosome aberration formation. *Cytogenetic and Genome Research* **104,** 14-20.

Jackson, S. P. (2002). Sensing and repairing DNA double-strand breaks. *Carcinogenesis* **23**(5)**,** 687-96.

Jaco, I., Munoz, P., Goytisolo, F., Wesoly, J., Bailey, S., Taccioli, G., and Blasco, M. A. (2003). Role of Mammalian Rad54 in Telomere Length Maintenance. *Molecular and Cellular Biology* **23,** 5572-5580.

Jasin, M. (2002). Homologous repair of DNA damage and tumorigenesis: the BRCA connection. *Oncogene* **21,** 8981-8993.

Jeggo, P. A., and Löbrich, M. (2005). Artemis Links ATM to Double Strand Break Rejoining. *Cell Cycle* **4,** e-42-e-44.

Jones, G. D., Bowell, T. V., and Ward, J. F. (1994). Effects of postirradiation temperature on the yields of radiation-induced single- and double-strand breakage in SV40 DNA. *Radiation Research* **138**(2)**,** 291-296.

Jones, N. J., Stewart, S. A., and Thompson, L. H. (1990). Biochemical and genetic analysis of the Chinese hamster mutants *irs1* and *irs2* and their comparison to cultured ataxia telangiectasia cells. *Mutagenesis* **5,** 15-23.

Kanno, S.-i., Kuzuoka, H., Sasao, S., Hong, Z., Lan, L., Nakajima, S., and Yasui, A. (2007). A novel human AP endonuclease with conserved zinc-finger-like motifs involved in DNA strand break responses. *EMBO Journal* **26,** 2094-2103.

Karimi-Busheri, F., Rasouli-Nia, A., Allalunis-Turner, J., and Weinfeld, M. (2007). Human Polynucleotide Kinase Participates in Repair of DNA Double-Strand Breaks by Nonhomologous End Joining but not Homologous Recombination. *Cancer Research* **67**(14)**,** 6619-6625.

Karlsson, K. H. (2007). Extensive ssDNA end formation at DNA double-strand breaks in non-homologous end-joining deficient cells during the S phase **170,** 467-476.

Karlsson, K. H., Radulescu, I., Rydberg, B., and Stenerlöw, B. (2008). Repair of Radiation-Induced Heat-Labile Sites is Independent of DNA-PKcs, XRCC1 and PARP. *Radiation Research* **169,** 506-512.

Karlsson, K. H., and Stenerlöw, B. (2007). Extensive ssDNA end formation at DNA double-strand breaks in non-homologous end-joining deficient cells during the S phase *BMC Molecular Biology* **8,** 97.

Karmakar, P., Piotrowski, J., Brosh, R. M., Sommers, J. A., Lees-Miller, S. P., Cheng, W.-H., Snowden, C. M., Ramsden, D. A., and Bohr, V. A. (2002a). Werner Protein Is a Target of DNA-dependent Protein Kinase in Vivo and in Vitro, and Its Catalytic Activities Are Regulated by Phosphorylation. *Journal of Biological Chemistry* **277,** 18291-18302.

Karmakar, P., Snowden, C. M., Ramsden, D. A., and Bohr, V. A. (2002b). Ku heterodimer binds to both ends of the Werner protein and functional interaction occurs at the Werner N-terminus. *Nucleic Acids Research* **30,** 3583-3591.

Kim, J.-S., Krasieva, T. B., Kurumizaka, H., Chen, D. J., Taylor, A. M. R., and Yokomori, K. (2005). Independent and sequential recruitment of NHEJ and HR factors to DNA damage sites in mammalian cells. *Journal of Cell Biology* **170**(3)**,** 341-347.

Kurimasa, A., Kumano, S., Boubnov, N. V., Story, M. D., Tung, C.-S., Peterson, S. R., and Chen, D. J. (1999). Requirement for the kinase activity of human DNA-dependent protein kinase catalytic subunit in DNA strand break rejoining. *Molecular and Cellular Biology* **19,** 3877-3884.

Kusumoto, R., Dawut, L., Marchetti, C., Lee, J. W., Vindigni, A., Ramsden, D., and Bohr, V. A. (2008). Werner Protein Cooperates with the XRCC4-DNA Ligase IV Complex in End-Processing. *Biochemistry (Moscow)* **47,** 7548-7556.

Kysela, B., Chovanec, M., and Jeggo, P. A. (2005). Phosphorylation of linker histones by DNA-dependent protein kinase is required for DNA ligase IV-dependent ligation in the presence of histone H1. *Proceedings of the National Academy of Sciences of the United States of America* **102,** 1877-1882.

Lee, K.-J., Huang, J., Takeda, Y., and Dynan, W. S. (2000). DNA Ligase IV and XRCC4 Form a Stable Mixed Tetramer That Functions Synergistically with Other Repair Factors in a Cell-free End-joining System. *Journal of Biological Chemistry* **275**(44)**,** 34787-34796.

Lee, S. E., Mitchell, R. A., Cheng, A., and Hendrickson, E. A. (1997). Evidence for DNA-PK-dependent and -independent DNA double-strand break repair pathways in mammalian cells as a function of the cell cycle. *Molecular and Cellular Biology* **17,** 1425-1433.

Lees-Miller, S. P., Godbout, R., Chan, D. W., Weinfeld, M., Day, R. S., III, Barron, G. M., and Allalunis-Turner, J. (1995). Absence of p350 subunit of DNA-activated protein kinase from a radiosensitive human cell line. *Science* **267,** 1183-1185.

Lees-Miller, S. P., and Meek, K. (2003). Repair of DNA double strand breaks by non-homologous end joining. *Biochimie* **85,** 1161-1173.

Lees-Miller, S. P., Sakaguchi, K., Ullrich, S. J., Appella, E., and Anderson, C. W. (1992). Human DNA-activated protein kinase phosphorylates serines 15 and 37 in the amino-terminal transactivation domain of human p53. *Molecular and Cellular Biology* **12,** 5041-5049.

Lieber, M. R., Grawunder, U., Wu, X., and Yaneva, M. (1997). Tying loose ends: roles of Ku and DNA-dependent protein kinase in the repair of double-strand breaks. *Current Opinion in Genetics & Development* **7,** 99-104.

Lieber, M. R., Ma, Y., Pannicke, U., and Schwarz, K. (2003). Mechanism and regulation of human non-homologous DNA end-joining. *Nat Rev Mol Cell Biol* **4**(9)**,** 712-20.

Limbo, O., Chahwan, C., Yamada, Y., de Bruin, R. A. M., Wittenberg, C., and Russell, P. (2007). Ctp1 Is a Cell-Cycle-Regulated Protein that Functions with Mre11 Complex to Control Double-Strand Break Repair by Homologous Recombination. *Molecular Cell* **28,** 134-146.

Lu, C., Shi, Y., Wang, Z., Song, Z., Zhu, M., Cai, Q., and Chen, T. (2008). Serum starvation induces H2AX phosphorylation to regulate apoptosis via p38 MAPK pathway. *FEBS Letters* **582,** 2703-2708.

Ma, Y., Lu, H., Tippin, B., Goodman, M. F., Shimazaki, N., Koiwai, O., Hsieh, C.-L., Schwarz, K., and Lieber, M. R. (2004). A Biochemically Defined System for Mammalian Nonhomologous DNA End Joining. *Molecular Cell* **16,** 701-713.

Ma, Y., Pannicke, U., Schwarz, K., and Lieber, M. R. (2002). Hairpin Opening and Overhang Processing by an Artemis/DNA-Dependent Protein Kinase Complex in Nonhomologous End Joining and V(D)J Recombination. *Cell* **108,** 781-794.

Macrae, C. J., McCulloch, R. D., Ylanko, J., Durocher, D., and Koch, C. A. (2008). APLF (C2orf13) facilitates nonhomologous end-joining and undergoes ATM-dependent hyperphosphorylation following ionizing radiation. *DNA Repair* **7**(2)**,** 292-302.

Mahajan, K. N., McElhinny, S. A. N., Mitchell, B. S., and Ramsden, D. A. (2002). Association of DNA Polymerase μ (pol μ) with Ku and Ligase IV: Role for pol μ in End-Joining Double-Strand Break Repair. *Molecular and Cellular Biology* **22,** 5194-5202.

Martin, M., Genesca, A., Latre, L., Jaco, I., Taccioli, G. E., Egozcue, J., Blasco, M. A., Iliakis, G., and Tusell, L. (2005). Postreplicative Joining of DNA Double-Strand Breaks Causes Genomic Instability in DNA-PKcs-Deficient Mouse Embryonic Fibroblasts. *Cancer Research* **65**(22)**,** 10223-10232.

Masson, J.-Y., Tarsounas, M. C., Stasiak, A. Z., Stasiak, A., Shah, R., McIlwraith, M. J., Benson, F. E., and West, S. C. (2001). Identification and purification of two distinct complexes containing the five RAD51 paralogs. *Genes & Development* **15,** 3296-3307.

Matsuoka, S., Ballif, B. A., Smogorzewska, A., McDonald III, E. R., Hurov, K. E., Luo, J., Bakalarski, C. E., Zhao, Z., Solimini, N., Lerenthal, Y., Shiloh, Y., Gygi, S. P., and Elledge, S. J. (2007). ATM and ATR Substrate Analysis Reveals Extensive Protein Networks Responsive to DNA Damage. *Science* **316,** 1160-1166.

Meek, K., Gupta, S., Ramsden, D. A., and Lees-Miller, S. P. (2004). The DNA-dependent protein kinase: the director at the end. *Immunological Reviews* **200**(1)**,** 132-141.

Metzger, L., and Iliakis, G. (1991). Kinetics of DNA double strand breaks throughout the cell cycle as assayed by pulsed field gel electrophoresis in CHO cells. *International Journal of Radiation Biology* **59,** 1325-1339.

Mills, K. D., Ferguson, D. O., Essers, J., Eckersdorff, M., Kanaar, R., and Alt, F. W. (2004). Rad54 and DNA Ligase IV cooperate to maintain mammalian chromatid stability. *Genes & Development* **18,** 1283-1292.

Nevaldine, B., Longo, J. A., and Hahn, P. J. (1997). The *scid* defect results in much slower repair of DNA double-strand breaks but not high levels of residual breaks. *Radiation Research* **147,** 535-540.

Nick McElhinny, S. A., Havener, J. M., Garcia-Diaz, M., Juarez, R., Bebenek, K., Kee, B. L., Blanco, L., Kunkel, T. A., and Ramsden, D. A. (2005). A Gradient of Template Dependence Defines Distinct Biological Roles for Family X Polymerases in Nonhomologous End Joining. *Molecular Cell* **19,** 357-366.

Normanno, N., De Luca, A., Bianco, C., Strizzi, L., Mancino, M., Maiello, M. R., Carotenuto, A., De Feo, G., Caponigro, F., and Salomon, D. S. (2006). Epidermal growth factor receptor (EGFR) signaling in cancer. *Gene* **366**(1)**,** 2-16.

Nussenzweig, A., and Nussenzweig, M. C. (2007). A Backup DNA Repair Pathway Moves to the Forefront. *Cell* **131,** 223-225.

Nyati, M. K., Feng, F. Y., Maheshwari, D., Varambally, S., Zielske, S. P., Ahsan, A., Chun, P. Y., Arora, V. A., Davis, M. A., Jung, M., Ljungman, M., Canman, C. E., Chinnaiyan, A. M., and Lawrence, T. S. (2006). Ataxia Telangiectasia Mutated Down-regulates Phospho-Extracellular Signal-Regulated Kinase 1/2 via Activation of MKP-1 in Response to Radiation. *Cancer Research* **66**(24)**,** 11554-11559.

O'Driscoll, M., and Jeggo, P. A. (2006). The role of double-strand break repair - insights from human genetics. *Nature Reviews. Genetics* **7,** 45-54.

Okayasu, R., and Iliakis, G. (1989). Linear DNA elution dose response curves obtained in CHO cells with non-unwinding filter elution after appropriate selection of the lysis conditions. *International Journal of Radiation Biology* **55,** 569-581.

Okayasu, R., and Iliakis, G. (1991). The shape of DNA elution dose response curves under non-denaturing conditions:. *International Journal of Radiation Biology* **61,** 455-463.

Olive, P. L. (1998). The Role of DNA Single- and Double-Strand Breaks in Cell Killing by Ionizing Radiation. *Radiation Research* **150 (Suppl.),** S42-S51.

Ouyang, B. H., Nussenzweig, A., Kurimasa, A., da Costa Soares, V., Li, X., Cordon-Cardo, C., Li, W.-h., Cheong, N., Nussenzweig, M., Iliakis, G., Chen, D. J., and Li, G. C. (1997). Ku70 is required for DNA repair but not for T cell antigen receptor gene recombination in vivo. *Journal of Experimental Medicine* **186,** 921-929.

Paull, T. T., and Gellert, M. (2000). A mechanistic basis for Mre11-directed DNA joining at microhomologies. *Proceedings of the National Academy of Sciences of the United States of America* **97**(12)**,** 6409-6414.

Perrault, R., Wang, H., Wang, M., Rosidi, B., and Iliakis, G. (2004). Backup Pathways of NHEJ Are Suppressed by DNA-PK. *Journal of Cellular Biochemistry* **92,** 781-794.

Plank, J. L., and Hsieh, T.-s. (2006). A Novel, Topologically Constrained DNA Molecule Containing a Double Holliday Junction: DESIGN, SYNTHESIS, AND INITIAL BIOCHEMICAL CHARACTERIZATION. *Journal of Biological Chemistry* **281**(25)**,** 17510-17516.

Raben, D., Helfrich, B., Chan, D. C., Ciardiello, F., Zhao, L., Franklin, W., Baron, A. E., Zeng, C., Johnson, T. K., and Bunn, P. A. (2005). The Effects of Cetuximab Alone and in Combination With Radiation and/or Chemotherapy in Lung Cancer. *Clinical Cancer Research* **11**(2)**,** 795-805.

Rasouli-Nia, A., Karimi-Busheri, F., and Weinfeld, M. (2004). Stable down-regulation of human polynucleotide kinase enhances spontaneous mutation frequency and sensitizes cells to genotoxic agents. *Proceedings of the National Academy of Sciences of the United States of America* **101,** 6905-6910.

Rass, E., Grabarz, A., Plo, I., Gautier, J., Bertrand, P., and Lopez, B. S. (2009). Role of Mre11 in chromosomal nonhomologous end joining in mammalian cells. *Nature Structural & Molecular Biology* **16**(8)**,** 819-825.

Regulus, P., Duroux, B., Bayle, P.-A., Favier, A., Cadet, J., and Ravanat, J.-L. (2007). Oxidation of the sugar moiety of DNA by ionizing radiation or bleomycin could induce the formation of a cluster DNA lesion. *Proceedings of the National Academy of Sciences of the United States of America* **104**(35)**,** 14032-14037.

Riballo, E., Kühne, M., Rief, N., Doherty, A., Smith, G. C. M., Recio, M.-J., Reis, C., Dahm, K., Fricke, A., Krempler, A., Parker, A. R., Jackson, S. P., Gennery, A., Jeggo, P. A., and Löbrich, M. (2004). A pathway of double-strand break rejoining dependent upon ATM, artemis, and proteins locating to γ-H2AX foci. *Molecular Cell* **16,** 715-724.

Rijkers, T., Van Den Ouweland, J., Morolli, B., Rolink, A. G., Baarends, W. M., Van Sloun, P. P., Lohman, P. H., and Pastink, A. (1998). Targeted inactivation of mouse RAD52 reduces homologous recombination but not resistance to ionizing radiation. *Molecular and Cellular Biology* **18,** 6423-6429.

Robert, I., Dantzer, F., and Reina-San-Martin, B. (2009). Parp1 facilitates alternative NHEJ, whereas Parp2 suppresses IgH/c-myc translocations during immunoglobulin class switch recombination. *Journal of Experimental Medicine* **206**(5)**,** 1047-1056.

Roberts, S. A., Strande, N., Burkhalter, M. D., Strom, C., Havener, J. M., Hasty, P., and Ramsden, D. A. (2010). Ku is a 5'-dRP/AP lyase that excises nucleotide damage near broken ends. *Nature* **464**(7292)**,** 1214-1217.

Rosidi, B., Wang, M., Wu, W., Sharma, A., Wang, H., and Iliakis, G. (2008). Histone H1 functions as a stimulatory factor in backup pathways of NHEJ. *Nucleic Acids Research* **36**(5)**,** 1610-1623.

Rothkamm, K., Krüger, I., Thompson, L. H., and Löbrich, M. (2003). Pathways of DNA Double-Strand Break Repair during the Mammalian Cell Cycle. *Molecular and Cellular Biology* **23,** 5706-5715.

Rudat, V., Bachmann, N., Küpper, J.-H., and Weber, K.-J. (2001). Overexpression of the DNA-binding domain of poly(ADP-ribose) polymerase inhibits rejoining of ionizing radiation-induced DNA double-strand breaks. *International Journal of Radiation Biology* **77,** 303-307.

Rydberg, B. (2000). Radiation-induced heat-labile sites that convert into DNA double-strand breaks. *Radiation Research* **153,** 805-812.

Sak, A., Stuschke, M., Wurm, R., Schroeder, G., Sinn, B., Wolf, G., and Budach, V. (2002). Selective Inactivation of DNA-dependent Protein Kinase with Antisense Oligodeoxynucleotides: Consequences for the Rejoining of Radiation-induced DNA Double-Strand Breaks and Radiosensitivity of Human Cancer Cell Lines. *Cancer Research* **62,** 6621-6624.

Salles, B., Calsou, P., Frit, P., and Muller, C. (2006). The DNA repair complex DNA-PK, a pharmacological target in cancer chemotherapy and radiotherapy. *Pathologie-Biologie* **54**(4)**,** 185-193.

Sallmyr, A., Tomkinson, A. E., and Rassool, F. V. (2008). Up-regulation of WRN and DNA ligase IIIα in chronic myeloid leukemia: consequences for the repair of DNA double-strand breaks. *Blood* **112**(4)**,** 1413-1423.

Sarkaria, J. N., Tibbetts, R. S., Busby, E. C., Kennedy, A. P., Hill, D. E., and Abraham, R. T. (1998). Inhibition of phosphoinositide 3-kinase related kinases by the radiosensitizing agent wortmannin. *Cancer Research* **58,** 4375-4382.

Schmidt-Ullrich, R. K., Contessa, J. N., Lammering, G., Amorino, G., and Lin, P.-S. (2003). ERBB receptor tyrosine kinases and cellular radiation responses. *Oncogene* **22,** 5855-5865.

Schreiber, V., Dantzer, F. o., Ame, J.-C., and de Murcia, G. (2006). Poly(ADP-ribose): novel functions for an old molecule. *Nature Reviews. Molecular Cell Biology* **7**(7)**,** 517-528.

Schwartz, D. C., and Cantor, C. R. (1984). Separation of yeast chromosome-sized DNAs by pulsed field gradient gel electrophoresis. *Cell* **37,** 67-75.

Sharan, S. K., Morimatsu, M., Albrecht, U., Lim, D. S., Regel, E., Dinh, C., Sands, A., Eichele, G., Hasty, P., and Bradley, A. (1997). Embryonic lethality and radiation hypersensitivity mediated by Rad51 in mice lacking *Brca2*. *Nature* **386,** 804-810.

Shrivastav, M., De Haro, L. P., and Nickoloff, J. A. (2008). Regulation of DNA double-strand break repair pathway choice. *Cell Research* **18**(1)**,** 134-147.

Simsek, D., and Jasin, M. Alternative end-joining is suppressed by the canonical NHEJ component Xrcc4-ligase IV during chromosomal translocation formation. *Nat Struct Mol Biol* **17**(4)**,** 410-6.

Spina Purrello, V., Cormaci, G., Denaro, L., Reale, S., Costa, A., Lalicata, C., Sabbatini, M., Marchetti, B., and Avola, R. (2002). Effect of growth factors on nuclear and mitochondrial ADP-ribosylation processes during astroglial cell development and aging in culture. *Mech Ageing Dev* **123**(5)**,** 511-20.

Stackhouse, M. A., and Bedford, J. S. (1993a). An ionizing radiation-sensitive mutant of CHO cells: irs-20. I. Isolation and initial characterization. *Radiation Research* **136,** 241-249.

Stackhouse, M. A., and Bedford, J. S. (1993b). An ionizing radiation-sensitive mutant of CHO cells: irs-20. II Dose-rate effects and cellular recovery processes. *Radiation Research* **136,** 250-254.

Stackhouse, M. A., and Bedford, J. S. (1994). An ionizing radiation-sensitive mutant of CHO cells: *irs*-20. III. Chromosome aberrations, DNA breaks and mitotic delay. *International Journal of Radiation Biology* **65,** 571-582.

Stenerlöw, B., Karlsson, K. H., Cooper, B., and Rydberg, B. (2003). Measurement of prompt DNA double-strand breaks in mammalian cells without including heat-labile sites: Results for cells deficient in nonhomologous end joining. *Radiation Research* **159,** 502-510.

Sugiyama, T., and Kowalczykowski, S. C. (2002). Rad52 Protein Associates with Replication Protein A (RPA)-Single-stranded DNA to Accelerate Rad51-mediated Displacement of RPA and Presynaptic Complex Formation. *Journal of Biological Chemistry* **277,** 31663-31672.

Sung, P. (1994). Catalysis of ATP-dependent homologous DNA pairing and strand exchange by yeast RAD51 protein. *Science* **265,** 1241-1243.

Sung, P., and Klein, H. (2006). Mechanism of homologous recombination: mediators and helicases take on regulatory functions. *Nature Reviews. Molecular Cell Biology* **7,** 739-750.

Süsse, S., Scholz, C.-J., Bürkle, A., and Wiesmüller, L. (2004). Poly(ADP-ribose) polymerase (PARP-1) and p53 independently function in regulating double-strand break repair in primate cells. *Nucleic Acids Research* **32,** 669-680.

Sutherland, B. M., Bennett, P. V., Sidorkina, O., and Laval, J. (2000). Clustered DNA damages induced in isolated DNA and in human cells by low doses of ionizing radiation. *Proceedings of the National Academy of Sciences of the United States of America* **97,** 103-108.

Sutherland, R. M., Bennett, P. V., Sutherland, J. C., and Laval, J. (2002). Clustered DNA Damages Induced by X Rays in Human Cells. *Radiation Research* **157,** 611-616.

Suwa, A., Hirakata, M., Takeda, Y., Jesch, S. A., Mimori, T., and Hardin, J. A. (1994). DNA-dependent protein kinase (Ku protein-p350 complex) assembles on double-stranded DNA. *Proceedings of the National Academy of Sciences of the United States of America* **91,** 6904-6908.

Takata, M., Sasaki, M. S., Sonoda, E., Morrison, C., Hashimoto, M., Utsumi, H., Yamaguchi-Iwai, Y., Shinohara, A., and Takeda, S. (1998). Homologous recombination and non-homologous end-joining pathways of DNA double-strand break. *EMBO Journal* **17,** 5497-5508.

Takeda, S., Nakamura, K., Taniguchi, Y., and Paull, T. T. (2007). Ctp1/CtIP and the MRN Complex Collaborate in the Initial Steps of Homologous Recombination. *Molecular Cell* **28**(3)**,** 351-352.

Tarsounas, M., Davies, D., and West, S. C. (2003). BRCA2-dependent and independent formation of RAD51 nuclear foci. *Oncogene* **22,** 1115-1123.

Taylor, E. M., Cecillon, S. M., Bonis, A., Chapman, J. R., Povirk, L. F., and Lindsay, H. D. (2010). The Mre11/Rad50/Nbs1 complex functions in resection-based DNA end joining in Xenopus laevis. *Nucleic Acids Research* **38**(2)**,** 441-454.

Terzoudi, G. I., Singh, S. K., Pantelias, G. E., and Iliakis, G. (2008). Premature chromosome condensation reveals DNA-PK independent pathways of chromosome break repair. *International Journal of Oncology* **31**(1)**,** 145-152.

Toulany, M., Kasten-Pisula, U., Brammer, I., Wang, S., Chen, J., Dittmann, K., Baumann, M., Dikomey, E., and Rodemann, H. P. (2006). Blockage of Epidermal Growth Factor Receptor-Phosphatidylinositol 3-Kinase-AKT Signaling Increases Radiosensitivity of K-RAS Mutated Human Tumor Cells In vitro by Affecting DNA Repair. *Clinical Cancer Research* **12**(13)**,** 4119-4126.

Toulany, M., Kehlbach, R., Florczak, U., Sak, A., Wang, S., Chen, J., Lobrich, M., and Rodemann, H. P. (2008). Targeting of AKT1 enhances radiation toxicity of human tumor cells by inhibiting DNA-PKcs-dependent DNA double-strand break repair. *Molecular Cancer Therapeutics* **7**(7)**,** 1772-1781.

Uematsu, N., Weterings, E., Yano, K.-i., Morotomi-Yano, K., Jakob, B., Taucher-Scholz, G., Mari, P.-O., van Gent, D. C., Chen, B. P. C., and Chen, D. J. (2007). Autophosphorylation of DNA-PKCS regulates its dynamics at DNA double-strand breaks. *Journal of Cell Biology* **177**(2)**,** 219-229.

Valerie, K., and Povirk, L. F. (2003). Regulation and mechanisms of mammalian double-strand break repair. *Oncogene* **22**(37)**,** 5792-812.

van Gent, D. C., Hoeijmakers, J. H., and Kanaar, R. (2001a). Chromosomal stability and the DNA double-stranded break connection. *Nat Rev Genet* **2**(3)**,** 196-206.

van Gent, D. C., Hoeijmakers, J. H. J., and Kanaar, R. (2001b). Chromosomal stability and the DNA double-stranded break connection. *Nature Reviews. Genetics* **2,** 196-206.

Verkaik, N. S., Esveldt-van Lange, R. E. E., van Heemst, D., Brüggenwirth, H. T., Hoeijmakers, J. H. J., Zdzienicka, M. Z., and van Gent, D. C. (2002). Different types of V(D)J recombination and end-joining defects in DNA double-strand break repair mutant mammalian cells. *European Journal of Immunology* **32,** 701-709.

Virsik-Köpp, P., Hofman-Hüther, H., Rave-Fränk, M., and Schmidberger, H. (2005). The Effect of Wortmannin on Radiation-Induced Chromosome Aberration Formation in the Radioresistant Tumor Cell Line WiDr. *Radiation Research* **164,** 148-156.

Virsik-Köpp, P., Rave-Fränk, M., Hofman-Hüther, H., and Schmidberger, H. (2003). Role of DNA-PK in the process of aberration formation as studied in irradiated human glioblastoma cell lines M059K and M059J. *International Journal of Radiation Biology* **79,** 61-68.

Wallace, S. S. (1998). Enzymatic Processing of Radiation-Induced Free Radical Damage in DNA. *Radiation Research* **150**(5)**,** S60-S79.

Wang, H., Perrault, A. R., Takeda, Y., Qin, W., Wang, H., and Iliakis, G. (2003). Biochemical evidence for Ku-independent backup pathways of NHEJ. *Nucleic Acids Research* **31,** 5377-5388.

Wang, H., Rosidi, B., Perrault, R., Wang, M., Zhang, L., Windhofer, F., and Iliakis, G. (2005). DNA Ligase III as a Candidate Component of Backup Pathways of Nonhomologous End Joining. *Cancer Research* **65**(10)**,** 4020-4030.

Wang, H., Zeng, Z.-C., Bui, T.-A., Sonoda, E., Takata, M., Takeda, S., and Iliakis, G. (2001a). Efficient rejoining of radiation-induced DNA double-strand breaks in vertebrate cells deficient in genes of the RAD52 epistasis group. *Oncogene* **20,** 2212-2224.

Wang, H., Zhao-Chong, Z., Perrault, A. R., Cheng, X., Qin, W., and Iliakis, G. (2001b). Genetic evidence for the involvement of DNA ligase IV in the DNA-PK-dependent pathway of non-homologous end joining in mammalian cells. *Nucleic Acids Research* **29,** 1653-1660.

Wang, M., Wu, W., Wu, W., Rosidi, B., Zhang, L., Wang, H., and Iliakis, G. (2006). PARP-1 and Ku compete for repair of DNA double strand breaks by distinct NHEJ pathways. *Nucleic Acids Research* **34**(21)**,** 6170-6182.

Weterings, E., and van Gent, D. C. (2004). The mechanism of non-homologous end-joining: a synopsis of synapsis. *DNA Repair (Amst)* **3**(11)**,** 1425-35.

Williams, R. S., Moncalian, G., Williams, J. S., Yamada, Y., Limbo, O., Shin, D. S., Groocock, L. M., Cahill, D., Hitomi, C., Guenther, G., Moiani, D., Carney, J. P., Russell, P., and Tainer, J. A. (2008). Mre11 Dimers Coordinate DNA End Bridging and Nuclease Processing in Double-Strand-Break Repair. *Cell* **135**(1)**,** 97-109.

Windhofer, F., Wu, W., Wang, M., Singh, S. K., Saha, J., Rosidi, B., and Iliakis, G. (2007). Marked dependence on growth state of backup pathways of NHEJ. *International Journal of Radiation Oncology Biology Physics* **68**(5)**,** 1462-1470.

Wipf, P., and Halter, R. J. (2005). Chemistry and biology of wortmannin. *Org Biomol Chem* **3**(11)**,** 2053-61.

Wold, M. S. (1997). Replication Protein A: A heterotrimeric, single-stranded DNA-binding protein required for eukaryotic DNA metabolism. *Annual Review of Biochemistry* **66,** 61-92.

Wu, L., Bachrati, C. Z., Ou, J., Xu, C., Yin, J., Chang, M., Wang, W., Li, L., Brown, G. W., and Hickson, I. D. (2006). BLAP75/RMI1 promotes the BLM-dependent dissolution of homologous recombination intermediates. *Proceedings of the National Academy of Sciences of the United States of America* **103**(11)**,** 4068-4073.

Wu, W., Wang, M., Wu, W., Singh, S. K., Mussfeldt, T., and Iliakis, G. (2008). Repair of radiation induced DNA double strand breaks by backup NHEJ is enhanced in G2. *DNA Repair* **7**(2)**,** 329-338.

Xie, A., Kwok, A., and Scully, R. (2009). Role of mammalian Mre11 in classical and alternative nonhomologous end joining. *Nature Structural & Molecular Biology* **16**(8)**,** 814-818.

Yacoub, A., McKinstry, R., Hinman, D., Chung, T., Dent, P., and Hagan, M. P. (2003). Epidermal Growth Factor and Ionizing Radiation Up-regulate the DNA Repair Genes XRCC1 and ERCC1 in DU145 and LNCaP Prostate Carcinoma through MAPK Signaling. *Radiation Research* **159,** 439-452.

Yacoub, A., Park, J. S., Qiao, L., Dent, P., and Hagan, M. P. (2001). MAPK dependence of DNA damage repair: ionizing radiation and the induction of expression of the DNA repair genes XRCC1 and ERCC1 in DU145 human prostate carcinoma cells in a MEK1/2 dependent fashion. *International Journal of Radiation Biology* **77**(10)**,** 1067-1078.

Yajima, H., Lee, K.-J., and Chen, B. P. C. (2006). ATR-Dependent Phosphorylation of DNA-Dependent Protein Kinase Catalytic Subunit in Response to UV-Induced Replication Stress. *Molecular and Cellular Biology* **26**(20)**,** 7520-7528.

Yan, C. T., Boboila, C., Souza, E. K., Franco, S., Hickernell, T. R., Murphy, M., Gumaste, S., Geyer, M., Zarrin, A. A., Manis, J. P., Rajewsky, K., and Alt, F. W. (2007). IgH class switching and translocations use a robust non-classical end-joining pathway. *Nature* **449,** 478-482.

Yano, K.-i., Morotomi-Yano, K., Wang, S.-Y., Uematsu, N., Lee, K.-J., Asaithamby, A., Weterings, E., and Chen, D. J. (2008). Ku recruits XLF to DNA double-strand breaks. *EMBO Reports* **9**(1)**,** 91-96.

Yokoya, A., Cunniffe, S. M. T., Stevens, D. L., and O'Neill, P. (2003). Effects of Hydration on the Induction of Strand Breaks, Base Lesions, and Clustered Damage in DNA Films by α-Radiation. *Journal of Physical Chemistry* **107,** 832-837.

Yonetani, Y., Hochegger, H., Sonoda, E., Shinya, S., Yoshikawa, H., Takeda, S., and Yamazoe, M. (2005). Differential and collaborative actions of Rad51 paralog proteins in cellular response to DNA damage. *Nucleic Acids Research* **33**(14)**,** 4544-4552.

Yoo, S., and Dynan, W. S. (1999). Geometry of a complex formed by double strand break repair proteins at a single DNA end: recruitment of DNA-PKcs induces inward translocation of Ku protein. *Nucleic Acids Research* **27,** 4679-4686.

Yurchenko, V., Xue, Z., and Sadofsky, M. J. (2006). SUMO Modification of Human XRCC4 Regulates Its Localization and Function in DNA Double-Strand Break Repair. *Molecular and Cellular Biology* **26**(5)**,** 1786-1794.

Zhang, Z., Fan, H.-Y., Goldman, J. A., and Kingston, R. E. (2007). Homology-driven chromatin remodeling by human RAD54. *Nature Structural & Molecular Biology* **14**(5)**,** 397-405.

Zhang, Z., Hu, W., Cano, L., Lee, T. D., Chen, D. J., and Chen, Y. (2004). Solution Structure of the C-Terminal Domain of Ku80 Suggests Important Sites for Protein-Protein Interactions. *Structure* **12**(3)**,** 495-502.

7. Appendix

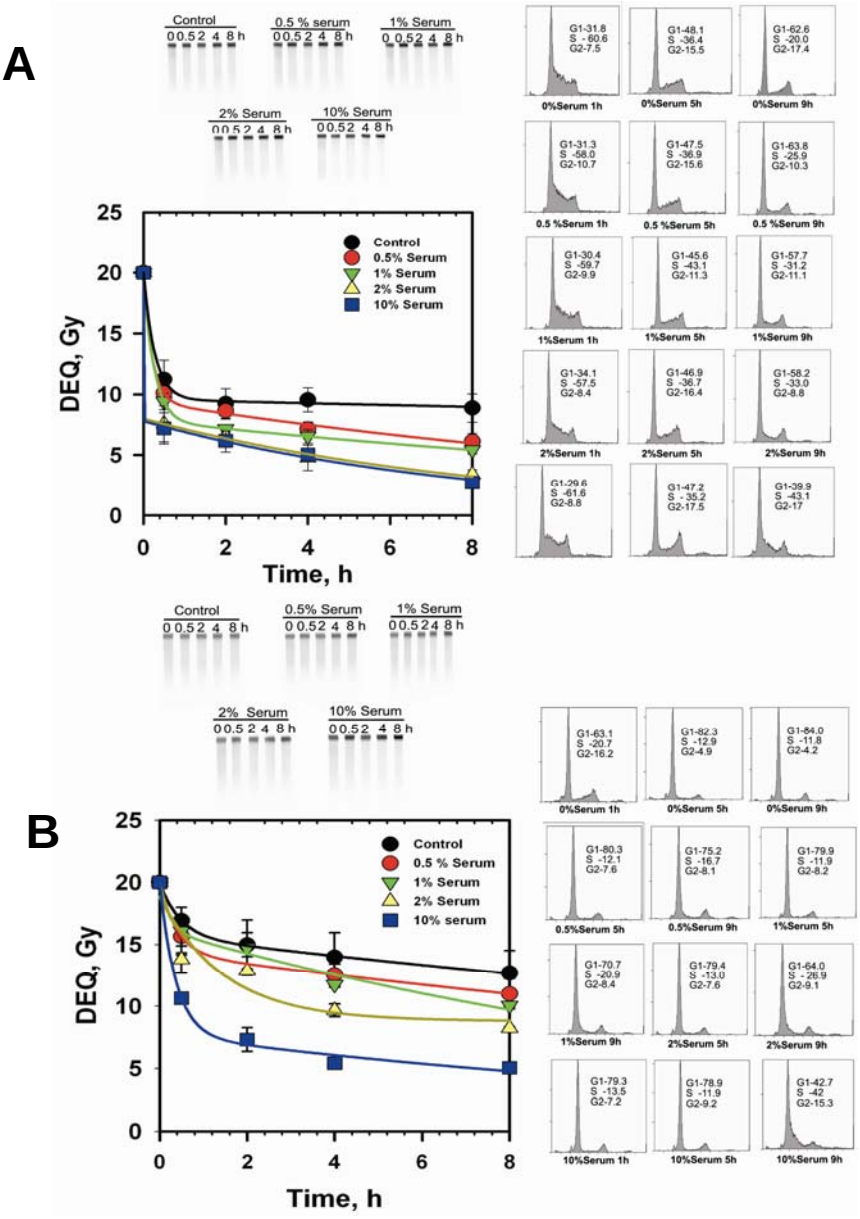

Recovery of repair capacity as a function of serum concentration applied immediately after the end of the serum deprivation period. *LIG4*$^{-/-}$ cells were serum deprived for 4 h and then returned to growth medium supplemented with the indicated amounts of serum. Serum deprived (SD) cells were treated with 0.5%, 1%, 2% and 10% serum just 1 h before IR and repair was followed by PFGE while incubating in the same media. Results shown are average and standard deviation of six determinations from two different experiments (A). Same experiment but with cells deprived from serum for 16 h and treated subsequently for 1 h with media containing different concentrations of serum. Cells were irradiated and DSB repair followed by PFGE (B).

Appendix 1

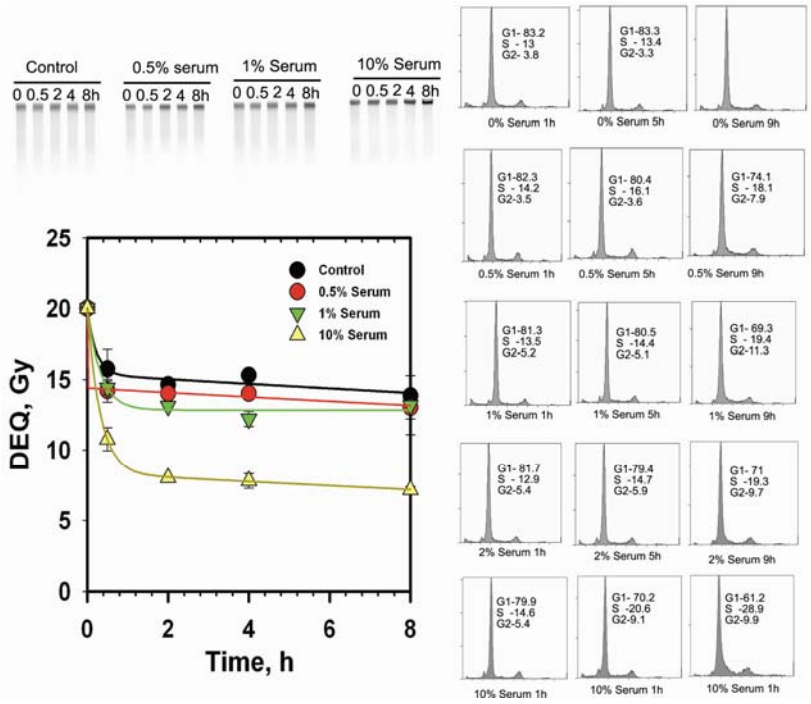

Recovery of repair capacity as a function of serum concentration applied immediately after the end of the serum deprivation period. *LIG4*$^{-/-}$ cells were serum deprived for 24 h and then returned to growth medium supplemented with the indicated amounts of serum. Serum deprived (SD) cells were treated with 0.5%, 1%, 2% and 10% serum just 1 h before IR and repair was followed by PFGE while incubating in the same media. Results shown are average and standard deviation of six determinations from two different experiments (A).

Appendix 2

8. Acknowledgement

I found an immense pleasure to acknowledge all the concerned people who were associated with the successful completion of my Ph.D. thesis. It's an honor to acknowledge each person who assisted me in my present work. I feel very grateful and indebted for their constant help and assistance throughout every stage of my doctoral dissertation.

I would like to express my deepest appreciation and gratefulness to the head of my Institute, advisor and mentor, Prof. Dr. George Iliakis, who has the attitude and the great temperament for good research. He continually and convincingly conveyed a spirit of adventure in regard to research. His constant and invaluable advice added new directions in the project. Without his guidance and persistent help this dissertation would not have been possible.

I would also like to thank Prof. Dr. Wolfgang-Ulrich Müller and Dr. Peter Tamulevicius for giving me insights into radiation protection, dosimetry and laboratory safety.

I am extremely thankful to Frau Jutta Müller, for excellent and timely administrative assistance during my stay in the institute. I am also very thankful to Dr. Lihua Zhang for teaching me survival assay and helping me at several occasions of ups and downs. I am also very thankful to Dr. Wenqi Wu for introducing me to amazing technique PFGE that I used intensively throughout my Ph.D dissertation. I would like to thank Dr. Minli Wang for her help to understand different ongoing techniques in the lab at the start of my Ph.D thesis.

I would like to thank Frau Tamara Musßfeldt, and Frau Elke Kouppers for excellent technical support, Frau Malihe Mesbah and Frau Lander for timely and very convenient support for ordering of chemicals and laboratory assistance. Their unconditional help made my work smooth and productive.

I would like to thank Dr. Hemant Agrawal, Dr. Savita Nair, Dr. Alena Bencsik, Dr. Xiaoxiang Fan and Dr. Mario Moscariello for formatting and editing my thesis. I especially want to thank Dr. Alena Bencsik for introducing me with certain features of MS word that helped me in formatting my thesis.

I would like to express my deep gratitude to my dedicated work group**.** Without their support this PhD work would have been a Herculean task. I would therefore like to specially thank them for giving me their full support in completing and solving problems pertaining to the experiments and help in maintaining a good environment during my project. It was really a fun to work in this work group.

Next, I would like to mention a word of thank to all, who helped and supported me constantly during my thesis, specially thank all my friends Aparna, Aruna, Ashish, Hemant, Kunal, Janapriya, Manoj, Minakshi Rani, Nisha, Preeti, Savita, Shreenath for their helpful suggestions, morale boosting and encouragement. I really appreciate their help during several occasions of turbulences in my life during last five years.

Above all, I would like to thank God for blessing me with everything that I have and especially this opportunity to come to Germany and introducing me to international standards of excellence. I would specially thank my **Family**, for being my pillars of strength and hope. I feel honored to mention about my parents for always being the source of inspiration and great support during my work. It is their good-will and prayers that have helped me immensely in pursuing my goals. I would thank my younger brother Shailendra too for constant moral boosting and support.

Finally, I would like to extend my special thanks to my wife, Shashi, for always being a source of encouragement and for believing in my dreams and supporting me through thick and thin.

9. Curriculum Vitae

Satyendra Kumar Singh

Institute for Medical Radiation Biology
Universitätsklinikum Essen
Hufelandstr. 55
Essen 45147, Germany

Phone: + 49-201-723-4153 *(Office)*
+ 49-17622723642 *(Mobile)*
E-mail: satyendra.singh@uni-due.de

PERSONAL DETAILS

Nationality : Indian

Date of birth : 10th June 1976

Sex : Male

ACADEMIC QUALIFICATIONS

1. **PhD (since Aug 2005—till date)**
   Department : Institute for Medical Radiation Biology,
   University : University Duisburg-Essen medical School
   Supervisor : Prof. (Dr). George Iliakis

2. **Junior Research Fellow (JRF) (2003 – 2005)**
   Department : Department of Biotechnology
   Organization : All India Institute of Medical Sciences (AIIMS) supported by Council of Scientific and Industrial research (CSIR), New Delhi, India
   Supervisor : Prof. Dr. S.N.Das

3. **Advanced PG Diploma in Bioinformatics (2002 – 2003)**
   Department : School of Computer and Systems Sciences (SCSS)
   Organization : Jawaharlal Nehru University, New Delhi, India

4. **Master in Science (M.Sc.) In Life Sciences (2000-02)**
   Department : School of Life Sciences (SLS)
   Organization : Jawaharlal Nehru University, New Delhi, India

RESEARCH EXPERIENCE

Since 2005 to till date: - **Ph.D student** – "The Function of Backup Pathways of Non-Homologous End Joining in Relation to Growth State of Chromatin Structure in Cells of Higher Eukaryotes"

University of Duisburg-Essen, Essen; Germany

Supervisor : Prof. Dr. George Iliakis

2003-2005 :- **Junior Research fellow (JRF)- "**BRCA1 and BRCA2 genes mutation in Familial breast cancer patients in North Indian population" All India Institute of Medical Sciences (AIIMS) supported by Council of Scientific and Industrial research (CSIR), New Delhi, India

Supervisor : Prof. Dr. S.N. Das

2002-2003 :- **Advanced PG Diploma in Bioinformatics –** Promoter Analysis Tool by using PSSM in E.coli. Jawaharlal Nehru University, New Delhi, India

Supervisor : Prof. Dr. Andrew Lynn

2000-2002 :- **Masters (research) student –** Comparison between *Entamoeba histolytica* and *Entamoeba dispar* Genomes by express sequence tags (ESTs).

School of Life Sciences, JNU, New Delhi. India

Supervisor: Prof. Dr. Alok Bhattacharya

ADDITIONAL QUALIFICATIONS

1. GATE (Graduate Aptitude Test in Engineering) qualified, conducted by Human Resource Development Ministry, Govt. of India in 2002.
2. Lectureship (LS) qualified in the exam conducted by Council for Scientific and Industrial Research (CSIR), Govt. of India in Dec`2001.
3. JRF (junior research fellowship) qualified, conducted by CSIR in Jun 2002.
4. One year fellowship provided by Department of Biotechnology, Govt. of India during Adv. Post Graduate Diploma in Bioinformatics.

10. Publications and Conferences

Publications

1. **Singh SK,** Staudt Christian, Wang M, Iliakis G "Delayed formation of DNA double strand breaks within clustered-damage sites from thermally unstable deoxyribose adducts in irradiated cells" (Manuscript prepared)

2. **Singh SK**, Wu W, Lihua Zhang, Wang M, Iliakis G. "The growth state dependence of backup NHEJ is general and observable after treatment with DNA-PK inhibitors" (Manuscript submitted) Int J Radiat Oncol Biol Phys.

3. **Singh SK**, Wu W, Wu W, Wang M, Iliakis G (2009) Extensive repair of DNA double-strand breaks in cells deficient in the DNA-PK-dependent pathway of NHEJ after exclusion of heat-labile sites. Radiation Research.Aug;172(2):152-64.

4. Terzoudi GI, **Singh SK**, Pantelias GE, Iliakis G. (2008) Premature chromosome condensation reveals DNA-PK independent pathways of chromosome break repair. Int J Oncol. Oct; 33(4):871-9.

5. Wu W, Wang M, Wu W, **Singh SK**, Mussfeldt T, Iliakis G.(2008) Repair of radiation induced DNA double strand breaks by backup NHEJ is enhanced in G2. DNA Repair (Amst) Feb 1;7(2):329-38. Epub 2007 Dec 26.

6. Windhofer F, Wu W, Wang M, **Singh SK**, Saha J, Rosidi B, Iliakis G.(2007) Marked dependence on growth state of backup pathways of NHEJ, Int J Radiat Oncol Biol Phys. Aug 1; 68(5):1462-70.

Poster Presentations

1. International Conference on ***Emerging Trends in Cancer Research*** held at the School of Life Sciences, Jawaharlal Nehru University, New Delhi, India **(14-16th Mar 2002).**

2. 24th Annual Convention of Indian Association for Cancer Research and International Symposium on ***Human Papillomavirus and Cervical Cancer*** at Indian Council of Medical Research, Noida, India **(Feb. 9-12, 2005).** Abstract was entitled "***BRCA1 and BRCA2 genes mutation in Familial breast cancer patients in North Indian population"*** **Satyendra Kumar Singh,** S.N.Das published in The **Indian Journal of Medical Research**, Volume 121; S -26 page no. 155, Feb.2005.

3. **10**th Biennial Meeting of the German Society for Research on DNA Repair DGDR, abstract was entitled ***Efficiency and dynamics of backup pathways of NHEJ in exponential and plateau phase of growth*** at Charité–Universitätsmedizin Berlin, Berlin , Germany (Sep. 2 – 5. 2008).

4. 11th International Wolfsberg Meeting on Molecular Radiation Biology/Oncology abstract was entitled ***Efficiency and dynamics of backup pathways of NHEJ in exponentially growing and plateau-phase cells*** at Ermatingen / Lake Constance, Switzerland (27-29 Jun 2009).

Oral Presentation

1. 12.Jahrestagung/12th Annual Conference Der/of the Gesellschaft für Biologische Strahlenforschung – GBS 30.9. – 2.10.2009, Essen

11. Declaration

Erklärung:

Hiermit erkläre ich, gem. § 6 Abs. 2, Nr. 7 der Promotionsordnung der Math.-Nat. Fakultäten zur Erlangung des Dr. *rer. nat*., dass ich das Arbeitsgebiet, dem das Thema: "*Titel der Dissertation*" zuzuordnen ist, in Forschung und Lehre vertrete und den Antrag von Herr Satyendra Kumar Singh befürworte.

Essen, den . _____

Unterschrift d. Wissenschaftl. Betreuers/Mitglieds

der Universität Duisburg-Essen

Erklärung:

Hiermit erkläre ich gem. § 6, Abs. 2, Nr. 6 der Promotionsordnung der Math.-Nat. Fakultäten zur Erlangung des Dr. *rer. nat*., dass ich die vorliegende Dissertation selbständig verfasst und mich keiner anderen als der angegebenen Hilfsmittel bedient habe.

Essen, den . _____

Unterschrift des/r Doktoranden/in

Erklärung:

Hiermit erkläre ich gem. § 6, Abs. 2, Nr. 8 der Promotionsordnung der Math.-Nat. Fakultäten zur Erlangung des Dr. *rer. nat*., dass ich keine anderen Promotionen bzw. Promotionsversuche in der Vergangenheit durchgeführt habe und dass diese Arbeit von keiner anderen Fakultät abgelehnt wurden ist.

Essen, den . _____

Unterschrift des/r Doktoranden/in